On the Computation of Loop Amplitudes Using the Loop-Tree Duality Formalism

Juan Pablo Vesga Simmons
geboren in Bogotá, Colombia

December 20, 2021

D77/ Dissertation der Johannes Gutenberg - Universität Mainz

For those that stand together

Contents

vi

Declaration of Authorship

I, Juan Pablo Vesga Simmons, hereby declare that I wrote the dissertation submitted without any unauthorized external assistance and used only sources acknowledged in the work. All textual passages which are appropriated verbatim or paraphrased from published and unpublished texts as well as all information obtained from oral sources are duly indicated and listed in accordance with bibliographical rules. In carrying out this research, I complied with the rules of standard scientific practice as formulated in the statutes of Johannes Gutenberg-University Mainz to insure standard scientific practice.

The main results of this dissertation, presented in Chapters 4 and 5, are based on original material previously published in collaboration with Robert Runkel, Stefan Weinzierl, Zoltán Szőr and myself in the following publications:

- [1] R. Runkel, Z. Szőr, J. P. Vesga and S. Weinzierl, "Causality and loop-tree duality at higher loops," Phys. Rev. Lett. **122** (2019) no.11, 111603, [erratum: Phys. Rev. Lett. **123** (2019) no.5, 059902] doi:10.1103/PhysRevLett.122.111603 [arXiv:1902.02135 [hep-ph]].

- [2] R. Runkel, Z. Szőr, J. P. Vesga and S. Weinzierl, "Integrands of loop amplitudes within loop-tree duality," Phys. Rev. D **101** (2020) no.11, 116014 doi:10.1103/PhysRevD.101.116014 [arXiv:1906.02218 [hep-ph]].

- [3] R. Runkel, Z. Szőr, J. P. Vesga and S. Weinzierl, "A new formulation of the loop-tree duality at higher loops," doi:10.22323/1.375.0073 [arXiv:1911.09610 [hep-ph]].

Abstract

The calculation of scattering amplitudes beyond the leading order or tree level approximation in perturbation theory is required to match the increasing precision of measurements at modern particle colliders where the fundamental structure of nature is put to test. The approach to higher-order calculations, based on the expansion on Feynman diagrams, becomes increasingly cumbersome beyond the simplest $2 \rightarrow 2$ processes. Moreover, the scattering amplitudes at a given perturbative order receive virtual and real corrections, which are given by divergent integrals over different integration measures. Although the divergences between the sum of all the contributions cancel against each other, realizing this cancellation in an automated fashion is difficult, and a framework to unify the integration measures is desired in order to pave the way for the possibility to cancel the divergences arising in the real and virtual contributions at the integrand level. In this thesis, the Loop-Tree Duality (LTD) formalism is utilized to reduce the dimension of the virtual loop integrals to that of the real radiation corrections. The formalism is applied in first instance to single Feynman integrals, resulting in the construction of integrands which have a tree-like structure where the usual Feynman propagators acquire a modified causal prescription for the position of the poles. Using the Feynman diagram expansion of the scattering amplitudes and the decomposition of each virtual contribution into trees, an expression in terms of a tree amplitude-like object is found for the integrand of the complete scattering amplitude in an arbitrary field theory. The tree structure of the integrand is then exploited to construct recursion relations which allow to compute the integrand without making reference to individual Feynman diagrams, providing a first step into the possible automation of the numerical calculation of higher-order amplitudes.

Zusammenfasung

Die Berechnung von Streuamplituden jenseits der Näherung führender Ordnung oder des Baumniveau in der Störungstheorie ist notwendig, um mit der ansteigenden Genauigkeit von Messungen an modernen Teilchenbeschleunigern mithalten zu können, bei denen die grundlegende Struktur der Natur auf die Probe gestellt wird. Die Herangehensweise an Berechnungen höherer Ordnung, basierend auf der Entwicklung in Feynman-Diagrammen, wird jenseits der einfachsten $2 \to 2$ Prozesse zunehmend umständlich. Zudem erhalten Streuamplituden zu einer bestimmten perturbativen Ordnung in der Störungstheorie virtuelle und reale Korrekturen, die durch divergente Integrale über verschiedene Integrationsgebiete gegeben sind. Obwohl sich die Divergenzen in der Summe aller Beiträge gegenseitig aufheben, ist die Realisierung der Aufhebungen in automatisierter Weise schwierig und ein Rahmen zur Vereinheitlichung der Integrationsgebiete ist erwünscht, um den Weg für die Möglichkeit zu ebnen, die Divergenzen, die in den realen und virtuellen Beiträgen auftreten auf dem Niveau des lntegranden aufzuheben. In dieser Arbeit wird der Loop-Tree Duality (LTD) Formalismus verwendet um die Dimension der virtuellen Schleifenintegrale auf die Dimension der realen Strahlungskorrekturen zu reduzieren.Der Formalismus wird zunächst auf einzelne Feynman-Integrale angewandt, was zur Konstruktion von Integranden führt, die eine baumartige Struktur haben, bei denen die üblichen Feynman-Propagatoren eine modifizierte kausale Vorschrift für die Position der Pole erhalten. Unter Verwendung der Entwicklung in Feynman-Diagrammen von Streuamplituden und der Zerlegung jedes virtuellen Beitrags in Bäume, wird ein Ausdruck in Form eines baumamplitudenartigen Objekts für den Integranden der vollständigen Streuamplitude in einer beliebigen Feldtheorie gefunden. Die Baumstruktur des Integranden wird dann ausgenutzt, um Rekursionsrelationen zu konstruieren, die es ermöglichen, den Integranden ohne Bezugnahme auf einzelne Feynman -Diagrammen zu berechnen, was einen ersten Schritt in Richtung einer möglichen Automatisierung der numerischen Berechnung von Amplituden höherer Ordnung darstellt.

Acknowledgements

There are moments in life which do not feel completely real a priori. Reaching the end of many years of learning and working in the fascinating topic of theoretical particle physics that lead to writing this thesis feels like one of those moments. The road to this point has been far from lonely, and the next few paragraphs are dedicated to those who helped me make happen such dream a reality.

In first place I would like to express my sincerest gratitude to my mentors. I want to thank Stefan Weinzierl, for without him I would not have had the opportunity to leave the comfort of my hometown, travel to a foreign country and pursue a PhD in physics. He has provided me with many valuables lessons, both about physics and the life of a professional for which I will be forever grateful. I would also like to thank Raffaele Fazio, whose attention and patience was key in me finding a passion for particle physics.

I would like to thank Zoltán Szőr for proving to be not only an incredible colleague who helped me better my understanding of particle physics and provide insightful feedback with some aspects of this work, but also one of the best persons I met in my time at Mainz and whom I am really happy to call a friend. My gratitude also goes to Sascha Kromin for catching typos and providing feedback with early drafts of this work, as well as helping my with my issues with the German language.

It certainly wouldn't have been possible for me to settle in Mainz if it wasn't for Ellen Luggert, whose help in sorting through the bureaucratic and administrative aspects of coming to Germany are something for which I will always be thankful. I would also like to thank all the administrative staff of the Theoretical High Energy Physics group for always being there to provide support with all the organizational issues I faced over the years at the institute.

Mainz was not only a possibility to study and challenge myself, but also a place where I met wonderful people. A big thanks as well to Ekta, Simon, Marco, Ina, Phillip, Robert and everybody else in the office at Mainz, for making my stay in Mainz such an amazing time from day one, making it feel sometimes like I wasn't an ocean apart from home. To Paolo, Julia and Swantje, for sharing so much of German, Italian and otherwise worldwide culture, long talks with beers and the not-so-occasional tabletop game. I hope our paths keep on crossing wherever each of us go.

Not a single word I've written nor any calculation I've done or any concept I've learned about physics would have been possible without the support of my mom and dad. They have encouraged me to pursue the crazy path of studying physics from day one. Even when they didn't understand what I was saying, they would listen to my every story about what I was

learning and that has kept me going through this road more times than I can count. For this and more, this work I also consider to be theirs.

Finally, I would like to express my infinite gratitude and love to Isabel, whose support, love and encouragement were vital to the writing of every single letter of this work. It is a strange and wonderful thing to find someone who resonates with you in the way we do, and for her being with me along the best part of this adventure I want to say: thank you!

Chapter 1

Introduction

1.1 The quest for precision in particle physics

The XX and XXI centuries have seen an amazing progress in humankind's understanding of nature. Starting with the discovery of quantum mechanics and relativity, physicists have embarked on a quest to understand the fundamental building blocks that make up our universe and how these blocks interact with each other.

The current theoretical paradigm asserts that there are four kinds of fundamental interactions among the known kinds of matter: the gravitational, electromagnetic, strong and weak nuclear interactions. These interactions can be mathematically described by fields which have values at different points in spacetime. There is, however, a divide in the properties of the field theories describing each of the interactions.

Gravity is described by Einstein's General Relativity, a classical field theory where the gravitational interaction is understood as a consequence of energy bending spacetime. It is responsible for sustaining the large-scale structure of the universe, providing the dominant force amongst celestial bodies such as stars, planets and galaxies. One characteristic property of the gravitational interaction is its attractive nature: two bodies that interact through a gravitational potential are always attracted to each other. As of today, there is no known consistent quantum-mechanical description of gravity, although there are indirect hints to the existence of gravitons, the hypothetical carrier of the interaction, thanks to the observation of gravitational waves by LIGO [4].

The three remaining interactions are described by gauge Quantum Field Theories. On one hand, the electromagnetic interaction is described by an Abelian gauge theory were the force carrier, the photon, is massless and is responsible for creating electric and magnetic fields. The charge associated to the electromagnetic interaction can have different signs, meaning that electrically charged particles can attract or repel each other, depending on their charges, which is in contrast to gravitation. Electromagnetism is the second interaction whose effects can most easily seen on a macroscopic scale, being responsible for a wide range of phenomena, from holding atoms together

through the attraction of nuclei and the electrons on their orbitals to the propagation of (visible) light. Meanwhile, the strong interaction, carried by massless, non-Abelian gauge bosons known as gluons, is responsible for the binding of quarks to form hadrons, such as the proton or the neutron. Finally, the weak interactions, mediated by the $W^{\pm}$ and Z_0 bosons, is responsible for the radioactive beta decay. These three interactions can be put together into a single framework, known as the standard model (SM) of particle physics.

The SM has proved to be an outstanding theory, not only correctly describing the dynamics of the particles known before and during its development, but also predicting the existence of a variety of particles which, time and time again, have been discovered through ever more ambitious experiments, with the discovery of a massive scalar of around 125 Gev discovered at the Large Hadron Collider (LHC) at CERN in 2012, which after extensive tests has shown to match all the expected properties of the Higgs boson.

Despite of its wide range of success, the SM is not a complete description of nature. Beyond its biggest limitation, which is the impossibility to consistently quantize Einstein's gravity due to the perturbative non-renormalizability of the theory, there is also no explanation in the SM for the existence and nature of dark matter and dark energy, which comprise around 94% of the universe's energy. Although we picked these two examples, there many more phenomena which the SM fails to explain, and the currently accepted picture is that the SM is a low-energy effective theory of a bigger framework which allows to explain all the currently observed discrepancies and the phenomena for which we do not have an explanation. As the history of physics has proved time and time again, independently of the soundness of the theoretical models that describe nature, discoveries that lead to a deeper understanding of the universe are found through observation, introducing the need to supersede the currently accepted paradigms and develop new models that adjust to the newly discovered aspects of reality. This means that the current goal of the particle physics community is to probe the predictions of the SM to a very high degree of accuracy and precision in order to look for clues of the hypothetical "higher structure" which reduces to the SM at low enough energies.

With the current machinery of particle colliders, there are two possible venues to put the SM to the test.

The first one is to increase the energy and luminosity at which the collisions occur. On this front, the LHC has provided the greatest improvements, having managed to operate at a collision energy of 7 TeV during its first run between 2009 and 2013, in which evidence for the Higgs boson was first discovered. The first improvements helped it achieve a collision energy of 14 TeV and, currently, further work on the collider plan to increase its luminosity by a factor of 10. Also at CERN, there are plans for the design of other

colliders, such as the Compact Linear Collider [5, 6] and the Future Circular Collider [7–10]. Elsewhere in the world, the International Linear Collider in Japan [11] and the Circular Electron-Positron Collider in China [12, 13] are currently under design. All these experiments will, through different observations, extend the limit to which the SM has been tested so far and, hopefully, shed some light into its possible extensions. The second possibility is to look at the values of very precise measurements, such as the ones provided by electron-positron colliders, and try to find tiny (but significant) discrepancies between the observed values and the predictions made by the calculations obtained from the framework of the SM. However, highly precise measurements require, in turn, highly precise calculations. As it turns out, increasing the predictions of calculations in the SM is no easy task.

The issue with the calculation of observables in the SM stems from the structure of Quantum Field Theory (QFT), the mathematical formalism used for its description. Due to the highly non-linear nature of the QFT's involved in the description of the SM, the equations of motion cannot be solved exactly and it is necessary to recur to the use of perturbation theory for the calculation of observables such as cross-sections at high energy. The perturbative series of an observable in an arbitrary QFT can be organized in terms of Feynman graphs, which give graphical representations of the terms appearing in the expansion. These graphs organize themselves by the number of external particles in the process, and by the number of internal closed loops in the graphs. Although these graphs provide an intuitive and, in principle, simple way to calculate the necessary contributions to an observable at any given perturbative order, in practice this is hardly what happens. One of the first issues is combinatorial in nature, because the number of graphs contributing to a particular observable grow rapidly with the number of external particles and the number of closed loops. Moreover, the nature of the contributions beyond the Leading Order (LO) approximation is complicated because of the appearance of integrals over all possible values of the momenta running through the loop. These integrals usually lead to divergences, and for a general observable these divergences cancel only in the combination of the so-called virtual and real corrections. Intuitively speaking, given the calculation of a LO observable with n external particles, some of the divergences that occur in the corrections with $L = 1$ closed loop and n external particles are cancelled against corrections with $(n + 1)$ external particles, but no additional closed loop. These first corrections, known as Next-to-Leading Order (NLO) corrections, are for the most part solved and can be performed in an automated fashion through the use of programs such as [14–17]. The current bottleneck for automation starts at Next-to-Next-to-Leading-Order (NNLO). Due to the increasing capacity of collider experiments, such contributions are necessary in order to compare to the current experimental benchmarks. Thus, it is of utmost importance to make progress towards breaking this bottleneck and design a framework in which one can compute NNLO corrections efficiently and automatically.

It is in this direction where the work of this thesis was done. We propose a new formulation of the Loop-Tree Duality (LTD) formalism [1–3], which allows to accommodate all the perturbative contributions at a given loop order in the same footing as the corrections with fewer amounts of loops and additional external particles. This unification of the structure of the different corrections allows for the definition of an object with properties similar to those of the leading order corrections prior to the integration over the loop momenta, aiming for the numerical computation of higher-order corrections bypassing some of the difficulties occurring in the typical analytic calculations of higher-order corrections.

1.2   Outline

This thesis is organized as follows.

In Chapter 2, we provide an introduction to QFT, illustrating some of its basic concepts, which set the framework to perform the calculation of scattering amplitudes and cross-sections. The Lagrangian formalism for scalar ϕ^3 theory, Quantum Electrodynamics (QED) and Quantum Chromodynamics (QCD) is introduced. Afterwards, the formula relating scattering amplitudes to cross sections is introduced, and a study of Feynman graphs and integrals is performed, focusing on the singular behaviour of loop integrals. We will see that there are two kinds of physical singularities present in higher-order corrections to scattering amplitudes: ultraviolet (UV) and infrared (IR) divergences. The energy regimes and the origin of each of these singularities will be discussed, along with a basic introduction to the theory of renormalization, which allows for the cancellation of UV divergences through the introduction of counterterms. Finally, we explicitly calculate the amplitude for the process $\gamma \to e^+e^-$ in QED at one-loop order. This calculation will serve as an example of the cancellation of IR divergences, which involve contributions from the virtual loop corrections and the so-called real corrections, given by diagrams with additional external edges.

Chapter 3 is devoted to the systematic classification of Feynman graphs. Here, we argue what kind of Feynman diagrams contribute to a scattering amplitude at a given perturbative order, and classify these diagrams into appropriate sets. Afterwards, we perform a graph-theoretical analysis of the relation between L-loop graphs with n external edges and tree graphs with $n + 2L$ external edges. The mechanism to relate these graphs will be the operations of cutting and sewing, which are inverse to each other. Essentially, cutting open an internal line of a loop graph reduces the loop order of the graph by one and increases its number of external legs by 2. Hence, cutting exactly L internal lines of an L-loop graph results into a connected tree graph with $n + 2L$ external legs. Given a specific tree graph, there will be more than a single set of cuts which of the associated loop graph which result into the same tree graph. We will see that this property implies that the symmetry factor associated to a loop graph will cancel after cutting when the overcounting

of tree graphs is properly taken into account, making it possible to exchange a summation over loop graphs for a summation over cut tree graphs.

The relation between loop and trees is further studied in Chapter 4, where we look at the analogue of the cutting operation for the Feynman integral associated to a given Feynman graph. It will be seen that cutting an internal line amounts to calculating the residue of the integrand at the pole in the energy component that arises when the associated momentum goes on-shell. We will first perform the analysis at the one-loop level, obtaining the Loop-Tree Duality (LTD) formula at one-loop, obtaining an integrand with the structure of a tree graph but with a modified causal prescription for the Feynman propagators and we present an example to illustrate the validity of the LTD formula. Finally, a generalization of the LTD formula is discussed, showing that it is possible to reproduce the behaviour at arbitrary loop order at the cost of introducing a set of combinatorial factors $S_{\sigma\alpha}$ which follow from the fact that, in general, multivariate residues cannot be calculated as the product of residues in a single complex variable. We discuss the non-uniqueness of the LTD representation for multiloop graphs, and provide a numerical example of the application of LTD to the two-loop sunrise graph in one spacetime dimension. The chapter is then concluded with a brief mention of the different approaches to LTD available in the current literature.

The extension of LTD to the integrand of the complete L-loop scattering amplitude is performed in Chapter 5. We begin by discussing the regularized forward-limit of tree amplitudes and tree amplitude-like objects, which is central to the definition of a non-singular loop integrand. The local representation of UV counterterms is then introduced, allowing us to write all of the virtual contributions to the scattering amplitude at a given perturbative order as integrals over L loop momenta. We will see that the local representation can be constructed such that residues of bare loop graphs originating from higher-order poles are cancelled against residues in the counterterms. This property will let us preserve the interpretation of the cut integrands as having a tree-like structure. Applying the LTD formula to every Feynman diagram contributing to a given scattering amplitude at L loops and using the relation between the sum of loop and tree graphs derived in Chapters 3 and 4 will then allow for the definition of an integrand which can be obtained without computing individual Feynman diagrams. The last step is then to introduce recursion relations that allow for the efficient calculation of the loop integrand. We conclude our discussion with a summary and an outlook of the further potential extensions of our work in Chapter 6.

Chapter 2

Basic notions of Quantum Field Theory

In this chapter, we give a brief overview of QFT and its applications in the phenomenology of the SM. We discuss how to construct cross-sections in terms of S-matrix elements and how these are computed order by order as a perturbative expansion in the couplings of the field theory under consideration. This will lead naturally to the introduction of Feynman diagrams and Feynman integrals, which are at the center of this thesis. We will study some of their properties and their singularity structure, exposing how these integrals often yield divergent results when treated at face value. This will lead us to discuss the different regularization procedures used in the literature to treat the divergences and how to remove them to obtain measurable predictions for physical observables.

2.1 Gauge Theories in Particle Physics

Our current understanding of particles and their interactions is based on QFT, where the fundamental objects are operator-valued distributions, the fields, whose excitations give rise to the different particles observed in nature. A particular field theory can be specified by a classical Lagrangian density[1]. For example, the Lagrangian describing the dynamics of a real scalar field ϕ of mass m in four dimensions can be written as

$$\mathcal{L}_{scalar} = \frac{1}{2}\left(\partial_\mu \phi \partial^\mu \phi - m^2 \phi^2\right) + \mathcal{L}_{int},\tag{2.1}$$

where $\mathcal{L}_{int}$ contains the interactions terms that are typically polynomials in ϕ (for example $\mathcal{L}_{int} = \frac{1}{3!}g\phi^3$), and the remaining terms make up the free Lagrangian, which describe the dynamics of the field when it is subject to no external potential.

For the calculation of physical observables, we will be interested in the so-called gauge theories: field theories whose Lagrangian is invariant under local transformations. Such a theory can be build up by considering a field theory that exhibits a global symmetry and promoting this symmetry to a local symmetry.

---

[1]In what follows, we will refer to a 'Lagrangian density' simply as a 'Lagrangian'.

Assume we are given a Dirac field Ψ with free Lagrangian

$$\mathcal{L}_D = \overline{\Psi}(i\slashed{\partial} - m)\Psi, \tag{2.2}$$

where $\slashed{p} = p_\mu\gamma^\mu, \overline{\Psi} = \Psi^\dagger\gamma^0$ and γ^μ denote the Dirac matrices. For any real number α, this Lagrangian is invariant under the transformation

$$\Psi \to e^{i\alpha}\Psi, \tag{2.3}$$

which implies that the theory has a global symmetry. We could then ask: what happens if α is a function of the spacetime coordinates? In this case, the mass term $m\overline{\Psi}\Psi$ is still invariant; however,

$$\partial_\mu e^{i\alpha(x)}\Psi \to e^{i\alpha(x)}\left(\partial_\mu\Psi + (i\partial_\mu\alpha)\Psi\right), \tag{2.4}$$

that is, the derivative term is not invariant under local phase transformations. The solution to this problem comes from the introduction of a covariant derivative, D_μ, which acting upon the Dirac field Ψ is given by

$$D_\mu\Psi(x) = \partial_\mu\Psi + ieA_\mu(x)\Psi(x), \tag{2.5}$$

where e is a constant and the vector field A_μ transforms according to

$$A_\mu(x) \to A_\mu(x) - \frac{1}{e}\partial_\mu\alpha(x), \tag{2.6}$$

so that multiplying the second term by $i\Psi(x)$ gives exactly the necessary quantity to cancel the term proportional to $\partial_\mu\alpha$ in the transformation of Ψ. Furthermore, we can construct another gauge invariant quantity by considering the commutator of two covariant derivatives:

$$\begin{aligned}
[D_\mu, D_\nu] &= [\partial_\mu + ieA_\mu, \partial_\nu + ieA_\nu] \\
&= ie\left([\partial_\mu, A_\nu(x)] - [\partial_\nu, A_\mu(x)]\right) \\
&= ie(\partial_\mu A_\nu - \partial_\nu A_\mu) \\
&= ieF_{\mu\nu}
\end{aligned} \tag{2.7}$$

where we define the field strength tensor $F_{\mu\nu} = \partial_\mu A_\nu - \partial_\nu A_\mu$. With these objects, we write down our final Lagrangian as

$$\mathcal{L}_{EM} = -\frac{1}{4}F_{\mu\nu}F^{\mu\nu} + \overline{\Psi}(i\slashed{D} - m)\Psi. \tag{2.8}$$

Interpreting the coupling e as the electric charge, the Lagrangian $\mathcal{L}_{EM}$ describes the dynamics of the electron, represented by the field Ψ, coupled to the gauge field A_μ that represents the photon. The classical equations of motion obtained by varying this Lagrangian with respect to the photon field can be seen to be the inhomogeneous Maxwell's equations with current $j^\mu = \overline{\Psi}\gamma^\mu\Psi$, and the variation with respect to Ψ will give Dirac's equation. Upon quantization of this theory, we obtain Quantum Electrodynamics (QED). This is the simplest example of a gauge theory that corresponds to

fields of physical particles and generalizing this construction to non-Abelian gauge groups (meaning that two successive transformations have non-trivial commutation properties), we obtain the most general type of gauge theories. The most important property of non-Abelian gauge theories is the fact that, contrary to the case of QED, the gauge field presents self-interaction terms: for a theory with gauge group $SU(N)$ for $N \geq 2$, we write

$$\mathcal{L}_{SU(N)} = -\frac{1}{4}F^a_{\mu\nu}F^{a\mu\nu} + i\overline{\Psi}(\slashed{D} - m)\Psi \tag{2.9}$$

where, now, we interpret Ψ as a multiplet of N Dirac fields whose covariant derivative acts as

$$D_\mu\Psi = \partial_\mu\Psi - igA^a_\mu t^a\Psi \tag{2.10}$$

where the generator matrices t^a are introduced, with the defining property

$$[t^a, t^b] = if^{abc}t^c \tag{2.11}$$

for some set of complex numbers f^{abc}, known as structure constants. The dimension of the matrices t^a depends on the underlying Lie group of the theory; in particular, there are $(N^2 - 1)$ generators in the adjoint representation of the group $SU(N)$. This means that a set of $(N^2 - 1)$ gauge fields A^a_μ is introduced to obtain a theory with local invariance with respect to transformations belonging to the Lie algebra of $SU(N)$.

Also, as in the case of QED, one can define the field strength tensor through the commutator of two covariant derivatives. In this case, however, because of Eq.(2.11), the two gauge fields do not commute, but rather satisfy

$$\begin{aligned} [D_\mu, D_\nu]\Psi &= [\partial_\mu - igA^a_\mu t^a, \partial_\nu - igA^b_\nu t^b]\Psi \\ &= \{[\partial_\mu, \partial_\nu] - ig[\partial_\mu, A^b_\nu t^b] - ig[A^a_\mu t^a, \partial_\nu] - g^2[A^a_\mu t^a, A^b_\nu t^b]\}\Psi \quad (2.12) \\ &= \{-ig\partial_\mu A^b_\nu t^b + ig\partial_\nu A^a_\mu t^a - ig^2 A^a_\mu A^b_\nu f^{abc}t^c\}\Psi. \end{aligned}$$

Defining the field strength tensor by the relation $[D_\mu, D_\nu] = -igF^a_{\mu\nu}t^a$, we then find

$$F^a_{\mu\nu} = \partial_\mu A^a_\nu - \partial_\nu A^a_\mu + gf^{abc}A^b_\mu A^c_\nu \tag{2.13}$$

thus, when squaring, we obtain not only a quadratic term in the derivatives of A_μ but also self-interaction terms with three and four gauge fields interacting. The most important application of gauge theories is the SM, which describes the interaction of matter, represented by fermionic fields mediated by the exchange of a set of gauge bosons. This theory is based on the gauge group

$$SU(3) \otimes SU(2) \otimes U(1) \tag{2.14}$$

where $SU(3)$ is the gauge group of the strong interaction and $SU(2) \otimes U(1)$ is the gauge group of the electroweak interaction. This gives raise to 8 colors of massless gluons g^a, as well as the three massive electroweak bosons W^+, W^-, Z and the massless photon γ. The electroweak bosons then acquire their mass through the Higgs mechanism.

2.2 Computation of observables and Perturbation Theory

Given that the theories we will be working with are quantum mechanical, the most general quantities we can calculate are probabilistic in nature. In particular, we are interested in giving a quantitative description of the phenomena of scattering, which can thought of as the consequence of localized collisions between particles. The mathematical description of scattering in quantum field theories is done via the S-matrix, which encodes the information about how particles interact with each other. We will do a short review of the definition of the S-matrix and its connection to cross-sections, our main object of interest, as well as how to compute the elements of the S-matrix from the knowledge of the Lagrangian. Detailed discussions of the subject can be found in standard textbooks [20, 21].

2.2.1 The S-Matrix and Cross-Sections

Consider the scattering process where n initial particles scatter into m final particles. A state formed in the asymptotic past where each particle has a definite momenta is known as an "in" state $|i\rangle_{in} = |p_1, p_2, ...p_n\rangle_{in}$. Similarly, a state formed in the asymptotic future where each particle has a definite momenta is an "out" state $|f\rangle_{out} = |k_1, k_2, ..., k_m\rangle_{out}$. We will be mainly interested in process where the initial state has no more than two particles. Thus, in what follows, we will assume that our "in" state is a two-particle state. The probability that the initial state $|i\rangle_{in}$ evolves into the final state $|f\rangle_{out}$ can be obtained by squaring the transition amplitude between the states,

$$
\begin{aligned}
P(i \to f) &= |_{out}\langle f|i\rangle_{in}|^2 \\
&= |_{out}\langle k_1, k_2, ..., k_m|p_1, p_2\rangle_{in}|^2.
\end{aligned}
\tag{2.15}
$$

Now, each of these states can be reached by starting from the states defined at some common reference time, for example, $t = 0$, taking the final state to time T and the initial state to $-T$ with a time evolution operator, and then let $T \to \infty$. The (unitary) operator that results from this limiting procedure is the S-matrix:

$$
\begin{aligned}
P(i \to f) &= |_{out}\langle k_1, k_2, ..., k_m|p_1, p_2\rangle_{in}|^2 \\
&= |\langle k_1, k_2, ..., k_m|S|p_1, p_2\rangle|^2
\end{aligned}
\tag{2.16}
$$

In an arbitrary scattering process, there exist the possibility that no scattering occurs at all. To separate this information from the actual interaction process, the S-matrix is written as

$$S = I + iT,$$ (2.17)

where I is the identity matrix in the Hilbert space where the "in" and "out" states are defined, and the T matrix contains all the information from the interactions. Momentum conservation should be encoded into either the S or T matrices, so we will define the matrix elements to contain an explicit momentum-conserving delta functions,

$$\langle k_1, k_2, ..., k_n | iT | p_1, p_2 \rangle$$
$$= (2\pi)^4 \delta^{(4)} \left(p_1 + p_2 - \sum_i k_i \right) iA(p_1, p_2; k_1, k_2, ..., k_m)$$ (2.18)

where the remaining factor, $A(p_1, p_2; k_1, k_2, ..., k_m)$, is the so-called scattering amplitude. We will usually assume that all the states are outgoing, and write

$$A(-p_1, -p_2; k_1, k_2, ..., k_m) = A_n(p_1, p_2, p_3..., p_n)$$ (2.19)

to denote the amplitude with n external particles. The minus sign in front of p_1 and p_2 in the left-hand side express the fact that, in a scattering process, an incoming particle with momentum p can be understood as an outgoing particle with momentum $-p$. The general rule of thumb is then to compute the amplitude with all states outgoing, and then change the signs of the momenta associated to the physically incoming particles of the process to obtain the correct value for the amplitude. These amplitudes may also depend on the polarizations of the external particles in theories with spin, but we will not write this dependence unless strictly necessary.

Scattering amplitudes are of central interest because of their relation to cross-sections. For a $2 \rightarrow (n-2)$ scattering process, the differential cross-section is given by

$$d\sigma = \frac{1}{F} \left(\prod_{i=3}^{n} \frac{d^3 p_i}{(2\pi)^3 2E_i} \right) |A_n(p_1, p_2, p_3, ..., p_n)|^2$$
$$\times (2\pi)^4 \delta^{(4)} \left(p_1 + p_2 - \sum_{i=3}^{n} p_i \right)$$ (2.20)

where F is a flux factor depending only on the initial kinematics and E_i are the on-shell energies of the final state particles. Assuming, then, that an expression for the amplitude A_n is known, one could obtain the cross section by performing the integrations over the final state momenta. Within the

current framework of QFT, there is no known technique that allows for the exact calculation of the scattering amplitude for interacting theories in four spacetime dimensions, which is related to the fact that there is no known exact solution to the classical equations of motion for interacting fields in four dimensions.

One can, however, find the solution to the equations of motion for free field theories and calculate the probability that a free particle propagates in space-time from one point to another. When including interactions, the solution to the free-field equations of motion serve as an useful first approximation for the observables of the interacting theory if the couplings of the theory are small. Therefore, what is done in practice is to organize the amplitude as a perturbative expansion in the couplings and keep only the first few orders of the expansion to obtain a meaningful approximation to the full amplitude. The problem, then, translates into the calculation of the coefficients of this expansion. We outline how this coefficients are calculated in the framework of perturbation theory.

2.2.2   The Perturbative Expansion and Feynman Diagrams

Consider a field theory with a single coupling g. According to our previous discussion, the n particle scattering amplitude can be written as a power series in g

$$A_n = A_n^{(0)} + g^2 A_n^{(1)} + g^4 A_n^{(2)} + \dots \qquad (2.21)$$

and, if the condition $g << 1$ is met, higher powers of g give smaller contributions to the amplitude. This condition usually depends on the energy scale at which the process occurs; for example, if we let g denote the coupling of QCD with n_f flavours of quarks, it is possible to show that, at a center of mass energy $E_{CM} = \sqrt{s}$, the coupling is given approximately by

$$g^2(s) = \frac{2\pi}{b_0 \log\left(\frac{\sqrt{s}}{\Lambda}\right)} \qquad (2.22)$$

where b_0 is a constant. We can see that, for values of s such that $\sqrt{s} >> \Lambda$, $g(k)$ is small. This phenomena is known as asymptotic freedom [18, 19] and implies that, at very high energies, the interactions of non-Abelian gauge theories become small enough so that one can apply perturbation theory to calculate observables. In this sense, Λ is the scale at which perturbation theory breaks down, since at energies lower than this scale, the coupling becomes large and higher-order contributions to the amplitude become large.

Each of the coefficients $A_n^{(L)}$ in Eq.(2.21) depend on the kinematics of the particles involved in the scattering process. The standard approach to calculate each of the terms in the perturbative expansion is through the use of Feynman diagrams, which give a pictorial representation of the different
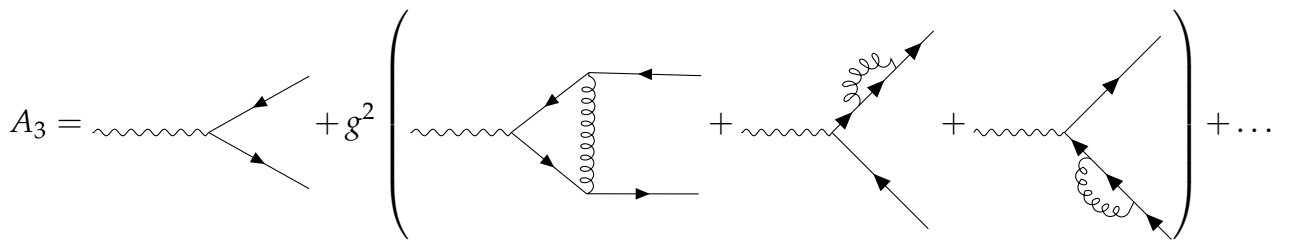
FIGURE 2.1: Contributions to off-shell photon decay into a quark-antiquark pair up to one-loop corrections in the strong interaction.

contributions that make up the quantities $A_n^{(l)}$ and are built using the Fenyman rules, which are specific to the field theory under consideration. We include the Feynman rules of some commonly encountered field theories in Appendix A.

The different sets of diagrams contributions to the scattering amplitude can then be organized by their number of external edges and loops, in such a way that the correction of order L contains diagrams with only L closed loops. Each closed loop introduces a momenta which is not constrained by momentum conservation, and thus should be integrated over. Therefore, every L loop diagram is associated with an integration over all of the spacetime components of L different momenta.

In Figure 2.1, we can see the first few contributions to the process where an off-shell photon decays into a quark-antiquark pair. The first order contribution to the amplitude is known as the tree-level or leading order (LO) contribution. Tree amplitudes have no unconstrained momenta, and therefore require no integration to obtain the amplitude. More interesting are the next-to-leading order, or NLO corrections. This kind of corrections include one closed loop, and according to our previous discussion, an integration should be performed over the so-called loop momenta. The extension to higher loops is natural, so that by considering graphs with higher number of loops introduces additional integrations to be performed in order to obtain the corresponding contributions.

2.2.3 Singularities of Feynman Integrals

The calculation of a scattering amplitude beyond tree-level involves the computation of Feynman integrals. The functions to be integrated are, in general, rational functions of the loop momenta. This implies that one might encounter singularities within the integration region, and dealing with the divergences that arise because of these singularities is an extremely non-trivial task.
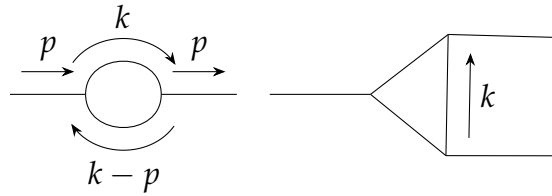
FIGURE 2.2: Diagrams corresponding to the scalar two- and three-point functions, $B_2^{(1)}$ and $T_3^{(1)}$, at one-loop order.

To illustrate this point, consider the diagrams of Figure 2.2, which show the contributions to the two- and three-point functions in ϕ^3 theory at one-loop.

The integral expression corresponding to the bubble diagrams is given by

$$B_2^{(1)}(p) = \int \frac{d^4k}{(2\pi)^4} \frac{1}{(k^2 + i\delta)((k-p)^2 + i\delta)} \tag{2.23}$$

while the triangle diagram can be written as

$$T_3^{(1)}(p) = \int \frac{d^4k}{(2\pi)^4} \frac{1}{(k^2 + i\delta)((p_1 - k)^2 + i\delta)((k + p_2)^2 + i\delta)} \tag{2.24}$$

where we have taken the internal lines to be massless, but we assume $p^2 \neq 0$. Let us first focus on the behaviour of the two-point function. For $k \to \infty$[2], we can take $(k - p) \approx k$ and then integral behaves as

$$\begin{aligned} B_2^{(1)}(p) &\propto \int \frac{d^4k}{k^4} \\ &\propto \int \frac{dk}{k} \\ &\propto \log k \end{aligned} \tag{2.25}$$

meaning that the integral will diverge logarithmically. Similarly, one can find situations in which the integral diverges linearly or quadratically with the magnitude of k. This type of divergence, which is related to modes with very high energies, are known as ultraviolet (UV) divergences and get their name from their similarity to the ultraviolet catastrophe of black-body radiation, the phenomena that gave birth to the discovery of quantum mechanics. These singularities are systematically removed through the process of renormalization, whose basic ideas we will discuss later.

---

[2]This statement only really makes sense if the momenta are Euclidean. This can always be accomplished by first performing a Wick rotation, so we ignore this technicality for the moment.

$$A_4^{(0)} = \text{[diagram]} + \text{[diagram]}$$
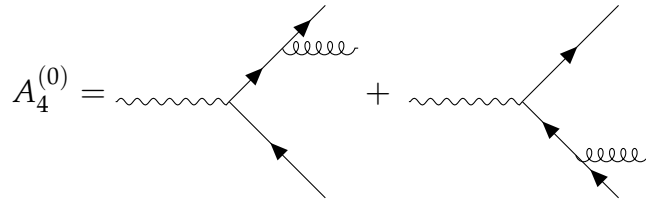
FIGURE 2.3: Real emission diagrams for the $\gamma^* \to q\bar{q}$ process

The other kind of singularities of Feynman integrals are known infrared (IR) divergences. These kind of divergences come from the regions where the momenta is small, and can only occur when one or more internal lines are massless. For example, from the $1/k^2$ term in the denominator of Eq.(2.24), we can see that the integral has a pole in the integration region as $k \to 0$. This kind of singularity is known as a soft singularity [22, 23]. Another kind of infrared divergence can occur for configurations where the loop momenta is collinear with one of the external momenta. In the case of the bubble integral, if we have $k \to zp$ for some real number z, then the propagator denominator $(k - p)^2$ behaves as p^2, and then the integral will diverge if $p^2 = 0$; these are known as collinear (or mass) divergences.

It is worth noticing that IR singularities not only appear in loop integrals, but that they can also be present in the phase-space integrals when one considers real corrections to a given process where the radiated particles are massless. From a physical point of view, these corrections are necessary because any detector has a finite resolution, which implies that if a given particle radiates another particle with very small energy or with small momenta collinear to the direction in which the original particle was scattered, the detector will not be able to distinguish between the process without the radiated particle and the actual physical process that occurred.

As an example, consider the process $\gamma^* \to q\bar{q}$. Similarly to the loop corrections in Fig. 2.1, one can also compute the corrections coming from diagrams of higher multiplicity. For this process, the contributing diagrams are given in Fig. 2.3.

In this case, when the integration over the three-particle phase space is performed, there can be soft singularities when the energy of the emitted gluon goes to zero and, if one is interested in the computation of observables where the masses of external quarks can be neglected, there will be also collinear singularities arising from the regions of phase-space where the gluon momenta is collinear with the momenta of the quark or antiquark.

The fact that both real and virtual corrections present IR singularities is not innocuous, but rather is at the root of their resolution: the Kinoshita-Lee-Nauenberg (KLN) theorem [24, 25] asserts that the IR singularities arising from the loop corrections to a particular order in perturbation theory are cancelled by the IR singularities that appear in the phase-space integration of

real corrections at the same perturbative order.

The KLN theorem, however, only applies to the so-called infrared safe observables, which are a set of observables insensitive to the inclusion of additional soft or collinear particles. This property is satisfied by various observables in the Standard Model, and is crucial to its predictive power.

Realizing the cancellation of IR divergences between real and virtual corrections in practical calculations is, in general, a very involved task, since the integrations are performed over different integration domains. Moreover, in all but the most simple of examples, performing the analytical computation of the phase-space integrals is in general not possible. Therefore, there are two general approaches to the calculation of loop amplitudes

- The virtual corrections are first integrated analytically over the loop momenta. As a first step, UV singularities must be regularized and removed by including renormalization counterterms. The introduction of the regulator and of the counterterms, as we will see, can be performed systematically and presents no difficulty. Performing the loop integrals, however, is rather difficult since beyond one-loop and low multiplicity, the loop integrations are quite non-trivial. The usual approach is not to perform these integrals directly, but rather to find systems of differential equations in the kinematic invariants which reduce the problem to the evaluation of a reduced set of basis integrals [26–32]. Moreover, the computations usually involve the manipulation of transcendental functions such as multiple or elliptic polylogarithms [33–41]. Afterwards, the phase-space integration of the virtual and real corrections is performed numerically. Although the sum of both contributions is free of IR divergences, each contribution is integrated over a different integration measure. Therefore, these singularities have to be first treated separately. An example of such a technique is the so-called dipole formalism [42–45], in which one introduces a set of counterterms given as integrals over the real radiation phase-space, that can be integrated over the phase-space measure of a single unresolved particle in such a way that adding and substracting the counterterms to the sum of virtual and real corrections appropriately to each of the contributions yields integrands, for both the virtual and real corrections, that contain only integrable singularities and therefore can be safely computed.

- One can attempt to perform the complete calculation numerically, for example, through numerical loop integration [46–58] or numerical unitarity [59–76]. In this approach, the difficulties in the treatment of the phase-space integrations are the same, but the challenges encountered in the analytic computation of the loop amplitudes is changed instead for a numerical computation. This process requires the computation of counterterms that can be written in a local representation [51, 53] in

such a way that they render the loop integrals UV integrable, while reproducing the correct value of the counterterms found in the analytic approach.

In general, the treatment of UV singularities can be performed in a systematic fashion, while that of IR singularities is more complicated and detailed. Let us, then, see how the UV singularities of Feynman integrals are parametrized and removed.

2.2.4 Regularization and Renormalization

In order to extract physically measurable quantities from the evaluation of Feynman integrals, their divergences must be treated and isolated, in order to associate a finite result to each integral which then allows to obtain a value for a given observable. The first step that is needed in order to treat this divergences is regularization: the integral is redefined by the introduction of a parameter which parametrizes the divergence, in such a way that the regularized integral is finite for some values of the parameter and that, in the limit where the original integral is recovered, the divergent behaviour emerges. As a very elementary example, consider the integral

$$I = \int_1^\infty \frac{dx}{x} \tag{2.26}$$

which is divergent as $x \to \infty$. This integral can be regularized by integrating up to some cut-off K. We obtain a modified integral, which can be evaluated

$$I(K) = \int_1^k \frac{dx}{x} = \log K \tag{2.27}$$

the new result is then finite, and we recover the original integral as $K \to \infty$. Although this process has not removed the divergence, we have managed to obtain a finite result where the singularities are clearly parametrized. A similar idea could be applied to the scalar two-point function of Eq.(2.23), where we could define the integral such that, when integrating over the magnitude of the momenta, we integrate only up to some very large, but finite, momentum Λ. This is an example of a regularization scheme, known as cut-off regularization. From the point of view of the properties of Feynman integrals this is not the most convenient regularization procedure, since the introduction of a preferred momentum scale breaks Lorentz invariance. There are many more regularization schemes, such as Pauli-Villar (PV) [77] and lattice regularization [78], among others. The regularization scheme most commonly encountered in perturbative Quantum Field Theory calculations is dimensional regularization (DR), which was introduced independently by Giambiagi and Bollini [79] and 't Hooft and Veltman [80]. The idea behind dimensional regularization is to redefine the integration in some arbitrary number of dimensions D, compute the integral as a meromorphic function for the values of D which make it convergent and then perform an analytic

continuation to the whole complex plane. The result, typically, is that if one performs a Laurent expansion of the D dimensional integral around the physical dimension (for example, taking $D = 4 - 2\epsilon$ and expanding around $\epsilon = 0$), the singularities will appear as poles in ϵ plus additional terms which are finite in the limit $\epsilon \to 0$. It is worth noticing that the integrations is performed as if D was an integer, but the analytic continuation guarantees that the result is valid even for non-integer values of D.

To illustrate this procedure, we consider the so-called tadpole integral

$$T_1^{(1)}(b, m) = \int \frac{d^4 k}{(2\pi)^4} \frac{1}{(k^2 - m^2 + i\delta)^b} \tag{2.28}$$

where we take the single propagator to have mass m and let it be raised to an arbitrary power b. For large k, the integral behaves as $k^{3-2b}dk$, such that for $b < \frac{3}{2}$ the integral has a UV divergence. For example, if $b = 1$, the integral diverges quadratically, while for $b = 2$ the integral has a logarithmic divergence. Now, we will compute this integral assuming that the momenta is D dimensional. The first step is to perform a Wick rotation, which allows us to rewrite this integral in terms of the magnitude of a D-dimensional Euclidean vector $k = (k_0^E, \vec{k})$ by means of the change of variables $k_0 = iK_0^E$, which doesn't change the integration limits of the integral over the Euclidean time component of the momenta thanks to the Feynman $i\delta$ prescription. The net result is to pick up a factor of $i(-1)^b$. Thus, we write

$$T_1^{(1)}(b, m; D) = i(-1)^b (\mu^2)^{\frac{D-4}{2}} \int \frac{d^D k}{(2\pi)^D} \frac{1}{(k^2 + m^2)^b} \tag{2.29}$$

where we have introduced an arbitrary scale μ, which ensures that the result has the same units as the result in $D = 4$ for every value of D. Now, since the integrand is spherically symmetric, we can work in D dimensional spherical coordinates. The measure can then be written in terms of the magnitude of the momenta and the D-dimensional solid angle,

$$d^D k = k^{d-1} dk d\Omega_D \tag{2.30}$$

and the integrations can be performed separately. The integral over the solid angle is a standard computation that can be found in textbooks, e.g. [20], with the result

$$\int d\Omega_D = \frac{2\pi^{\frac{D}{2}}}{\Gamma\left(\frac{D}{2}\right)} \tag{2.31}$$

where $\Gamma(x)$ is Euler's Gamma function. The remaining integral

$$I_{int}(D) = \int_0^\infty \frac{k^{D-1}}{(k^2 + m^2)^b} dk \tag{2.32}$$

can be performed by first changing variables to $u = k^2$, which results in

$$I_{int}(D) = \frac{1}{2} \int_0^\infty \frac{u^{\frac{D}{2}-1}}{(u+m^2)^b} du \tag{2.33}$$

and then a further change of variables $x = \frac{m^2}{u+m^2}$ puts the integral, after a bit of algebra, in the form

$$I_{int}(D) = \frac{1}{2} (m^2)^{\frac{D}{2}-b} \int_0^1 x^{b-\frac{D}{2}-1}(1-x)^{\frac{D}{2}-1} dx \tag{2.34}$$

This integral can be evaluated with Euler's Beta function and yields

$$\begin{aligned} I_{int}(D) &= \frac{1}{2}(m^2)^{\frac{D}{2}-b} B\left(b - \frac{D}{2}, \frac{D}{2}\right) \\ &= \frac{1}{2}(m^2)^{\frac{D}{2}-b} \frac{\Gamma\left(b - \frac{D}{2}\right) \Gamma\left(\frac{D}{2}\right)}{\Gamma(b)} \end{aligned}$$

so that, putting everything together, the final result for $T_1^{(1)}$ is, in terms of $2\epsilon = 4 - D$,

$$T_1^{(1)}(b, m; \epsilon) = \frac{i(-1)^b}{(4\pi)^{2-\epsilon}} (\mu^2)^\epsilon (m^2)^{2-\epsilon-b} \frac{\Gamma\left(b - 2 + \epsilon\right)}{\Gamma(b)} \tag{2.35}$$

We can now perform the Laurent expansion, using the properties of the Gamma function. For example, in the case $b = 2$ the resulting integral has an overall factor of $\Gamma(\epsilon)$. Its behaviour around $\epsilon = 0$ is

$$\Gamma(\epsilon) = \frac{1}{\epsilon} - \gamma + \mathcal{O}(\epsilon) \tag{2.36}$$

where $\gamma = 0,57721...$ is the Euler-Mascheroni constant. Hence, we can write the tadpole integral as

$$T_1^{(1)}(2, m; \epsilon) = \frac{i}{16\pi^2} \left(\frac{1}{\epsilon} - \gamma + \log(4\pi) - \log\left(\frac{m^2}{\mu^2}\right)\right) + \mathcal{O}(\epsilon) \tag{2.37}$$

This results has allowed us to separate the singular behaviour of the integral encapsulated as a pole in the regulator ϵ from a finite result in terms of m^2. From the point of view of a cut-off regulator, we expected the integral to diverge as $\log \Lambda$ for some momentum scale Λ. Thus, we can see that a logarithmic divergence of a loop integral translates into a simple pole in dimensional regularization. Moreover, polynomial divergences are related to higher-order poles in the regularization parameter ϵ. As a consequence of this procedure, we have introduced an additional scale μ^2 in order to keep the units of the calculated quantities consistent independent of the regulator[3].

---

[3]Physical observables should not be dependent on this scale, however. This observation lead to the development of the renormalization group and the Callan-Symansyk equations.

Although we have managed to extract the finite behaviour of the integral and parametrize its singularity structure in terms of a regulator, it is only half of the story: there is no escaping the fact that the integral still depends on ϵ and in order to obtain a physical result, we must take $\epsilon \to 0$. Therefore, what we need is a set of rules that allow us to subtract these poles, leaving as the result of our calculation a finite result. The procedure of removing the UV singularities of a Feynman integral is known as renormalization. This processes relies on the fact that the parameters that enter our calculations, which generally come from a Lagrangian through the Feynman rules, are not the physical quantities measured in an experiment. Thus, performing a redefinition of the quantities in the Lagrangian (that is, renormalizing the basic quantities that make up a field theory) by demanding that the parameters that enter our calculations match their measured values we can get rid of the divergences and obtain finite results for our predictions.

At the level of amplitudes and Feynman integrals, the effect of renormalization is to modify the values of the quantities being calculated by adding additional contributions known as counterterms. For example, the renormalized tadpole integral in Eq.(2.37) would take the form

$$T_{1,ren}^{(1)}(2, m; \epsilon) = T_1^{(1)}(2, m; \epsilon) + \delta T \qquad (2.38)$$

where the counterterm δT is picked such that the divergent term, proportional to ϵ^{-1}, is cancelled. Thus, we can see that, in general, the counterterms depend on the regulator and are by themselves divergent quantities. Their singular behaviour, however, is such that the divergences of the physically observable quantities being calculated are cancelled. In this case, we could simply pick

$$\delta T = -\frac{i}{16\pi^2 \epsilon} \qquad (2.39)$$

which would render the tadpole finite. In this case, we have defined the counterterm to have no finite contribution but one can in general pick it such that it also leaves a finite contribution after cancelling the divergences. A set of rules to pick the finite part of the counterterms is called a renormalization scheme[4].

The example given in Eq. (2.39) is known as the minimal substraction (MS) scheme, where the counterterms are constructed to only remove the

---

[4]In general, every choice of renormalization scheme must guarantee that the divergences are cancelled, leaving the arbitrariness to choose some non-vanishing finite contribution to the counterterms. If a calculation is performed with a particular renormalization scheme, it is always possible to do a further finite renormalization to translate the result into another renormalization scheme. The renormalization scheme that is most convenient to use initially depends on the particular calculation under consideration.

divergences. A related renormalization scheme is the modified minimal substraction ($\bar{M}S$) scheme [80, 81], where the counterterms are defined to cancel both the divergence and the term proportional to $(-\gamma + \log(4\pi))$, which tends to appear after expanding around $\epsilon = 0$ in calculations using dimensional regularization. Along with these two, the other most commonly used scheme is the on-shell renormalization scheme. In order to introduce it, we will discuss the systematic process of renormalization by starting from a Lagrangian and see how the counterterms arise from the redefinition of the parameters defining the theory.

Consider, once again, the QED Lagrangian of Eq.(2.8). We will rewrite this Lagrangian by using the explicit expressions for the field strength tensor and the covariant derivative, as

$$
\begin{aligned}
\mathcal{L}_{EM} = -\frac{1}{4}(\partial_\mu (A_b)_\nu - \partial_\nu (A_b)_\mu)(\partial^\mu (A_b)^\nu - \partial^\nu (A_b)^\mu) \\
+ \overline{\Psi}_b(i\slashed{\partial} - m_b)\Psi_b - e_b\overline{\Psi}_b\gamma_\mu(A_0)^\mu\Psi_b
\end{aligned}
\tag{2.40}
$$

where we have added a subscript b to all of the quantities in the Lagrangian, which is used to denote that none of the values of the parameters appearing in the Lagrangian correspond to the measured values, nor are the fields properly normalized to compute the correct scattering amplitudes. We refer to this as the bare Lagrangian, and give a similar name to each of its quantities.

The quantities appearing in the bare Lagrangian are related to the physical quantities through the process of renormalization. On one hand, the renormalized fields are defined as

$$
\Psi_b = Z_2^{1/2}\Psi
\tag{2.41}
$$

in the case of the fermion field, and

$$
(A_b)_\mu = Z_3^{1/2}A_\mu
\tag{2.42}
$$

where Z_2, Z_3 are formally infinite constants which allow the amplitudes obtained from a perturbative expansion using the renormalized fields Ψ and A_μ to have the proper normalization by setting the residues of the propagators at their poles equal to 1. With these modifications, the Lagrangian becomes

$$
\mathcal{L}_{EM} = -\frac{1}{4}Z_3 F_{\mu\nu}F^{\mu\nu} + Z_2\overline{\Psi}(i\slashed{\partial} - m_b)\Psi - Z_2 Z_3^{1/2}e_b\overline{\Psi}\gamma_\mu A^\mu\Psi.
\tag{2.43}
$$

Now, we must properly define the remaining parameters of the Lagrangian: the mass m_b and the charge e_b. The renormalized charge e is defined by introducing an additional factor Z_1 such that

$$e_b Z_2 Z_3^{\frac{1}{2}} = Z_1 e. \tag{2.44}$$

Before we write out the renormalization of the mass, notice that no renormalization is necessary in order to obtain the appropriate tree-level amplitudes. Thus, we should expect the renormalization factors Z_i to have the expansion

$$Z_i = 1 + \delta_i \tag{2.45}$$

where δ_i are a set of coefficients which can be expanded as a power series in the couplings (in this case, the electric charge) such that they cancel the divergences that appear in the amplitudes beyond the tree-level approximation order by order in perturbation theory. These coefficients is what we referred to previously as the counterterms. With this in mind, we introduce the mass counterterm δ_m as

$$\delta_m = Z_2 m_b - m \tag{2.46}$$

written in terms of the renormalized mass m. The QED Lagrangian takes the form

$$\mathcal{L}_{EM} = -\frac{1}{4} F_{\mu\nu} F^{\mu\nu} + \overline{\Psi}(i\slashed{\partial} - m)\Psi - e\overline{\Psi}\gamma_\mu A^\mu \Psi + \mathcal{L}_{CT} \tag{2.47}$$

where the first set of contributions is written completely in terms of the renormalized fields and parameters, and the last term, known as the counterterm Lagrangian, is given by

$$\mathcal{L}_{CT} = -\frac{1}{4} \delta_3 F_{\mu\nu} F^{\mu\nu} + \overline{\Psi}(i\delta_2 \slashed{\partial} - \delta_m)\Psi - e\delta_1 \overline{\Psi}\gamma_\mu A^\mu \Psi \tag{2.48}$$

where all the fields, as well as the mass and electric charge, are renormalized. The different contributions to the counterterm Lagrangian are then treated as further interaction vertices, and the corresponding Feynman rules are shown in A.

By a suitable fixing of the counterterms, the amplitudes calculated using the renormalized Lagrangian will result in finite values. This fixing is realized by imposing renormalization conditions, which will be relations that fix the behaviour of the higher-order corrections to the tree-level propagators and the interaction vertex. In QED, this relations read

$$\Sigma(\slashed{p} = m_P) = 0,$$

$$\frac{d}{d\slashed{p}} \Sigma(\slashed{p})\big|_{\slashed{p}=m_P} = 0, \tag{2.49}$$

$$\Pi(q^2 = 0) = 0,$$

$$-ie\Gamma^\mu(q = 0) = -ie\gamma^\mu$$

where $\Sigma(\not{p})$ is the value by which the pole of the fermion propagator is displaced from the bare mass m_b by quantum corrections[5]. Therefore, the first condition in Eq.(2.49) fixes the location of the simple pole of the electron propagator at a finite mass value m_P, known as the pole mass, while the second condition guarantees that the residue of the propagator at the pole mass is simply the imaginary unit i.

On the other hand, $\Pi(q^2)$ denotes the quantum corrections to the photon propagator, and the third equation fixes the value of the residue of the photon propagator at $q^2 = 0$. Finally, Γ^μ is made up of the higher-order contributions to the electromagnetic interaction vertex. Its renormalization condition fixes the electromagnetic charge appearing in the interaction vertex to have the value of the measured electric charge of the electron or any other fermion under consideration.

Notice that we have written the renormalization conditions such that the fermion propagator has a pole at m_P, where m_P is some finite mass which we define as the locations of its pole. The purpose of this is to provide a definition for the physical mass, that may be different from the renormalized mass m that one computes in an arbitrary renormalization scheme. With this in mind, we define the on-shell scheme to be the renormalization scheme where the value of the renormalized mass m coincides with the value of the pole mass m_P. This renormalization scheme will be the most useful to us, as we will see later on when the application of the LTD formalism to define the integrand for loop amplitudes is exposed.

2.2.5 Cancellation of IR divergences

We conclude this chapter by explicitly calculating the NLO corrections to the process $\gamma^* \to e^+ e^-$, in order to show a concrete example of the cancellation of infrared divergences. We will perform this computation using dimensional regularization. The diagrams contributing to this process are given by the two first diagrams in Figs 2.1 and the two diagrams in Fig. 2.3, but with every gluon replaced by a photon. We will need various identities involving sums of polarization vectors, spinors and traces of Dirac matrices, the proof of which can be found in any standard textbook, for example in [20].

The first contribution we must compute is the tree-level contribution. The Feynman rules used in this calculation can be found in Appendix A. The three particle tree amplitude is given, according to these rules, simply by the QED vertex dressed with the appropriate spinors and polarization vector; if we let q denote the momentum of the photon, p_1 the momentum of the electron and p_2 the momentum of the positron, we find

---

[5]It is common terminology to refer to quantities coming from contributions beyond tree-level or leading order as quantum corrections. This is because the leading order contributions to a scattering amplitude are essentially the predictions that the classical theory associated to the Quantum Field Theory under consideration would make.

$$A_3^{(0)} = -ie\bar{u}(p_1)\gamma^\mu v(p_2)\epsilon_\mu(q) \tag{2.50}$$

where, due to momentum conservation, $q = p_1 + p_2$. Here, we take the electron line to be on-shell, and to simplify the subsequent calculations, we take them to be massless, i.e. $p_1^2 = p_2^2 = 0$. Since we are interested in the cross-section, we consider the square of the amplitude, summed over spins and polarizations. Using the identity

$$(\bar{u}\gamma^\mu v)^\dagger = \bar{v}\gamma^\mu u \tag{2.51}$$

valid for any pair of spinors u and v, we find

$$\sum_{spins} |A_3^{(0)}|^2 = e^2 \sum_{s,s'} \bar{u}(p_1)\gamma^\mu v(p_2)\bar{v}(p_2)\gamma^\nu u(p_1) \sum_h \epsilon_\mu(q)\epsilon_\nu^*(q) \tag{2.52}$$

where the sums go over the spins s, s' of the electron and positron, respectively, and the polarizations of the photon, denoted by h. To proceed, we need the completeness relations

$$\sum_s u(p)\bar{u}(p) = \slashed{p} + m$$

$$\sum_s' v(p)\bar{v}(p) = \slashed{p} - m \tag{2.53}$$

$$\sum_h \epsilon_\mu(q)\epsilon_\nu^*(q) = -g_{\mu\nu} + \frac{q_\mu n_\nu + q_\nu n_\mu}{q \cdot n}$$

where m is the mass of the fermion described by the spinors u or v, and n_μ is the so-called reference vector, characterized by the properties $n^2 = 0$ and $q \cdot n \neq 0$. By evaluating the sum in a convenient order, we can realize that the contributions depending on the reference vector vanishes. For example, contracting the term $q_\mu n_\nu$ into the Gamma matrices results in a contribution proportional to

$$\bar{u}(p_1)\slashed{q}v(p_2) = \bar{u}(p_1)(\slashed{p}_1 + \slashed{p}_2)v(p_2) \tag{2.54}$$

which, due to the momentum-space Dirac equations,

$$\bar{u}(p)\slashed{p} = \bar{u}(p)m$$
$$\slashed{p}u(p) = mu(p)$$
$$\bar{v}(p)\slashed{p} = -\bar{v}(p)m \tag{2.55}$$
$$\slashed{p}v(p) = -mv(p)$$

vanish for massless external states. Thus, putting all of these identities together, we obtain

$$\sum_{spins} |A_3^{(0)}|^2 = e^2 Tr(\not{p}_1 \gamma^\mu \not{p}_2 \gamma_\mu). \tag{2.56}$$

In order to evaluate the trace, we use the D-dimensional contraction identity

$$\gamma^\mu \gamma^\nu \gamma_\mu = -(D-2)\gamma^\nu, \tag{2.57}$$

while replacing $D = 4 - 2\epsilon$ and $e^2 = 4\pi\alpha$, with α the fine structure constant. This results in

$$\sum_{spins} |A_3^{(0)}|^2 = -4\pi\alpha(2 - 2\epsilon) Tr(\not{p}_1 \not{p}_2). \tag{2.58}$$

Finally, using the defining property of the Gamma matrices

$$\{\gamma^\mu, \gamma^\nu\} = 2g^{\mu\nu}, \tag{2.59}$$

which is independent of the dimensions of spacetime, we can see that

$$\begin{aligned} Tr(\not{p}_1 \not{p}_2) &= Tr(2p_1 \cdot p_2 - \not{p}_2 \not{p}_1) \\ &= 8p_1 \cdot p_2 - Tr(\not{p}_1 \not{p}_2) \end{aligned} \tag{2.60}$$

where, in the second line, we used the property that the trace of a product of matrices is cyclic to exchange the order of $\not{p}_1$ and $\not{p}_2$. We can solve this equation for the trace to obtain

$$Tr(\not{p}_1 \not{p}_2) = 4p_1 \cdot p_2 \tag{2.61}$$

with which we find the square of the tree amplitude to be

$$\sum_{spins} |A_3^{(0)}|^2 = 16\pi\alpha(1-\epsilon)s_0 \tag{2.62}$$

where we defined $s_0 = (p_1 + p_2)^2 = 2p_1 \cdot p_2$. The integration over the two-particle phase space yields the cross-section for this process. We will not need to compute this integral, however, and proceed with computation of the virtual and real corrections.

At the one-loop level, there is a only one correction to the scattering amplitude, given by a vertex correction, which has the topology of a triangle diagram. This contribution will involve an integration over the loop momenta; taking this momenta to coincide with the momenta of the virtual photon propagating in the loop, we can write this contribution as

$$A_3^{(1)} = \epsilon_\mu \int \frac{d^D k}{(2\pi)^D} \times$$
$$\frac{\overline{u}(p_1)(-ie\gamma^\alpha)i(\not{p}_1 + \not{k})(-ie\gamma^\mu)i(\not{k} - \not{p}_2)(-ie\gamma^\beta)(-ig_{\alpha\beta})v(p_2)}{(k^2 + i\delta)((k + p_1)^2 + i\delta)((k - p_2)^2 + i\delta)}. \tag{2.63}$$

As a first step, let us simplify the integral where possible. Cancelling the different factors of i, putting together the corresponding powers of the electric charge and contracting the Lorentz indices with the metric tensor, we find

$$A_3^{(1)} = -e^3 \epsilon_\mu \int \frac{d^D k}{(2\pi)^D} \frac{\overline{u}(p_1)(\gamma^\alpha(\not{p}_1 + \not{k})\gamma^\mu(\not{k} - \not{p}_2)\gamma_\alpha)v(p_2)}{k^2(k + p_1)^2(k - p_2)^2}, \tag{2.64}$$

where we have dropped momentarily the $i\delta$ prescription. We can simplify the integrand further using the contraction identity

$$\gamma^\alpha \gamma^\mu \gamma^\nu \gamma^\rho \gamma_\alpha = -2\gamma^\rho \gamma^\nu \gamma^\mu + (4 - D)\gamma^\mu \gamma^\nu \gamma^\rho \tag{2.65}$$

and the Dirac equations, as in the tree calculation. As a result, we arrive at the integral

$$A_3^{(1)} = 2e^3 \epsilon_\mu \int \frac{d^D k}{(2\pi)^D} \frac{\overline{u}(p_1)((\not{k} - \not{p}_2)\gamma^\mu(\not{k} + \not{p}_1) - \epsilon \not{k}\gamma^\mu \not{k})v(p_2)}{(k + p_1)^2(k - p_2)^2 k^2} \tag{2.66}$$

where, in the denominator of the integrand, we have replaced $D = 4 - 2\epsilon$. Now, we want to rewrite the integrand in such a way that there is a single denominator. One way to achieve this is to introduce the so-called Feynman parameters, which arise from the formula

$$\frac{1}{A_1 A_2 \dots A_n} = (n - 1)! \int_{[0,1]^n} d^n \alpha \frac{\delta\left(1 - \sum_{i=1}^n \alpha_i\right)}{\left(\sum_{i=1}^n \alpha_i A_i\right)^n}. \tag{2.67}$$

Since we have three denominators, we need to introduce three Feynman parameters. We can then see that

$$\begin{aligned}
&\alpha_1(k + p_1)^2 + \alpha_2(k - p_2)^2 + \alpha_3 k^2 \\
&= (\alpha_1 + \alpha_2 + \alpha_3)k^2 + \alpha_1 2k \cdot p_1 - \alpha_2 2k \cdot p_2 \\
&= k^2 + 2k \cdot (\alpha_1 p_1 - \alpha_2 p_2) + (\alpha_1 p_1 - \alpha_2 p_2)^2 - (\alpha_1 p_1 - \alpha_2 p_2)^2 \\
&= (k + \alpha_1 p_1 - \alpha_2 p_2)^2 + \alpha_1 \alpha_2 s_0
\end{aligned} \tag{2.68}$$

where, going from the first to the second line, we used the fact that $p_1^2 = p_2^2 = 0$, in the third line we used $\alpha_1 + \alpha_2 + \alpha_3 = 1$ and completed the square, and in the last line we expanded $(\alpha_1 p_1 - \alpha_2 p_2)^2$ and kept the only

non-vanishing term, which is then expressed in terms of s_0. This allows us to rewrite

$$
A_3^{(0)} = 4e^3 \epsilon_\mu \int_0^1 d\alpha_1 \int_0^{1-\alpha_1} d\alpha_2
$$
$$
\int \frac{d^D k}{(2\pi)^D} \frac{\bar{u}(p_1)((\slashed{k} - \slashed{p}_2)\gamma^\mu(\slashed{k} + \slashed{p}_1) - \epsilon \slashed{k} \gamma^\mu \slashed{k})v(p_2)}{((k + \alpha_1 p_1 - \alpha_2 p_2)^2 + \alpha_1 \alpha_2 s_0)^3}. \tag{2.69}
$$

Now, we can focus on the loop integration. Since the integration is performed over all values of the loop momenta k, we can perform the shift $k \to k - \alpha_1 p_1 + \alpha_2 p_2$ without changing the integration measure. This results in the denominator of the integral being invariant under the $k \to -k$. Thus, any term with an odd power of k in the numerator vanishes by symmetry. With this in mind, we end up with the integral

$$
\int \frac{d^D k}{(2\pi)^D} \frac{\bar{u}(p_1)\left((1 - \epsilon)\slashed{k}\gamma^\mu\slashed{k} + (\epsilon\alpha_1\alpha_2 - (1 - \alpha_1)(1 - \alpha_2))\slashed{p}_2\gamma^\mu\slashed{p}_1\right)v(p_2)}{(k^2 + \alpha_1\alpha_2 s_0)^3}.
$$

Using the anticommutator of the Gamma matrices, we find

$$
\slashed{k}\gamma^\mu\slashed{k} = (2k^\mu - \gamma^\mu\slashed{k})\slashed{k}
$$
$$
= 2k^\mu\slashed{k} - \gamma^\mu k^2 \tag{2.70}
$$

and

$$
\slashed{p}_2\gamma^\mu\slashed{p}_1 = (2p_2^\mu - \gamma^\mu\slashed{p}_2)\slashed{p}_1
$$
$$
= 2p_2^\mu\slashed{p}_1 - \gamma^\mu(2p_1 \cdot p_2 - \slashed{p}_1\slashed{p}_2) \tag{2.71}
$$
$$
= -s_0\gamma^\mu
$$

where the last line is only valid when the expression is inside the spinors $\bar{u}(p_1)$ and $v(p_2)$, by virtue of the Dirac equation. Having reduced the integrand to this form, we can perform the loop integrations via the Tadpole integral of Eq.(2.28), as well as

$$
\int \frac{d^D k}{(2\pi)^D} \frac{k^\mu k^\nu}{(k^2 - \Delta)^n} = \frac{(-1)^{n-1} i}{(4\pi)^{\frac{D}{2}}} \frac{g^{\mu\nu}}{2} \frac{\Gamma(n - \frac{D}{2} - 1)}{\Gamma(n)} (\Delta)^{\frac{D}{2} + 1 - n} \tag{2.72}
$$

which can be obtained by noting that, due to the spherical symmetry of the integral and the fact that there is no preferred four-vector upon which the integral depends, the only possible tensor structure that can be obtained after integration is $g^{\mu\nu}$. From this integral, one immediately obtains, after contracting with the metric tensor,

$$\int \frac{d^D k}{(2\pi)^D} \frac{k^2}{(k^2 - \Delta)^n} = \frac{(-1)^{n-1} i}{(4\pi)^{\frac{D}{2}}} \frac{D}{2} \frac{\Gamma\left(n - \frac{D}{2} - 1\right)}{\Gamma(n)} (\Delta)^{\frac{D}{2} + 1 - n}. \qquad (2.73)$$

With these formulas at hand, we can evaluate

$$\begin{aligned}
\int \frac{d^D k}{(2\pi)^D} & \frac{2k^\mu \slashed{k} - k^2 \gamma^\mu}{(k^2 + \alpha_1 \alpha_2 s_0)^3} \\
&= \frac{i}{2(4\pi)^{\frac{D}{2}}} \Gamma\left(2 - \frac{D}{2}\right) (-\alpha_1 \alpha_2 s_0)^{\frac{D}{2} - 2} \gamma^\mu \\
&\quad - \frac{iD}{4(4\pi)^{\frac{D}{2}}} \Gamma\left(2 - \frac{D}{2}\right) (-\alpha_1 \alpha_2 s_0)^{\frac{D}{2} - 2} \gamma^\mu \\
&= \frac{i}{2(4\pi)^{\frac{D}{2}}} \Gamma\left(2 - \frac{D}{2}\right) (-\alpha_1 \alpha_2 s_0)^{\frac{D}{2} - 2} \left(1 - \frac{D}{2}\right) \gamma^\mu \\
&= \frac{i}{32\pi^2 (4\pi)^{-\epsilon}} \Gamma(\epsilon) (-\alpha_1 \alpha_2 s_0)^{-\epsilon} (-1 + \epsilon) \gamma^\mu
\end{aligned} \qquad (2.74)$$

while, on the other hand, we can use the tadpole integral formula to obtain

$$\int \frac{d^D k}{(2\pi)^D} \frac{1}{(k^2 + \alpha_1 \alpha_2 s_0)^3} = -\frac{i}{32\pi^2 (4\pi)^{-\epsilon}} \Gamma(1 + \epsilon)(-\alpha_1 \alpha_2 s_0)^{-1-\epsilon}. \qquad (2.75)$$

Using these results, we can write the one-loop correction to the amplitude as a two-dimensional integral over the Feynman parameters

$$\begin{aligned}
A_3^{(1)} = & \frac{4ie^3 \epsilon_\mu (-s_0)^{-\epsilon}}{32\pi^2 (4\pi)^{-\epsilon}} \int_0^1 d\alpha_1 \int_0^{1-\alpha_1} d\alpha_2 \bar{u}(p_1) \gamma^\mu \Big[-(1 - \epsilon)^2 \Gamma(\epsilon)(\alpha_1 \alpha_2)^{-\epsilon} \\
& ((1 - \alpha_1)(1 - \alpha_2) - \epsilon \alpha_1 \alpha_2) \Gamma(1 + \epsilon)(\alpha_1 \alpha_2)^{-1-\epsilon} \Big] v(p_2).
\end{aligned} \qquad (2.76)$$

We can see at this point that the remaining integrations have no Lorentz structure and depend only on the regularization parameter ϵ. That means that we can write

$$A_3^{(1)} = \frac{4ie^3 \epsilon_\mu \Gamma(\epsilon)(-s_0)^{-\epsilon}}{32\pi^2 (4\pi)^{-\epsilon}} \bar{u}(p_1) \gamma^\mu v(p_2) F(\epsilon) \qquad (2.77)$$

where

$$F(\epsilon) = \int_0^1 d\alpha_1 \int_0^{1-\alpha_1} d\alpha_2 \left[-(1-\epsilon)^2 (\alpha_1 \alpha_2)^{-\epsilon} \right.$$
$$\left. ((1-\alpha_1)(1-\alpha_2) - \epsilon\alpha_1\alpha_2)\epsilon(\alpha_1\alpha_2)^{-1-\epsilon} \right] \tag{2.78}$$

and we used $\Gamma(1+\epsilon) = \epsilon\Gamma(\epsilon)$ to factor out the Gamma function. This integral can be split into two different integrations, according to the power of $(\alpha_1\alpha_2)$ that appears in each of them. The first of these integrals is

$$I_1 = (\epsilon - (1-\epsilon)^2 - \epsilon^2) \int_0^1 d\alpha_1 \int_0^{1-\alpha_1} d\alpha_2 (\alpha_1\alpha_2)^{-\epsilon}$$
$$= -(1-\epsilon)(1-2\epsilon) \int_0^1 d\alpha_1 \alpha_1^{-\epsilon} \frac{(1-\alpha_1)^{1-\epsilon}}{1-\epsilon}$$
$$= -(1-2\epsilon) \int_0^1 d\alpha_1 \alpha_1^{-\epsilon} (1-\alpha_1)^{1-\epsilon} \tag{2.79}$$
$$= -(1-2\epsilon) \frac{\Gamma(1-\epsilon)\Gamma(2-\epsilon)}{\Gamma(3-2\epsilon)}$$

where we used the definition of Euler's Beta function to perform the last integration. The remaining integral is given by

$$I_2 = \epsilon \int_0^1 d\alpha_1 \int_0^{1-\alpha_1} d\alpha_2 (1-\alpha_1-\alpha_2)(\alpha_1\alpha_2)^{-1-\epsilon}. \tag{2.80}$$

In this case, we have contributions with three different integrands: $(\alpha_1\alpha_2)^{-1-\epsilon}$, $\alpha_1(\alpha_1\alpha_2)^{-1-\epsilon}$ and $\alpha_2(\alpha_1\alpha_2)^{-1-\epsilon}$. By virtue of the symmetry of the integral under the exchange of α_1 and α_2, the last two integrals give the same result. For the first one, a procedure identical to the calculation of I_1 yields

$$\int_0^1 d\alpha_1 \int_0^{1-\alpha_1} d\alpha_2 (\alpha_1\alpha_2)^{-1-\epsilon} = -\frac{1}{\epsilon} \frac{\Gamma(-\epsilon)\Gamma(1-\epsilon)}{\Gamma(1-2\epsilon)} \tag{2.81}$$

while, for example,

$$\int_0^1 d\alpha_1 \int_0^{1-\alpha_1} d\alpha_2 \alpha_1 (\alpha_1\alpha_2)^{-1-\epsilon}$$
$$= \int_0^1 d\alpha_1 \alpha_1^{-\epsilon} \int_0^{1-\alpha_1} d\alpha_2 \alpha_2^{-1-\epsilon}$$
$$= \int_0^1 d\alpha_1 \alpha_1^{-\epsilon} \frac{(1-\alpha_1)^{-\epsilon}}{-\epsilon} \tag{2.82}$$
$$= -\frac{1}{\epsilon} \int_0^1 d\alpha_1 \alpha_1^{-\epsilon} (1-\alpha_1)^{-\epsilon}$$
$$= -\frac{1}{\epsilon} \frac{\Gamma^2(1-\epsilon)}{\Gamma(2-2\epsilon)}$$

with the remaining integral giving the same result.

Recalling that the tree amplitude is given by $A_3^{(0)} = -ie\epsilon_\mu \bar{u}(p_1)\gamma^\mu v(p_2)$ and using the result of the Feynman parameter integrals, we can write

$$
A_3^{(1)} = -A_3^{(0)} \frac{4e^2 \Gamma(\epsilon)(-s_0)^{-\epsilon}}{32\pi^2 (4\pi)^{-\epsilon}} \left[-(1 - 2\epsilon)\frac{\Gamma(1-\epsilon)\Gamma(2-\epsilon)}{\Gamma(3-2\epsilon)} \right.
$$
$$
\left. -\frac{\Gamma(-\epsilon)\Gamma(1-\epsilon)}{\Gamma(1-2\epsilon)} + 2\frac{\Gamma^2(1-\epsilon)}{\Gamma(2-2\epsilon)} \right]
\tag{2.83}
$$

We can now rewrite all the Gamma functions in order to factorize a single ratio of Gammas. In order to do this, we write

$$
\Gamma(2-\epsilon) = (1-\epsilon)\Gamma(1-\epsilon)
$$
$$
\Gamma(3-2\epsilon) = (2-2\epsilon)(1-2\epsilon)\Gamma(1-2\epsilon)
$$
$$
\Gamma(2-2\epsilon) = (1-2\epsilon)\Gamma(1-2\epsilon)
\tag{2.84}
$$
$$
\Gamma(-\epsilon) = -\frac{\Gamma(1-\epsilon)}{\epsilon}
$$

with which we arrive at the result

$$
A_3^{(1)} = -A_3^{(0)} \frac{\alpha}{2\pi}\left(-\frac{s_0}{4\pi}\right)^{-\epsilon} \frac{2\epsilon^2 - \epsilon + 2}{2\epsilon^2(1-2\epsilon)}\frac{\Gamma(1+\epsilon)\Gamma^2(1-\epsilon)}{\Gamma(1-2\epsilon)}
\tag{2.85}
$$

where we replaced $e^2 = 4\pi\alpha$. This means that we can write the complete amplitude, up to one-loop order, as

$$
A_3 = A_3^{(0)} + A_3^{(1)} + \mathcal{O}(\alpha^2)
$$
$$
\approx A_3^{(0)}\left(1 - \frac{\alpha}{2\pi}\left(-\frac{s_0}{4\pi}\right)^{-\epsilon} \frac{2\epsilon^2 - \epsilon + 2}{2\epsilon^2(1-2\epsilon)}\frac{\Gamma(1+\epsilon)\Gamma^2(1-\epsilon)}{\Gamma(1-2\epsilon)}\right)
\tag{2.86}
$$

When we square this quantity, we will keep contributions only to next-to-leading order in α. That means that we will throw away the square of the loop amplitude, and only keep the interference term between the tree and loop amplitudes. This means that, for our calculation, we take

$$
|A_3|^2 = |A_3^{(0)}|^2\left(1 - \frac{\alpha}{\pi}\left(-\frac{s_0}{4\pi}\right)^{-\epsilon} \frac{2\epsilon^2 - \epsilon + 2}{2\epsilon^2(1-2\epsilon)}\frac{\Gamma(1+\epsilon)\Gamma^2(1-\epsilon)}{\Gamma(1-2\epsilon)}\right)
$$
$$
+ \mathcal{O}(\alpha^2)
\tag{2.87}
$$

We would like to expand this around $\epsilon = 0$. In order to get rid of innocuous factors of Euler's constant γ, we multiply and divide by $e^{\epsilon\gamma}$. Restoring the renormalization scale μ to obtain a result with consistent units, we obtain
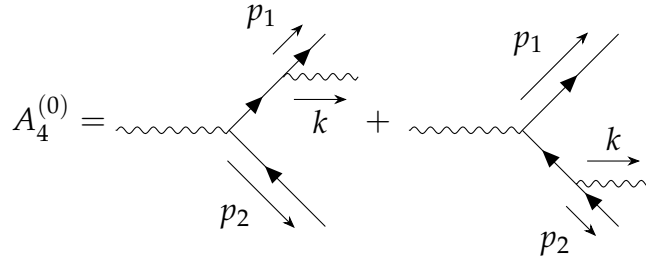
FIGURE 2.4: Real emission diagrams for the $\gamma^* \to e^+e^-$ process

$$|A_3|^2 = |A_3^{(0)}|^2 \left(1 - \frac{\alpha}{\pi} S_\epsilon \left(\frac{s_0}{\mu^2} \right)^{-\epsilon} \left(\frac{1}{\epsilon^2} + \frac{3}{2\epsilon} + 4 - \frac{\pi^2}{12} \right) + \mathcal{O}(\epsilon) \right), \quad (2.88)$$

where we define $S_\epsilon = (4\pi)^\epsilon e^{-\epsilon\gamma}$. Having this expansion, we clearly see that the integral is singular when $\epsilon \to 0$. Hence, we expect that the poles in ϵ will be cancelled by the corresponding real corrections. Without any further ado, we go on to tackle this calculation.

The corresponding diagrams, with the momenta of the final-state lines, are shown in Fig. 2.4. The expression for the amplitude is then

$$
\begin{aligned}
A_4^{(0)} &= \bar{u}(p_1)(-ie\gamma^\alpha) \frac{i(\not{p}_1 + \not{k})}{(p_1 + k)^2}(-ie\gamma^\mu)v(p_2)\epsilon_\alpha^*(k)\epsilon_\mu(q) \\
&+ \bar{u}(p_1)(-ie\gamma^\mu)\frac{i(-\not{p}_2 - \not{k})}{(-k - p_2)^2}(-ie\gamma^\alpha)v(p_2)\epsilon_\alpha^*(k)\epsilon_\mu(q) \\
&= -ie^2\bar{u}(p_1)\frac{\gamma^\alpha(\not{p}_1 + \not{k})\gamma^\mu}{(p_1 + k)^2}v(p_2)\epsilon_\alpha^*(k)\epsilon_\mu(q) \qquad (2.89) \\
&+ ie^2\bar{u}(p_1)\frac{\gamma^\mu(\not{p}_2 + \not{k})\gamma^\alpha}{(p_2 + k)^2}v(p_2)\epsilon_\alpha^*(k)\epsilon_\mu(q) \\
&= -ie^2\epsilon_\alpha^*\epsilon_\mu\bar{u}(p_1)\left[\frac{\gamma^\alpha(\not{p}_1 + \not{k})\gamma^\mu}{(p_1 + k)^2} - \frac{\gamma^\mu(\not{p}_2 + \not{k})\gamma^\alpha}{(p_2 + k)^2} \right]v(p_2)
\end{aligned}
$$

Before squaring to obtain the contribution to the cross-section, we can simplify this expression a bit. First, we notice that

$$
\begin{aligned}
\bar{u}(p_1)\gamma^\alpha\not{p}_1 &= \bar{u}(p_1)\left(2p_1^\alpha - \not{p}_1\gamma^\alpha \right) \\
&= \bar{u}(p_1)2p_1^\alpha
\end{aligned} \qquad (2.90)
$$

where we used the anticommutator of the Dirac matrices on the first line and then the Dirac equation on the second line. Similarly,

$$\not{p}_2\gamma^\alpha v(p_2) = 2p_2^\alpha v(p_2). \qquad (2.91)$$

These relations, along with the fact that the external momenta are massless, allow us to write

$$
A_4^{(0)} = -ie^2 \epsilon_\alpha^*(k)\epsilon_\mu(q)\bar{u}(p_1) \left[\frac{2p_1^\alpha \gamma^\mu + \gamma^\alpha \slashed{k}\gamma^\mu}{2p_1 \cdot k} - \frac{2p_2^\alpha \gamma^\mu + \gamma^\mu \slashed{k}\gamma^\alpha}{2p_2 \cdot k} \right] v(p_2)
\tag{2.92}
$$

Now, we proceed similarly as with the three-point tree amplitude, by computing the square of the amplitude and summing over spins. In this case there are two polarization vectors which will yield two metric tensors, and we find

$$
\sum_{spins} |A_4^{(0)}|^2 = e^4 Tr \left[\slashed{p}_1 \left(\frac{2p_1^\alpha \gamma^\mu + \gamma^\alpha \slashed{k}\gamma^\mu}{2p_1 \cdot k} - \frac{2p_2^\alpha \gamma^\mu + \gamma^\mu \slashed{k}\gamma^\alpha}{2p_2 \cdot k} \right) \right.
$$
$$
\left. \slashed{p}_2 \left(\frac{2p_{1\alpha}\gamma_\mu + \gamma_\mu \slashed{k}\gamma_\alpha}{2p_1 \cdot k} - \frac{2p_{2\alpha}\gamma_\mu + \gamma_\alpha \slashed{k}\gamma_\mu}{2p_2 \cdot k} \right) \right].
\tag{2.93}
$$

Expanding the product inside the trace we obtain four different contributions, that we can distinguish by the structure of their appropriate denominators. Two of them have a denominator of the form $(2p_1 \cdot k)(2p_2 \cdot k)$, while the remaining two are of the form $(2p_1 \cdot k)^2$ and $(2p_2 \cdot k)^2$. The calculation of these traces is performed in Appendix B. The result for the amplitude squared is given by

$$
\sum_{spins} |A_4^{(0)}|^2 = e^4 \left[\frac{32(1-\epsilon)^2(p_1 \cdot k)(p_2 \cdot k)}{(2p_1 \cdot k)^2} + \frac{32(1-\epsilon)^2(p_1 \cdot k)(p_2 \cdot k)}{(2p_2 \cdot k)^2} \right.
$$
$$
\left. + \frac{64(1-\epsilon)(p_1 \cdot p_2)(p_1 \cdot p_2 + p_1 \cdot k + p_2 \cdot k) - 64\epsilon(1-\epsilon)(p_1 \cdot k)(p_2 \cdot k)}{(2k \cdot p_1)(2k \cdot p_2)} \right]
\tag{2.94}
$$

This result can be further simplified. First, let

$$
s = q^2 = (p_1 + p_2 + k)^2
\tag{2.95}
$$

be the center-of-mass energy squared of the collision process. Next, define

$$
x_1 = \frac{2p_1 \cdot q}{q^2} = \frac{2p_1 \cdot k + 2p_1 \cdot p_2}{s},
$$
$$
x_2 = \frac{2p_2 \cdot q}{q^2} = \frac{2p_2 \cdot k + 2p_1 \cdot p_2}{s},
\tag{2.96}
$$
$$
x_3 = \frac{2k \cdot q}{q^2} = \frac{2p_1 \cdot k + 2p_2 \cdot k}{s},
$$

which can be interpreted as the ratio of each particles energy to the total energy of the process. These variables satisfy the relation $x_1 + x_2 + x_3 = 2$. Solving for the kinematic invariants, we obtain

$$
\begin{aligned}
2p_1 \cdot k &= s(1 - x_2), \\
2p_2 \cdot k &= s(1 - x_1), \\
2p_1 \cdot p_2 &= s(1 - x_3).
\end{aligned}
\tag{2.97}
$$

Replacing $e^2 = 4\pi\alpha$, the squared amplitude can be written in terms of x_1 and x_2 as

$$
\begin{aligned}
\sum_{spins} |A_4^{(0)}|^2 = 128\pi^2\alpha^2(1-\epsilon) \Bigg[(1-\epsilon) \left(\frac{1-x_1}{1-x_2} + \frac{1-x_2}{1-x_1} \right) \\
- \frac{2(x_1 + x_2 - 1)}{(1-x_1)(1-x_2)} - 2\epsilon \Bigg].
\end{aligned}
\tag{2.98}
$$

Let us perform a further change of variables, namely $y_i = 1 - x_i$, for $i = 1, 2, 3$. These variables satisfy $y_1 + y_2 + y_3 = 1$, and

$$
\begin{aligned}
\sum_{spins} |A_4^{(0)}|^2 = 128\pi^2\alpha^2(1-\epsilon) \Bigg[(1-\epsilon) \left(\frac{y_1}{y_2} + \frac{y_2}{y_1} \right) \\
- \frac{2}{y_1 y_2} + \frac{2}{y_1} + \frac{2}{y_2} - 2\epsilon \Bigg].
\end{aligned}
\tag{2.99}
$$

We can factorize the squared three-point tree amplitude from this quantity, obtaining

$$
\begin{aligned}
\sum_{spins} |A_4^{(0)}|^2 = 8\pi\alpha \sum |A_3^{(0)}|^2 \Bigg[(1-\epsilon) \left(\frac{y_1}{y_2} + \frac{y_2}{y_1} \right) \\
- \frac{2}{y_1 y_2} + \frac{2}{y_1} + \frac{2}{y_2} - 2\epsilon \Bigg].
\end{aligned}
\tag{2.100}
$$

In terms of the variables y_i, the three-particle phase-space $d\phi_3$ can be factorized as

$$
d\phi_3 = d\phi_2 d\tilde{\phi}
\tag{2.101}
$$

where $d\phi_2$ is the two-particle phase space measure, and

$$
d\tilde{\phi} = \frac{(4\pi)^{\epsilon-2}}{\Gamma(1-\epsilon)} s^{1-\epsilon} d^3 x \delta(1 - y_1 - y_2 - y_3)(y_1 y_2 y_3)^{-\epsilon}
\tag{2.102}
$$

Hence, one only needs to integrate the squared amplitude against $d\tilde{\phi}$. We must compute

$$I = \int d^3 y \delta(1 - y_1 - y_2 - y_3)(y_1 y_2 y_3)^{-\epsilon} \left[\frac{2}{y_1 y_2} - \frac{2}{y_1} - \frac{2}{y_2} \right.$$
$$\left. + (1 - \epsilon)\left(\frac{y_1}{y_2} + \frac{y_2}{y_1} \right) - 2\epsilon \right] \tag{2.103}$$

Before performing any integration with the delta function, we notice that the integrand is invariant under $y_1 \to y_2$. Therefore, we can simplify the integral to

$$I = \int d^3 y \delta(1 - y_1 - y_2 - y_3)(y_1 y_2 y_3)^{-\epsilon} \left[\frac{2}{y_1 y_2} - \frac{4}{y_1} + (1 - \epsilon)\frac{2y_1}{y_2} - 2\epsilon \right] \tag{2.104}$$

Each of these integrals can be evaluated separately with the help of Mathematica. The final result, with the appropriate prefactor of $(4\pi)^{\epsilon-2}/\Gamma(1 - \epsilon)$ simplifies to

$$I = \frac{2^{2\epsilon-3}\pi^{\epsilon-2}(1 - 2\epsilon)(\epsilon^2 - 2\epsilon + 2)\Gamma^2(-\epsilon)}{\Gamma(3 - 3\epsilon)}. \tag{2.105}$$

Multiplying by the customary factor $e^{-\epsilon\gamma}$ and expanding the result around $\epsilon = 0$ yields

$$\int d\phi_3 \sum_{spins} |A_4^{(0)}|^2 = \frac{\alpha}{\pi} \left(\frac{1}{\epsilon^2} + \frac{3}{2\epsilon} + \frac{19}{4} - \frac{7}{12}\pi^2 \right)$$
$$\times \left(\frac{s_0}{\mu^2} \right)^{-\epsilon} S_\epsilon \int d\phi_2 |A_3^{(0)}|^2, \tag{2.106}$$

where we restored the appropriate units by introducing the factor $(s_0/\mu^2)^{-\epsilon}$. Integrating Eq.(2.88) over the two-particle phase space and adding both results, we can see that the poles in ϵ cancel exactly against each other, leading to our desired result. An exploration of the IR structure of the related process $e^+e^- \to 3$ jets is presented in [82].

Having done an overview of renormalization and explicitly shown in an example how the cancellation of IR divergences between virtual and real corrections goes through in an infrared-safe process, we have introduced all the fundamental concepts of QFT necessary for the calculation of scattering amplitudes. Our next task, which is the organization of the different kind of Feynman diagrams that may appear in a general L-loop computation, is the topic of the next chapter.

Chapter 3

Tree and Loop Feynman Graphs

The perturbative expansion of an amplitude in QFT, as discussed in Chapter 2, can be organized in terms of Feynman diagrams, with higher-order contributions being represented by diagrams with a higher amount of loops. Any graph with closed loops can be associated to a set of tree graphs through the concept of a spanning tree or a cut graph, which represent all the possible ways to open up a loop diagram into fully connected trees. In terms of Feynman integrals, this implies that it is possible to rewrite the integrand of an amplitude in such a way that it has a tree-like structure. Moreover, not every possible loop diagram gives a direct contribution to the amplitude at a given order in perturbation theory.

In this chapter, we will give a systematic classification of the different type of Feynman graphs that can contribute to a scattering amplitudes at all orders in perturbation theory. We will see how some of these give vanishing contributions or are removed after renormalization. A general notation which includes counterterm diagrams will be provided and the relation between a linear combination of loop diagrams weighted with symmetry factor and a sum of tree diagrams will be derived. Although the relations studied in this chapter are purely diagrammatic in nature, they set the ground for the possibility to write integrands of L-loop amplitudes which are given only in terms of tree-like objects.
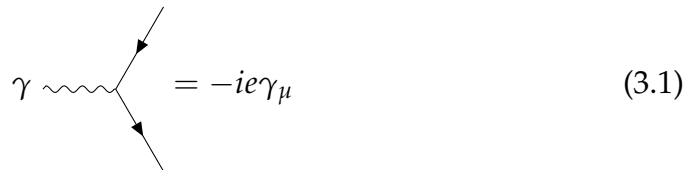
3.1   Connected Graphs

As a starting point, we want to look at the elements that define a Feynman graph[1]. In general, a graph is a set of vertices together with a set of edges, which are lines connecting some of the vertices according to some prescribed rules.

In the case of a Feynman graph, it is important to distinguish between internal and external edges: an internal edge corresponds to a propagator, while an external edge corresponds to an external particle. In a general

---

[1]Feynman diagrams are an example of the mathematical objects studied by graph theory, which is a branch of discrete mathematics. Although we will use some of the concepts of graph theory, a thorough exposition of these can be found in [84]

graph, there is an external vertex at the end of each external line. For a Feynman graph, the external vertices are not associated to the value of any physical quantity, so it is common practice to omit them. The internal vertices, however, are related to the interactions terms of the Lagrangian and contribute powers of the coupling of the theory. Finally, the set of rules which tells us how to connect the different vertices and edges of a Feynman graph are the Feynman rules of the specific field theory. Thus, a Feynman graph can be characterized by the number of external lines (and the particles associated to these lines), n, the number of internal vertices (which we will simply call vertices), V, and the rules to put them together to compute their values.

One can further characterize a vertex by its valency, which is the number of edges that join at a given vertex. For example, a vertex of valency 3 would be a vertex where three edges meet; these are the most typical kind of vertices we encounter in Quantum Field Theory. In the QED Lagrangian of Eq. (2.8), the interaction term $\overline{\Psi} A_\mu \Psi$ is represented by the vertex

$$\gamma \sim\sim\sim\!\!\!< \quad = -ie\gamma_\mu \tag{3.1}$$

where the electromagnetic field A_μ is connected to the fermion and antifermion fields Ψ and $\overline{\Psi}$. The resulting expression carries a power of the coupling, which in this case is the electric charge e. A particular feature of the Standard Model is that there are no vertices with valency greater than four.

Another important property of graphs in the context of Feynman diagrams is that of connectivity. An edge or a vertex is said to be a connected component of a graph if it can be reached from another element of the graph by following a continuous path throughout the graph. If there is no such continuous path between two elements of the graph, such elements are said to be disconnected.

Figure 3.1 show two different graphs with four external edges. The graph on the left has all the edges connected to a single vertex and is a connected graph. The graph on the right, however, is composed of two disconnected edges that connect two pairs of external edges; in this case, we say that the graph has two connected components.

The most general graph is then made up of k connected components, n external edges and V vertices. Using these quantities, one can define the first Betti number or the cyclotomic number of the graph [83]

$$L = n - V + k \tag{3.2}$$

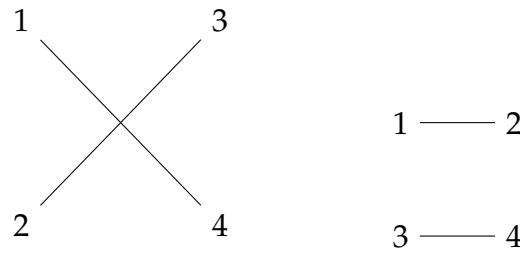which, in the physics literature, is what we refer as the number of loops.

FIGURE 3.1: The left figure shows a connected graph with a single vertex of valency 4. The left diagram shows a graph with two disconnected lines.
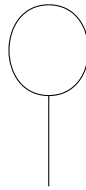

FIGURE 3.2: One-loop tadpole diagram in a generic theory with a cubic coupling.

Given this relation, instead of describing a graph by its number of vertices, one can use the number of loops. This is the approach usually found in the Quantum Field Theory literature, since the perturbative expansion of the S-matrix organizes itself in diagrams with an increasing number of loops. A particular property of the S-matrix is that only fully connected diagrams contribute to the scattering amplitudes at any given perturbative order [20]. Therefore, our focus will be centered around these kind of diagrams. This also implies that vacuum diagrams do not contribute to the S-matrix, since they would always be disconnected from the components which contain the external particles.

As we discussed previously, diagrams containing loops are often divergent due to the integration over the loop momenta. There are, however, diagrams that contain further possible singularities: diagrams with a tadpole insertion, which introduce a propagator with momentum zero, and diagrams with a self-energy insertion on an external leg, which are divided through by an on-shell propagator. We will digress into the role of these two types of diagrams on the calculation of scattering amplitudes before we discuss the general classification of all loop diagrams that typically appear in the perturbative computation of the S-matrix.

3.1.1 Tadpole Diagrams

Tadpoles are a type of loop diagrams with the property that only one external leg is attached to them, which can be itself attached to another part of a bigger diagram. These diagrams contribute to the one-point correlation function, thus giving quantum corrections to the classical vacuum-expectation value
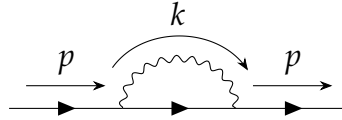
FIGURE 3.3: One-loop self-energy correction to the fermion propagator in QED

of the fields. We will see later that, after renormalization, these diagrams are non-vanishing only if one deals with massive scalar fields.

A typical example of a tadpole diagram is shown in Fig.3.2. We can see that if we were to attach this tadpole to another diagram, the line attached to the tadpole would then become an internal propagator. Because of momentum conservation, this propagator would have momentum zero. In the case of a massless field, since the propagator is proportional to $1/p^2$, we would divide the whole diagram by zero, which means that any such diagram diverges and thus is ill-defined.

The expression for the Feynman integral associated to the one-loop tadpole was derived in Eq.(2.35) within dimensional regularization and its Laurent expansion around $D = 4$ was given in Eq. (2.37). We saw that the only scale upon which the integral could depend was the mass of the particle propagating in the loop. A massless tadpole integral in arbitrary space-time dimension would be an integral of the form

$$T_1^{(1)}(b,0) = \int \frac{d^D k}{(2\pi)^D} \frac{1}{(k^2)^b}. \tag{3.3}$$

A general property of dimensional regularization [85] is that Eq.(3.3) vanishes for any value of $b \neq -\frac{D}{2}$. For this reason, tadpole diagrams are usually excluded from the calculation of scattering amplitudes in theories were the fields have a vacuum expectation value equal to zero. If this is not the case, the particle that attaches the tadpole to the rest of the diagram contributes a massive, zero momentum propagator, which then multiplies the rest of the diagram by a factor of $1/m$, where m is the mass of the propagating particle. In this case, moreover, the tadpole integral does not vanish and requires any associated source term[2] to be renormalized in order to deal with its UV divergences.

3.1.2 Self-Energy Diagrams

Self-Energy diagrams are, in general, the quantum corrections to two-point correlation functions. This means that the loop-level corrections to the tree-level propagators are obtained by evaluating self-energy diagrams. A typical example of a one-loop self-energy contribution to the fermion propagator in QED is shown in Fig.3.3. From the structure of this diagram, it can be

---

[2]A source is any term in the Lagrangian which is linear in a single field.

seen that in any kind of diagram with a self-energy insertion on an external leg, the propagator that connects the self-energy attachment to the rest of the diagram will have the same momentum as the on-shell external particle. This means that we would have a contribution of the form

$$\frac{1}{p^2 - m^2}\bigg|_{p^2=m^2} \to \infty \tag{3.4}$$

making any diagram with such an insertion divergent.

The resolution to this problem is found through the use of the Lehmann-Symanzik-Zimmermann (LSZ) reduction formula [86], which instructs us to compute S-matrix elements by first calculating the n-point (off-shell) correlation function, Fourier transforming into momentum space and then looking at its behaviour close to the region where the momenta go on-shell. Then, the S-matrix element will be proportional to the coefficient of the multiple pole of the correlation function.

In terms of Feynman diagrams, this means that we do not include diagrams with self-energy corrections attached to external legs in the computation of scattering amplitudes. This does not mean, however, that the self-energy diagrams do not play a role in the calculation of higher order contributions.

For example, in a scalar theory, the bare and renormalized amplitudes $\mathcal{A}_n^{bare}$ and $\mathcal{A}_n^{ren}$ are related to each other, at every order in perturbation theory, by

$$\mathcal{A}_n^{ren}(\{p\}, g, m) = (Z_\phi^{1/2})^n \mathcal{A}_n^{bare}(\{p\}, g_b, m_b), \tag{3.5}$$

where the renormalized amplitude depends on the momenta

$$\{p\} = \{p_1, ..., p_n\}, \tag{3.6}$$

the renormalized coupling g and the renormalized mass m, while the bare amplitude depends on the bare parameters, which are related to the renormalized parameters of the theory through renormalization constants, similar to those defined in the case of QED in Eq.(2.45). Here, the factor $Z_\phi^{1/2}$ relate the bare scalar field ϕ_b and the renormalized field ϕ as

$$\phi_b = Z_\phi^{1/2}\phi, \tag{3.7}$$

in the same way that Z_2 relates the bare and renormalized fermionic fields Ψ in QED. The higher-order corrections to $Z_\phi = 1 + \delta_{Z_\phi}$ are then computed by evaluating the self-energy and counterterm diagrams to the desired order and then apply the renormalization conditions to determine the value of the counterterms. An example of the computation of a wave-function renormalization at one-loop order in QED is given in Appendix C.
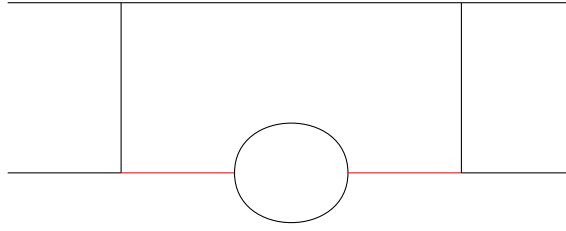
FIGURE 3.4: Two-loop diagram with a self-energy insertion on
an internal propagator. The diagram contains a squared propa-
gator, coming from the two red lines.

A different situation occurs when we consider a diagram with a self-
energy insertion on an internal edge. We illustrate one such diagram in
Fig.3.4. As a consequence of momentum conservation on the two vertices
connecting the red propagators with the self-energy insertion, these two will
have the same momenta, and then the complete diagram will have a propa-
gator raised to a power greater than one. These diagrams, as opposed to the
insertions on external legs, do contribute to the scattering amplitude and we
make a distinction between both kinds of graphs.

3.1.3 General Organization of Loop Graphs

Having found the solution to the problems that arise when dealing with tad-
pole and self-energy insertions, we can start organizing the loop graphs that
appear in the calculation of a scattering amplitude. To begin with, let

$$U_{L,n} \tag{3.8}$$

denote the set of all graphs, including tadpoles and any kind of self-
energy insertion, with n external edges and L loops. This means that, if the
theory has a single coupling g, the resulting integral will be multiplied by a
factor of g^{2l+n-2}. Since we are interested in the diagrams that contribute to
the scattering amplitudes, we will denote by

$$U_{L,n}^{S} \tag{3.9}$$

the set of all diagrams in $U_{L,n}$ without tadpoles or self-energy insertions
on external legs. Diagrams such as the one in Fig.3.4 are included in $U_{L,n}^{S}$.
Now, we assume that counterterm diagrams have integral representations
with the structure of the associated loop diagrams whose divergences they
cancel; for example, it is possible to write a counterterm to a propagator as a
two-point function, such that the integrand obtained by adding both the bare
and counterterm diagrams is free of UV divergences. The fact that this is pos-
sible has been shown in [87]. This allows us to treat counterterm diagrams as
elements of $U_{L,n}$ or $U_{L,n}^{S}$, instead of treating the bare and counterterm contri-
butions differently. Thus, we need to further define two sets: first,
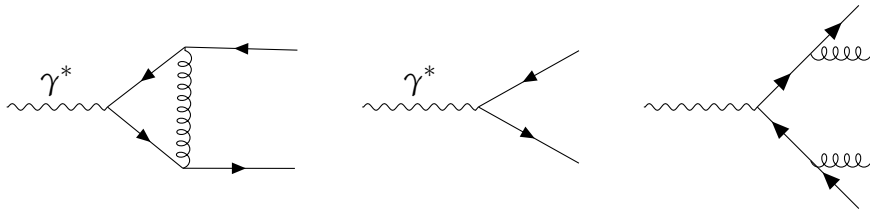
$$U_{L,n}^{CT} \tag{3.10}$$

FIGURE 3.5: The graph on the left correspond to a one-loop correction to the process $\gamma^* \to q\bar{q}$. The graph on the center is the spanning tree obtained by removing the internal gluon line, while the third graph denotes the cut graph obtained by cutting open the gluon propagator

which is the set of all counterterm diagrams with L loops and n external edges, and

$$U_{L,n}^{S,CT} \tag{3.11}$$

which is the restriction of $U_{L,n}^{CT}$ to the counterterm diagrams that contribute to the scattering amplitude.

3.2 Relations Between Loop and Tree Graphs

In the language of graph theory, any graph with closed loops can be associated to a set of tree graphs through the concept of a spanning tree: for any graph $\Gamma \in U_{L,n}$, we let $E_\Gamma = \{e_1, e_2, ..., e_N\}$ denote the set of its internal edges. A spanning tree is a sub-graph of Γ which contains all of its vertices and is a connected tree graph. Such a graph, which we denote by $T_{sp} \in U_{0,n}$, can be obtained by deleting L of the N internal edges of Γ. There are, in general, many ways to obtain a spanning tree from a single loop graph Γ. We can specify the deleted edges by a set $\{e_{\sigma_1}, ..., e_{\sigma_L}\}$, and let $\sigma = \{\sigma_1, ..., \sigma_L\}$ denote the set of indices of the deleted edges.

Every spanning tree T_{sp} of the graph Γ is in one-to-one correspondence with a cut graph T_{cut}, which is obtained from Γ by taking each of the edges deleted to form the spanning tree and cutting them open so that they become a pair of external edges of a new tree graph, which we call a cut graph. In contrast to spanning trees, cut graphs belong to the set $U_{0,n+2L}$. These will be of special interest to us, because cutting a single line of a loop graph translates directly to the computation of a residue of the integrand associated to it via the Feynman rules. In what follows, we will denote by $\mathcal{T}_\Gamma$ the set of spanning trees of the graph Γ and $\mathcal{C}_\Gamma$ the set of all set of indices of the edges of Γ that can be deleted or cut to obtain a spanning tree or a cut graph, respectively.

Let us illustrate the difference between a spanning tree and a cut graph and why the concept of a cut graph is more useful to us, using the example

of the NLO corrections to $\gamma^* \to q\bar{q}$.

In Fig.3.5, we can see the one-loop graph coming from the QCD vertex correction, alongside two different tree graphs. In the first case, the gluon line is removed, leaving the tree level photon-quark-antiquark vertex. The last graph shows a tree graph with five external particles, obtained by cutting open the gluon propagator. This diagram is not associated in any way to the real corrections we saw in Fig.2.3, but as we will see, its structure matches exactly with the residue of the one-loop integral associated to the triangle diagram when the gluon propagator goes on-shell. This is a first hint at the relation between cut tree graphs and loop graphs at the level of the Feynman integrals and not only at a purely graph-theoretical level.

Conversely, any connected tree graph can be associated to a loop graph through the use of the operation of sewing [2].

To see how sewing works, we begin by considering a graph $\Gamma \in U_{L-1,n+2}$ such that each of its external edges is labelled by a set of momenta

$$\{p_1, ..., p_n, k_1, \bar{k}_1\}. \tag{3.12}$$

We then say that we sew the edges with momenta k_1 and $\bar{k}_1$ if we take both edges and put them together to form a new internal line. The result is an L-loop graph that has n external edges labelled by the momenta p_i[3].

In general, if we start from a tree graph $\Gamma_{tree} \in U_{0,n+2L}$, we can pick L pairs of external edges labelled by momenta of the form $\{k_1, \bar{k}_1, ..., k_L, \bar{k}_L$ and sew them together to obtain a graph $\Gamma_{L-loop} \in U_{L,n}$. In this sense, sewing and cutting are inverse operations of each other. Similarly to the way in which the cut graph corresponds to taking a residue of a Feynman integral when one of its propagators goes on-shell, we would like to know what it means, in terms of Feynman integrals, to sew two external edges of a graph.

The first thing to notice is that sewing only makes sense in the context of Feynman integrals if, for every pair of sewed external lines, $\bar{k}_i = -k_i$. This is because each internal propagator of a Feynman integral has a unique momenta flowing through it, up to redefinitions of the loop momenta. If we let k denote the momenta flowing through an internal edge and we cut it open, the resulting external edges can only be assigned the momentum k evaluated on its mass shell. The direction of the original momentum flow will then translate to one of the cut edges having outgoing momentum k and the other having outgoing momentum $-k$. This implies that, when we try to sew two edges together in order to invert the process of cutting, the selected edges must have equal and opposite momenta. This means that graphs that can be

---

[3]Notice that this is a purely graphical statement and is independent of the quantities used to label the graphs; that is, there is no need at this point to refer to the momenta, but it will prove useful to use this labelling.

sewed have the structure of a forward limit.

In theories with spin, the external particles of a Feynman graph are dressed with their respective wave-functions; fermions are associated with spinors $u(k)$ or $\overline{u}(k)$, anti-fermions with spinors $v(k)$ or $\overline{v}(k)$, while gauge bosons come with polarization vectors $\epsilon^\mu(k)$ and their complex conjugates. When we sew a pair of external lines associated with particles with spin, we must perform a sum over the physical and unphysical polarizations of these particles. In the case of a pair of fermions, this means that the spinors are replaced as

$$\sum_s u^s(k)\overline{u}^s(k) = \slashed{k} + m, \quad \sum_s v^s(k)\overline{v}^s(k) = \slashed{k} - m \qquad (3.13)$$

which is just the completeness relation for Dirac spinors. These are the usual numerators of the fermion propagators. In this sense, the additional summing procedure allows for the sewing operation to introduce the correct propagator into the resulting diagram. In addition to this, one must include a factor of (-1) whenever a fermion line is sewed, independent of whether the resulting loop is a fermion loop or not. While this statement makes sense in the case of fermion loops, which always include a factor of (-1) due to the anticommuting nature of the fermion fields, the necessity of this factor is not so evident when one obtains different kinds of loops after sewing[4].

Diagrams with fermions running in non-fermion loops do not have the prefactor of (-1), which implies that there must be a mechanism to cancel out this minus sign in the sewing procedure in order to obtain results consistent with the standard Feynman rules. The resolution to this problem is found by looking at amplitudes with identical fermion-antifermion pairs. Such amplitudes can, in general, be written as a linear combination of amplitudes where all fermion-antifermion pairs have different flavours.

An example of a process with scattering of fermions of different flavours in QED is the annihilation of an electron-positron pair into a muon-antimuon pair. At tree level, there is only a single diagram that contributes to this process

Similarly, at leading order, the amplitude for the process $e^-\mu^- \to e^-\mu^-$ can be calculated from the single diagram

---

[4]An example of a non-fermion loop that includes a fermion line is a graph like the one in Fig.3.3. Such a diagram could be obtained by sewing two external electron edges of a graph contributing to a $e^+e^- \to e^+e^-$ process at tree level.
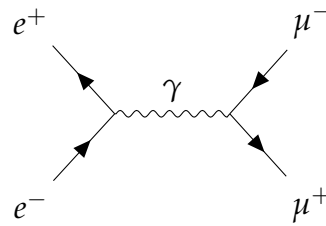
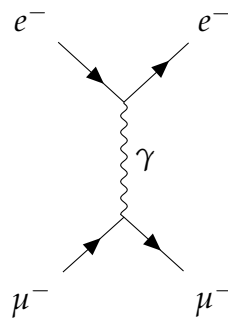FIGURE 3.6: Tree-level contribution to the amplitude $A_4(e^+e^- \to \mu^+\mu^-)$

FIGURE 3.7: Tree-level contribution to the amplitude $A_4(e^-\mu^- \to e^-\mu^-)$

Note that, in either of these diagrams, the only sewing procedures that make sense are between particles of the same flavour. In both cases, the resulting diagram is a tadpole insertion into the electron or muon propagator, which by virtue of having a fermion loop include a minus sign. Now, in the case of electron-positron scattering, the tree-level amplitude receives contributions from two different diagrams, namely
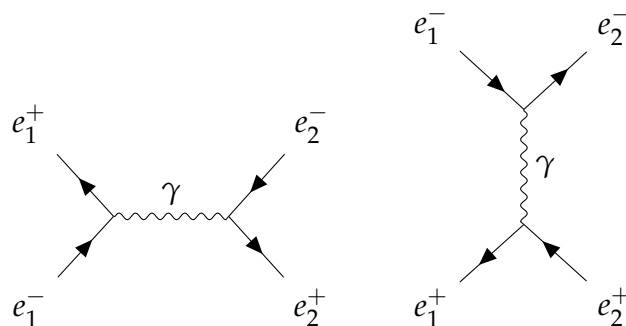

FIGURE 3.8: Contributions to electron-positron scattering at leading order in QED. The tree-level amplitude is given by the difference between the diagram on the left and the diagram on the right.

The diagrams on the left and right of Fig.3.8 can be related to the diagram

for the processes $e^+e^- \to \mu^+\mu^-$ and $e^-\mu^- \to e^-\mu^-$, respectively, by substitution of the muon mass with the electron mass. In this sense, one can obtain the amplitude $A_4(e^+e^- \to e^+e^-)$ as a combination of two amplitudes with fermions of different flavours. Now, this amplitude is given by the difference between the two diagrams in Fig.3.8, with the relative minus sign between the two contributions being a consequence of Fermi statistics. Now, when we try to sew, for example, e_1^- with e_1^+, we get two different kinds of contributions: from the diagram on the left, we get a tadpole insertion into the $e_2^- e_2^+$ edge. On the other hand, sewing these two edges on the diagram on the right leads to a self-energy insertion into the remaining electron edge. The minus sign coming from the sewing procedure will then multiply the minus sign in front of the tree diagram, resulting in the correct sign for this contribution to the electron two-point function at one-loop. The same behaviour occurs with general graphs, were a pair of fermion-antifermion lines are sewn together.

In the case of massless gauge bosons, such as photons or gluons, we have

$$\sum_s \left(\epsilon_\mu^s(k, n) \right)^* \epsilon_\nu^s(k, n) = -g_{\mu\nu} + \frac{k_\mu n_\nu + k_\nu n_\mu}{k \cdot n}, \tag{3.14}$$

where n is a reference vector. As in the fermion case, we would like to use this relation to restore the numerator of the boson propagator. These propagators, however, are gauge-dependent. In particular, in Feynman gauge, the numerator of the gauge boson propagator is given simply by (-1) times the metric tensor. Using the completeness relation for $g_{\mu\nu}$, we can write

$$-g_{\mu\nu} = \sum_s \left(\epsilon_\mu^s(k, n) \right)^* \epsilon_\nu^s(k, n) - \frac{k_\mu n_\nu + k_\nu n_\mu}{k \cdot n} \tag{3.15}$$

the gauge dependence of the propagator is reflected on the fact that one cannot write the metric tensor in terms of only physical polarizations, but rather also needs to include the terms that depend explicitly on the reference vector n. The contributions coming from these unphysical polarizations are cancelled by diagrams including Fadeev-Popov ghosts. Thus, we also need to consider tree diagrams with external ghosts and develop sewing rules for them. Since ghosts are anticommuting scalar particles, there is no need to introduce any external wave function. However, in analogy to the sewing of fermion edges, a factor of (-1) is included whenever a pair of ghost edges are sewn together.

So far, we have seen how to go from loop to tree graphs, and vice versa, at the level of individual loop graphs. On one hand, from an L-loop graph we can obtain various tree graphs by choosing a set of L internal edges and cutting then open into a pair of external edges. On the other hand, a tree graph can be turned into a loop graph by identifying pairs of external edges and sewing them together. In terms of Feynman integrals, these operations are related to the calculation of residues. We would like to see what happens when we try to relate the complete set of graphs that contribute to an arbitrary L-loop amplitude with n external edges to the set of graphs obtained

FIGURE 3.9: One-Loop contribution to the two-point function
in a theory with cubic interactions. Exchanging the internal
edges leads to an equivalent expression, leading to the appear-
ance of a symmetry factor.

by sewing all possible tree graphs with $n + 2L$ external edges into the graphs
that contribute to the L-loop amplitude. Our findings constitute the main re-
sult of this chapter: we will see how a sum over loop graphs, weighted with
their corresponding symmetry factors, can be replaced by a sum over a set of
sewed tree graphs.

3.3   Cancellation of Symmetry Factors

There is one aspect of loop integrals that we have ignored so far, but is crucial
for the correct calculation of a scattering amplitude: the presence of symme-
try factors. These are combinatorial factors associated to the fact that a given
loop graph might be invariant under the exchange of some of its internal
edges.

The need for symmetry factors can be seen already in the simple exam-
ple of the two-point function of Fig. 3.9. One might start by drawing the
diagram as the graph on the left, with the red propagator on the top and the
blue on the bottom. Equivalently, one could swap the position of these inter-
nal edges. The corresponding expression for the Feynman integral associated
to either of these diagrams is the same, so we must multiply by a factor of $\frac{1}{2}$
when adding it's contribution to a correlation function or a scattering ampli-
tude. The reciprocal of this number, $S = 2$, is known as the symmetry factor
of the diagram.

For higher-loop graphs, the computation of the symmetry factors becomes
an exercise in combinatorics. However, we know that, through the process
of cutting, one can identify an arbitrary loop graph with a set of tree graphs,
and since the external edges of these graphs always fix the position of the
internal edges, their symmetry factors are always trivial. Hence, we are in-
terested in seeing what happens with the symmetry factors of a set of loop
graphs if we cut them all open. In order to do this, we must first introduce
some additional notation which will allow our treatment of the problem to
be as general as possible. The arguments in this section closely follows [2].

Let us define a new set

$$U_{L,n}^{\otimes L} \tag{3.16}$$

called the set of *L*-marked, *L* loop graphs with *n* external edges. The elements of this set are the graphs $\Gamma \in U_{L,n}$ that can be obtained by marking a set of *L* internal edges of Γ, labelling them with the indices $\{1, 2, ..., L\}$ and an orientation of each of these edges, such that when cutting the marked edges, we obtain a connected tree graph $\Gamma_{cut} \in U_{0,n+2L}$. Two marked graphs are different if they are obtained by marking different edges of the same graph. Moreover, two marked graphs are also considered to be different if the order of the markings is different; that is, choosing the same set of internal edges, but labelling them with different indices, yields two different marked graphs. Finally, two marked graphs are different if the orientation of one or more of the marked internal edges is different.

We can characterize each graph of $U_{L,n}^{\otimes L}$ by identifying an ordered tuple of edges $\{e_{\sigma_1}, ..., e_{\sigma_L}\}$ such that cutting these edges results in a connected tree graph, together with a map $e_{\sigma_j} \to j$ that performs the marking of the selected internal edges, and an orientation of each of the lines, which means assigning each of the lines e_{σ_j} a pair of signs of the form $\{+, -\}$ or $\{-, +\}$. We define a projection map

$$\pi_f : U_{L,n}^{\otimes L} \to U_{L,n} \tag{3.17}$$

that takes a marked graph into its corresponding loop graph by getting rid of the marking of the internal edges. We can see a connection between marked graphs and spanning trees by noting that, for any graph $\Gamma \in U_{L,n}$, the number of spanning trees $|\mathcal{T}_\Gamma|$ is equal to the number of ways one can select a set of markings. This implies that there are

$$N_{marked} = 2^L L! |\mathcal{T}_\Gamma| \tag{3.18}$$

marked graphs that project to Γ under π_f, which is obtained from the number of spanning trees by multiplying by the number of possible ways to assign an orientation (2^L) and by all the possible ways to assign the labels $\{1, 2, ..., L\}$ to the selected edges ($L!$). We define also a set

$$U_{L,n}^{S,\otimes L} \tag{3.19}$$

which is the subset of $U_{L,n}^{\otimes L}$ which only contains diagrams that contribute to the scattering amplitude. At this point, its useful to introduce an "intermediate" set

$$U_{L,n}^{\otimes L, nh} \tag{3.20}$$

whose elements are obtained from those of $U_{L,n}^{\otimes L}$ by forgetting the information on the ordered tuple $\{e_{\sigma_1}, ..., e_{\sigma_L}\}$, but keeping both the marking and the orientation. The elements of $U_{L,n}^{\otimes L, nh}$ are then characterized by marking *L* internal edges and assigning an orientation to each of these edges. This

means that two graphs where the L marked edges are not the same, but where the orientation of both sets of L edges is equal, are considered to be the same element of $U_{L,n}^{\otimes L, nh}$. We can furthermore define projections

$$\pi_h : U_{L,n}^{\otimes L} \to U_{L,n}^{\otimes L, nh} \tag{3.21}$$

defined by dropping the information on the ordered tuple of edges, and

$$\pi_m : U_{L,n}^{\otimes L, nh} \to U_{L,n} \tag{3.22}$$

defined by getting rid of the marking and orientation of the internal edges. It is in this sense that $U_{L,n}^{\otimes L, nh}$ is an intermediate set between $U_{L,n}^{\otimes L}$ and $U_{L,n}$. These projections satisfy the relation

$$\pi_f = \pi_m \circ \pi_h. \tag{3.23}$$

Now, we can build a set of tree graphs by considering the set of momenta $\{P\} = \{p_1, ..., p_n, k_1, ..., k_L, \bar{k}_1, ..., \bar{k}_L\}$. Then, let

$$U_{0,n+2L}^{L-Sew} \tag{3.24}$$

be the set of all tree graphs with $(2n + L)$ external lines with momenta in $\{P\}$ where all the pairs $(k_i, \bar{k}_i)$ are sewn together for all $i \in \{1, 2, ..., L\}$. This results in graphs with n external edges and L loops. Assigning the momenta k_i and $\bar{k}_i$ to the sewn edges defines a marking and an orientation of the new internal edge, which we take to be from k_i to $\bar{k}_i$. With this properties in mind, we can define a bijection

$$B : U_{0,n+2L} \to U_{L,n}^{\otimes L, nh} \tag{3.25}$$

which sends the j-th sewed edge labelled by the momenta k_j to the orientation label $+$ and the j-th sewed edge labelled by the momenta $\bar{k}_j$ to the orientation label $-$.

Let F denote an arbitrary operator acting on a graph Γ. For example, we could let F be the operator that maps the graph its algebraic expression according to the Feynman rules. We want to show that

$$\sum_{\Gamma \in U_{L,n}^{\otimes L}} \frac{1}{S(\pi_f(\Gamma))} F(\pi_f(\Gamma)) = \sum_{\Gamma \in U_{0,n+2L}^{L-Sew}} F(B(\Gamma)) \tag{3.26}$$

where $S(\Gamma)$ denotes the symmetry factor of the graph. This relation allows to exchange a sum of marked loop graphs weighted by the symmetry factors associated to the unmarked graph with a sum over the corresponding cut graphs.

To prove this statement, first notice that we have established that there is bijection between the graphs in $U_{0,n+2L}^{L-sew}$ and $U_{L,n}^{\otimes L, nh}$. However, there might be several graphs in $U_{L,n}^{\otimes L}$ which project into the same graph in $U_{L,n}^{\otimes L, nh}$. What

we have to show is that the symmetry factor exactly compensates the over-counting when going form the marked graphs to the tree graphs.

Consider a graph $\Gamma \in U_{L,n}^{\otimes L}$. An automorphism on Γ is an isomorphism from the graph to itself; that is, it corresponds to a symmetry of the graph. Such a transformation permutes the edges and vertices of $\pi_f(\Gamma)$, leaving it invariant. If we let $Aut(\pi_f(\Gamma))$ denote the group of automorphisms of $\pi_f(\Gamma)$, we can see that the dimension of this group exactly corresponds to the symmetry factor of the graph $\pi_f(\Gamma)$, that is

$$S(\pi_f(\Gamma)) = |Aut(\pi_f(\Gamma))|. \tag{3.27}$$

Adopting this point of view will allow us to use concepts from group theory to prove Eq.(3.26).

Let $T \in Aut(\pi_f(\Gamma))$. T induces a transformation on each graph $\Gamma \in U_{L,n}^{\otimes L}$ by permutting the corresponding edges and vertices together with the markings and orientations of the original marked graph. This means that T induces a group action on the set of marked graphs. We denote such a group by G_T and an arbitrary transformation in this set by g_T. Now, let

$$G_T(\Gamma) = \{g_T(\Gamma)|g_T \in G_T\} \tag{3.28}$$

be the orbit of Γ under G_T, that is, all the graphs that can be obtained from the graph Γ by applying transformations from G_T. Since any transformation in G_T permutes the markings and orientations of Γ, but leave the same internal edges marked, all graphs in the orbit of Γ project to the same graph $\pi_h(\Gamma)$ in $U_{L,n}^{\otimes L,nh}$. On the other hand, a graph $\Gamma \in U_{L,n}^{\otimes L}$ corresponds, due to the markings, to a tree graph. Since tree graphs have no symmetry factors, their automorphism group is trivial. This means that the only transformation leaving the marked graphs invariants is the identity, implying that the group action G_T is free. Thus, $G_T(\Gamma)$ generates all graphs which project to $\pi_h(\Gamma)$ and the symmetry factor correctly compensates the over-counting.

Let us discuss some examples to make our argument a bit more clear. We begin by looking a the one-loop two point function. This graph has a symmetry factor $S = 2$. Any graph obtained by marking one of its internal edges will inherit this symmetry factor. The two marked graphs, which project to the one-loop bubble graph, are shown in Fig. 3.10.

From the perspective of the sewn graphs, the two marked bubbles are obtained from the same graph:

hence, the symmetry factor of 2 cancels the over-counting of the marked graphs.

More involved examples can be found at two loops and beyond. We consider the so-called sunrise diagram,
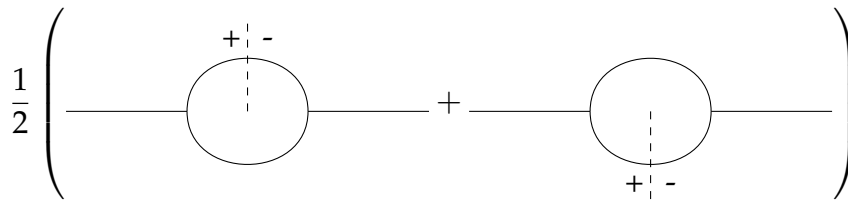
FIGURE 3.10: Possible markings of the one-loop bubble graph. These inherit the symmetry factor $S = 2$ from the original unmarked graph.
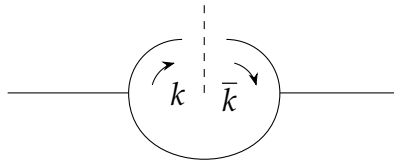

FIGURE 3.11: Cut graph obtained from the marked one-loop bubble.

which contributes to the NNLO corrections to the propagator. Notice that exchanging any two of the three propagators at a single vertex leaves the diagram invariant. Since there are 3! ways of doing this, the diagram has a symmetry factor of $S = 6$. Moreover, there are three ways of marking two out of the three propagators, and for each of these markings, there are two possible ways to assign the labels 1 or 2 to each of the marked edges. This means that there are six graphs in $U_{2,2}^{\otimes 2}$ which project to the sunrise graph.

An example of these graphs is given in Fig.3.13.The remaining five marked graphs are obtained by assigning the labels 1 and 2 to each possible way to pick two of the three internal edges. All of these six marked graphs project onto the same sewn graph of Fig. 3.14. As in the previous one-loop example, the symmetry factor cancels the over-counting of loop graphs which produce the same sewn graph, just as we expected from Eq.(3.26).

Having shown how to relate tree and loop graphs through the operations of cutting and sewing, we have seen that, at the level of graph theory, we can translate any problem involving loop graphs to the study of tree graphs. By looking at the particular kind of loop graphs contributing to the scattering amplitude at arbitrary loop order, we have been able to construct a compact notation to reference the different kinds of graphs we might encounter in a given calculation, and we have seen how the symmetry factors of loop graphs are cancelled by the different ways to open up a loop graph once we have given special labels to each of its internal edges. It is time to see how these relations between tree and loop graphs translates to Feynman integrals.
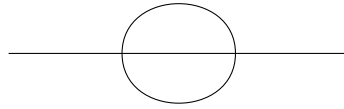
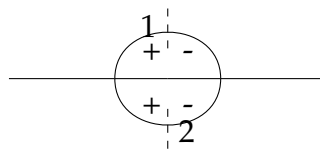FIGURE 3.12: Two-loop sunrise graph. This is an element of $U_{2,2}$.

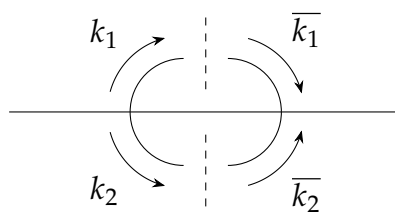FIGURE 3.13: One of the six possible marked graphs obtained from the two-loop sunrise.

FIGURE 3.14: Cut graph obtained from the marked two-loop sunrise graph.

Chapter 4

Loop-Tree Duality

Loop-Tree Duality, or LTD for short, is an approach to the calculation of Feynman integrals based on Cauchy's residue theorem. The main motivation behind this approach is the fact that the virtual corrections to a scattering amplitude at any fixed perturbative order are given as integrals over all the components of the momenta running through the loops, while the radiative corrections are calculated as phase-space integrals. Therefore, it becomes beneficial to write all the corrections in terms of the same integration measure. The LTD formalism attempts to do this by performing the integration over a single component of each of the loop momenta (usually the energy) by calculating the residues of the integrand obtained when the propagators go on-shell. In terms of the underlying Feynman graphs, calculating a residue is equivalent to cutting an internal line into two external lines with opposite on-shell momenta. The result is then a sum of integrals performed over the spatial components of the loop-momenta where the new, so-called dual integrands, have a tree-like structure.

In this chapter, we will derive the LTD formula for individual Feynman integrals. As a first step, we provide the derivation of the LTD formula at one-loop and give explicit analytic computations of some cut integrals in ϕ^3 theory. We then proceed to the multiloop case, where complications arise due to the calculation of residues in more than one complex variable.

4.1 Loop-Tree Duality at One-Loop

We introduce the LTD formalism [1] for Feynman integrals by first deriving the formula at the one-loop level.

Let $\Gamma \in U_{1,n}$ denote a one-loop graph with n external edges and N internal edges. Let $E_\Gamma = \{e_1, ..., e_N\}$ denote the set of the internal edges. Assume that all the momenta $p_1, p_2, ..., p_n$ are outgoing, and define

$$q_j = \sum_{i=1}^{j} p_i$$

We are interested in the calculation of the integral

$$I_n^{(1)} = \int \frac{d^D k}{(2\pi)^D} \frac{P(k)}{\prod_{e_j \in E_\Gamma} D_j^{\nu_j}} \tag{4.1}$$

where $P(k)$ is a polynomial in the loop (and external) momenta, and the inverse propagators D_j are given by

$$D_j = k_j^2 - m_j^2 + i\delta \tag{4.2}$$

where $k_j = k + q_j$, m_j the mass of the j-th line and δ is an infinitesimally small quantity. We assume that $D_i \neq D_j$ for $i \neq j$ without loss of generality and that each propagator can be raised to an arbitrary integer power ν_j. It will be convenient to denote the integrand of Eq.(4.1) as

$$f(E, \vec{k}) = \frac{P(k)}{\prod_{e_j \in E_\Gamma} D_j^{\nu_j}}, \tag{4.3}$$

where we choose to make the dependence on the energy and the spatial components of the loop momenta explicit and separate.

The loop integrand becomes singular when any of the propagators goes on-shell. Letting E denote the energy component of k, this means that each propagator develops a pair of poles in E which are solutions to

$$D_j = 0 \longrightarrow E + q_{j,0} = \pm\sqrt{|\vec{k} + \vec{q_j}|^2 + m_j^2 - i\delta}$$

We now expand the square root to first order in δ in order to determine the location of the poles in the complex E plane. This results in

$$E^\pm = -q_{j,0} \pm \left(E_j - \frac{i\delta}{2E_j} \right) \tag{4.4}$$

where we define $E_j = \sqrt{|\vec{k_j}|^2 + m_j^2}$. Each propagator gives a pole located in either the upper- or lower-half of the complex E plane and we can use the residue theorem to perform the integral over E, under the assumption that the polynomial $P(k)$, seen as a function of E, is such that the integrations over half-circles at infinity vanish, by picking a contour in either of the half-planes. The election of closing the contour on either side of the complex plane is arbitrary and the result of the integration is independent of this choice. We can also average over the two possibilities:

$$\begin{aligned} I_n^{(1)} = -\frac{i}{2} \int \frac{d^{D-1}k}{(2\pi)^{D-1}} \times \\ \sum_r \left(res\left(f(E, \vec{k}), E = E_r^+ \right) + res\left(f(E, \vec{k}), E = E_r^- \right) \right) \end{aligned} \tag{4.5}$$

where $E_r^\pm$ denote the pole of the r-th propagator whose real part has the sign $\pm$ and both sums go over all the positive or negative energy poles. We

now specialize to the case where $\nu_j = 1$. This means that each pole is simple, and we can directly compute each residue. In general, the residues will be the product of the factors

$$res\left(\frac{1}{k_j^2 - m_j^2 + i\delta}, E = E^+\right) = \frac{1}{2E_j} \tag{4.6}$$

for the pole at $E^+ = -q_{j,0} + E_j - \frac{i\delta}{2E_j}$ or

$$res\left(\frac{1}{k_j^2 - m_j^2 + i\delta}, E = E^-\right) = -\frac{1}{2E_j} \tag{4.7}$$

for the pole at $E^- = -q_{j,0} - E_j + \frac{i\delta}{2E_j}$, with the remaining propagators evaluated at $E = E^+$ or $E = E^-$, respectively. This modifies the $i\delta$ prescription of each propagator, for $a \neq j$, as

$$
\begin{aligned}
D_a(E = E^+) &= (E^+ + q_{a,0})^2 - |\vec{k}_a|^2 - m_a^2 + i\delta \\
&= \left(-q_{j,0} + E_j + q_{a,0} - \frac{i\delta}{2E_j}\right)^2 - |\vec{k}_a|^2 - m_a^2 + i\delta \\
&= (-q_{j,0} + E_j + q_{a,0})^2 - \frac{-q_{j,0} + E_j + q_{a,0}}{E_j}i\delta - |\vec{k}_a|^2 - m_n^2 + i\delta \\
&= (-q_{j,0} + E_j + q_{a,0})^2 - |\vec{k}_a|^2 - m_a^2 + \frac{q_{ja,0}}{E_j}i\delta
\end{aligned}
\tag{4.8}
$$

where we have kept terms only up to order δ and we define $q_{ja} = q_j - q_a$. The result for $E = E^-$ is obtained by the simple shift $E_j \to -E_j$. Finally, in each residue, we evaluate the polynomial $P(k)$ at the corresponding energy.
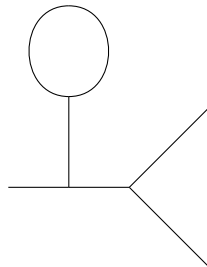
The cut integrands obtained by this procedure are tree-like objects built from propagators that have a modified $i\delta$ prescription that, at one loop, depends on the external momenta[1]. These are known as dual propagators [88].

An obvious question at this point is: why is it convenient to consider the average over the different contour closings, if one ends up with more contributions than by considering just a single contour? Let us answer this question at the one-loop level, and postpone the discussion for higher-loop integrals for the derivation of the multi-loop LTD formula.
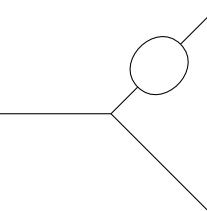
---

[1]Notice that the role of the $i\delta$ prescription is to specify the position of the poles of the propagators in the complex plane. Therefore, when the modified $i\delta$ prescription is taken into account, one only cares about the sign of the prefactor in front of $i\delta$. At the one-loop level, these signs are defined completely once the external momenta is fixed. This doesn't hold beyond two-loops, which is the main problem one has to solve in order to generalize the LTD formula for multiloop integrals.

If there are massless particles propagating in the loop, and integral such as Eq.(4.1) will develop IR singularities whose structure might be difficult to parametrize. However, the behaviour of tree amplitudes in soft and collinear limits is very well understood: the amplitudes factorizes in soft limits while the squared amplitudes factorizes in collinear limits [22, 23] into an amplitude with fewer external particles, multiplied by a factor that depends only on the kind of soft or collinear particles. Thus, if it were possible to write the integrand of a loop amplitude as a tree amplitude-like object with similar factorization properties close to their IR singularities, it would be possible to identify the regions where the IR divergences of the virtual corrections occur and achieve a cancellation, at the integrand level, of the IR divergences of the virtual and real corrections to a cross-section at NLO. This is achieved precisely by the averaging procedure.
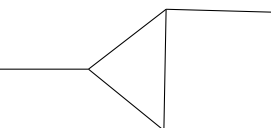
To illustrate this point, let us consider the 5-point tree-level amplitude in ϕ^3 theory. There are 15 diagrams that contribute to this amplitude, corresponding to the insertion of an additional scalar to each of the lines of the three diagrams that contribute to the 4-point scalar amplitude, which are simply the sum of an s, t, and u channel diagrams. If we let two of the external lines be labelled by a pair of momenta $(k, \bar{k})$, where $\bar{k} \to -k$, we can sew their corresponding edges together to obtain various one-loop graphs. Out of the 15 diagrams, three of them sew into a tadpole insertion

$$A_3^{(1-TP)} = \qquad\qquad\qquad\qquad \tag{4.9}$$

another six sew into self-energy insertions

$$A_3^{(1-SE)} = \qquad\qquad\qquad\qquad \tag{4.10}$$

while the remaining six all sew into the triangle diagram

$$A_3^{(1-triangle)} = \qquad\qquad\qquad\qquad \tag{4.11}$$

Now, the one-loop amplitude with three external massless scalars is calculated only from the triangle diagram and its possible counterterms. If we applied the LTD formula and only picked one contour closure, we would

miss half the possible tree diagrams contributing to the five-point tree amplitude that are consistent with the LSZ formula. The resulting integrand has the structure of a tree amplitude where the contributions that are singular in the forward limit $\bar{k} \to -k$ have been removed. This new tree-like object enjoys the same factorization properties as the tree amplitude, which simplifies the study of the IR singularities of the whole virtual contribution to the cross section. This is the reason why it is useful to perform an averaging procedure at one-loop.

4.1.1 Computation of simple integrals using LTD

Before we introduce the generalization of the LTD theorem to multiloop integrals, let us illustrate the consistency of the theorem with the computation of some simple cut integrals and how their contributions sum up to the result obtained for the Feynman integral after direct integration.

We begin by considering the triangle integral in Eq.(4.11), where we take the outgoing momenta to be p_1 and p_2, and we take every particle massless. The expression for this integral, in dimensional regularization, is then

$$I_3^{(1)}(p_1, p_2) = \mu^{4-D} \int \frac{d^D k}{(2\pi)^D} \frac{1}{(k^2 + i\delta)((k + p_1)^2 + i\delta)((k - p_2)^2 + i\delta)}$$
(4.12)

including the renormalization scale. Using standard Feynman parameters and reflection identities for Gamma functions, the massless triangle integral evaluates to [89]

$$I_3^{(1)}(s) = \frac{i}{16\pi^2 s} \left(\frac{s}{4\pi\mu^2} \right)^{-\epsilon} \frac{\Gamma(1 + 2\epsilon)\Gamma(1 - \epsilon)}{\epsilon^2} \cos \pi\epsilon$$
(4.13)

which depends only on the kinematic invariant $s = (p_1 + p_2)^2$.

In order to apply LTD, we notice that each of the three propagators has two residues, whose location in the complex k_0 plane are given by

$$k^2 + i\delta = 0 \longrightarrow k_0^{\pm} = \pm \left(|\vec{k}| - \frac{i\delta}{2|\vec{k}|} \right)$$

$$(k + p_1)^2 + i\delta = 0 \longrightarrow k_0^{\pm} = -E_1 \pm \left(|\vec{k} + \vec{p}_1| - \frac{i\delta}{2|\vec{k} + \vec{p}_1|} \right)$$
(4.14)

$$(k - p_2)^2 + i\delta = 0 \longrightarrow k_0^{\pm} = E_2 \pm \left(|\vec{k} - \vec{p}_2| - \frac{i\delta}{2|\vec{k} - \vec{p}_2|} \right)$$

where we have kept terms only up to $\mathcal{O}(\delta)$. Applying LTD, we can write the triangle integral as the linear combination

$$I_3^{(1)}(p) = \frac{1}{2}\left(\sum_{i=1}^{3} Cut(i^+) + \sum_{i=1}^{3} Cut(i^-)\right)$$

$$= \frac{1}{2}\sum_{\alpha=-1,1}\sum_{i=1}^{3} Cut(i^{(\alpha)})$$

(4.15)

where, labelling the inverse propagators as $D_1 = (k+p_1)^2 + i\delta$, $D_2 = (k-p_2)^2 + i\delta$ and $D_3 = k^2 + i\delta$, the quantity $Cut(i^{(\alpha)})$ denotes the cut obtained by evaluating the residue of the propagator D_i at the pole $k_0^{(\alpha)}$. As we mentioned previously, at one loop one obtains equivalent results when closing the contour upwards or downwards. Thus, we will show the results only for the integrals obtained by closing the contour on the lower-half of the complex plane.

In order to simplify the resulting integrals, we work on the Center of Momentum (CoM) frame, where the external momenta p_1 and p_2 are given by

$$p_1 = (E, \vec{p}), \quad p_2 = (E, -\vec{p})$$

(4.16)

with $E = |\vec{p}|$, since the external momenta are massless. Furthermore, the invariant s takes the value $4E^2$. Using this coordinates, we can write

$$Cut(1^+) = -i\mu^{4-D}\int \frac{d^{D-1}k}{(2\pi)^{D-1}2|\vec{k}+\vec{p}|} \times$$

$$\frac{1}{((|\vec{k}+\vec{p}|-E)^2 - |\vec{k}|^2)((|\vec{k}+\vec{p}-2E)^2 - |\vec{k}+\vec{p}|^2)}$$

$$= -i\mu^{4-D}\int \frac{d^{D-1}k}{(2\pi)^{D-1}2k} \times$$

$$\frac{1}{(k-E)^2 - |\vec{k}-\vec{p}|^2)((k-2E)^2 - k^2)}$$

(4.17)

where we perform the shift $\vec{k} \to \vec{k} - \vec{p}$ to go from the first to the second line, and we introduce the short-hand notation $k = |\vec{k}|$. If we let θ be the angle between $\vec{k}$ and $\vec{p}$, we can parametrize the integration measure as

$$d^{D-1}k = k^{D-2}dk \sin^{D-3}\theta d\theta d\Omega_{D-2}$$

(4.18)

were Ω_D denotes the solid angle in D dimensions. Further rescaling $k = Ex = \frac{\sqrt{s}}{2}x$ and evaluating the solid angle using Eq.(2.31) turns the cut into the two dimensional integral

$$Cut(1^+) = \frac{i}{(2\pi)^{D-1}2s} \frac{\pi^{\frac{D}{2}-1}}{\Gamma\left(\frac{D}{2}-1\right)} \left(\frac{\sqrt{s}}{2\mu}\right)^{D-4}$$
$$\times \left(\int_0^\infty \frac{x^{D-4}}{1-x}dx\right)\left(\int_0^\pi \frac{\sin^{D-3}\theta}{1-\cos\theta}d\theta\right)$$

(4.19)

The remaining integrals depend only on the dimension D, and we set $D = 4 - 2\epsilon$, keeping in mind an expansion around $D = 4$. The first one is performed with the transformations $x = \frac{y}{1-y}$,

$$\int_0^\infty \frac{x^{-2\epsilon}}{1-x}dx = \int_0^1 \frac{1-y}{1-2y}\frac{y^{-2\epsilon}}{(1-y)^{-2\epsilon}}\frac{1}{(1-y)^2}dy$$
$$= \int_0^1 \frac{y^{-2\epsilon}(1-y)^{2\epsilon-1}}{1-2y}dy$$
$$= \frac{\pi}{2}\left(-2i - \cot(\pi\epsilon) + \tan(\pi\epsilon)\right)$$
$$= -\pi\csc(2\pi\epsilon)e^{i2\pi\epsilon},$$

(4.20)

while the second one requires $\cos\theta = 1 - 2z$. This then yields

$$\int_0^\pi \frac{\sin^{1-2\epsilon}\theta}{1-\cos\theta}d\theta = \int_0^1 \frac{(4z(1-z))^{-\epsilon}}{2z}2dz$$
$$= 4^{-\epsilon}\int_0^1 z^{-\epsilon-1}(1-z)^{-\epsilon}dz$$
$$= 4^{-\epsilon}\frac{\Gamma(-\epsilon)\Gamma(1-\epsilon)}{\Gamma(1-2\epsilon)}$$

(4.21)

where we used the definition of the Euler's Beta function and written it in terms of Gamma functions. Simplifying the resulting expression using the identity

$$\Gamma(z)\Gamma(1-z) = \pi\csc(\pi z)$$

(4.22)

the final result for this integral is

$$Cut(1^+) = \frac{i}{32\pi^2 s}\left(\frac{s}{4\pi\mu^2}\right)^{-\epsilon}\frac{\Gamma(1+2\epsilon)\Gamma(1-\epsilon)}{\epsilon^2}e^{i2\pi\epsilon}$$

(4.23)

The result for the second cut is obtained in an analogous fashion, and we simply quote the final result:

$$Cut(2^+) = \frac{i}{32\pi^2 s}\left(\frac{s}{4\pi\mu^2}\right)^{-\epsilon}\frac{\Gamma(1+2\epsilon)\Gamma(1-\epsilon)}{\epsilon^2}.$$

(4.24)

At this point, by noticing that

$$1 + e^{i2\pi\epsilon} = 2e^{i\pi\epsilon}\cos\pi\epsilon$$
$$= 2(-1)^{-\epsilon}\cos\pi\epsilon \tag{4.25}$$

we can see that the adding the two cuts already yields the result of Eq.(4.13). The remaining cut integral $Cut(3^+)$ can be seen to be proportional to an expression of the form

$$\frac{1}{\epsilon_{UV}} - \frac{1}{\epsilon_{IR}} \tag{4.26}$$

where each of the parameters regularize either an UV or an IR divergence. However, since we are working in dimensional regularization, we can take these two regulators to be the same, which implies that the integral vanishes. This phenomena, where a cancellation occurs between UV and IR divergences, is only present when working in dimensional regularization. The steps involved in the calculation when the contour is closed on the upper-half of the complex plane is identical, resulting in the three same integrals. Hence, we can see that the LTD theorem reproduces the result for the direct integration of the loop integral.

4.2   Loop-Tree Duality for Multi-Loop Integrals

We will now see how to generalize Eq.(4.5) to L-loop integrals. As a first step, we will highlight the additional complications that arise beyond one loop by looking at a particular example.

Consider the integral

$$I_{sun}^{(2)}(p^2; m_1, m_2, m_3) = \int \prod_{i=1}^{2} \left(\frac{d^D K_i}{(2\pi)^D} \right) \times$$
$$\frac{1}{(k_1^2 - m_1^2 + i\delta)(k_2^2 - m_2^2 + i\delta)(k_3^2 - m_3^2 + i\delta)} \tag{4.27}$$

which corresponds to the sunrise graph of Fig. 3.12 and the momenta satisfy the constraint

$$k_1 + k_2 + k_3 = p. \tag{4.28}$$

The two integration variables K_i can be any two of the momenta of the three propagators $\{k_1, k_2, k_3\}$. This is an example of the general idea that we can pick different bases of independent loop momenta by picking L out of the N propagators in a given loop integral, with the momenta of the remaining $(N - L)$ propagators written as a linear combination of the independent loop momenta and the external momenta.

We want to find an LTD formula for the integral of Eq.(4.27). As a first attempt, we notice that each inverse propagator $D_i = k_i^2 - m_i^2 + i\delta$ produces two poles at

$$k_{i,0} = \pm \left(\sqrt{|\vec{k}_i|^2 + m_i^2} - \frac{i\delta}{2\sqrt{|\vec{k}_i|^2 + m_i^2}} \right),\tag{4.29}$$

where we have expanded to first order in δ. Now, we consider all the possible ways to cut two propagators that yields a connected tree graph. In the case of the sunrise, this will happen when we pick any two propagators, meaning that here are

$$n_{cut} = \binom{3}{2} = 3\tag{4.30}$$

possible ways to choose the propagators[2]. Using the translation invariance of the loop integral, we can choose the independent loop momenta K_1 and K_2 so that they match the momenta of the cut propagators. Thus, we can perform the calculation of the residues as two independent complex variables. For each variable, we can close the integration contour on either hemisphere of the complex plane. There are four different ways to close the two contours of each possible cut, and we average over them as we did in the one-loop case. Let us define

$$Cut(i^{\lambda_i}, j^{\lambda_j}) = \lambda_i \lambda_j Res(f, k_{i,0} = E_i, k_{j,0} = E_j)\tag{4.31}$$

where $\lambda = \pm 1$ and $E_i = \lambda_i \sqrt{|\vec{k}_i|^2 + m_i^2} - \frac{i\delta}{2\sqrt{|\vec{k}_i|^2+m_i^2}}$ and we let f denote the integrand of Eq.(4.27). For example, if we pick $K_1 = k_1$ and $K_2 = k_2$,

$$Cut(1^+, 2^+) = \frac{1}{2\sqrt{|\vec{k}_1|^2 + m_1^2}} \frac{1}{2\sqrt{|\vec{k}_2|^2 + m_2^2}}$$
$$\times \frac{1}{(p - k_1 - k_2)^2 - m_3^2 + s_3(\{1,2\})i\delta}\tag{4.32}$$

where $s_3(\{1,2\})$ depends on the energies of the cut propagators, and the momenta k_1 and k_2 entering the combination $k_3 = (p - k_1 - k_2)$ are now on-shell. Applying this procedure and then shifting back so that every cut is integrated over the same pair of Euclidean momenta, we would obtain

$$I_{sun}^{(2)}(p^2; m_1, m_2, m_3) = \frac{(-i)^2}{4} \int \frac{d^{D-1}k_1}{(2\pi)^{D-1}} \frac{d^{D-1}k_2}{(2\pi)^{D-1}}$$
$$\sum_{i \neq j}^{3} \sum_{\lambda \in \{-1,+1\}} Cut(i^{\lambda_i}, j^{\lambda_j})\tag{4.33}$$

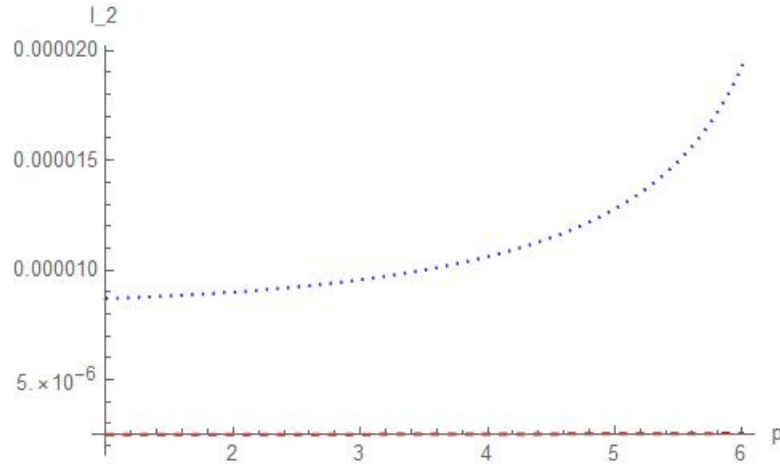[2]This means that are there are three possible marked graphs

FIGURE 4.1: Plots of the 1D sunrise integral evaluated using the LTD ansatz of Eq.(4.33) (dotted line) and numerical evaluation of Eq.(4.34) (dashed line) as functions of p for $m_1 = 11, m_2 = 13, m_3 = 17$.

Before we proceed, let us compare the values of the sunrise integral evaluated in two different ways: by direct integration and by using the formula in terms of cuts. To make this comparison as simple as possible, we will work in $D = 1$.

Using Feynman parameters, the integral can be rewritten as

$$I_{sun}^{(2)}(p; m_1, m_2, m_3) = \frac{1}{4\pi} \int_0^1 \int_0^{1-a_1} d^2 a \frac{\mathcal{U}^{\frac{3}{2}}}{\mathcal{F}^2} \tag{4.34}$$

where

$$\mathcal{U} = a_1 a_2 + a_1(1 - a_1 - a_2) + a_2(1 - a_1 - a_2) \tag{4.35}$$

and

$$\mathcal{F} = (-a_1 a_2(1 - a_1 - a_2)p^2 + \mathcal{U}(a_1 m_1^2 + a_2 m_2^2 + (1 - a_1 - a_2)m_3^2)^2 \tag{4.36}$$

The resulting integral can be performed numerically. On the other hand, since each momenta is one dimensional, applying the residue theorem once in each variable amounts to calculating the integral. Therefore, the integral should simply be the sum of the cuts, evaluated at their corresponding poles in K_1 and K_2.

Figure 4.1 show the values of the 1D sunrise integral as a function of p for fixed values of the masses obtained by using our LTD ansatz and the numerical evaluation of the integral after Feynman parametrization. Clearly, there is something wrong: while both results appear to have the same order of magnitude, the values and the behaviour of the integral are completely different from one another. This means that there must we something wrong

with our approach to the residue calculation.

In order to see what is happening, let us consider the iterative application of LTD to the sunrise integral, computing first the residues in one of the two energy components, say, of k_2, and then trying to apply the residue theorem in the remaining energy integral. To simplify the discussion, we will take all propagators to be massless. We rewrite the integral as

$$I_{sun}^{(2)}(p^2) = \int \frac{d^D k_1}{(2\pi)^D} \frac{1}{k_1^2 + i\delta} I_{bub}(k_1) \tag{4.37}$$

where

$$I_{bub}(k_1) = \int \frac{d^D k_2}{(2\pi)^D} \frac{1}{(k_2^2 + i\delta)((p - k_1 - k_2)^2 + i\delta)} \tag{4.38}$$

has the structure of a one-loop bubble integral, and we have taken k_1 and k_2 as our two independent loop momenta, while explicitly writing $k_3 = (p - k_1 - k_2)$. The two denominators result in poles on the $k_{2,0}$ plane located at

$$k_2^2 + i\delta = 0 \longrightarrow k_{2,0}^{\pm} = \pm \left(|\vec{k}_2| - \frac{i\delta}{2|\vec{k}_2|} \right),$$

$$(p - k_1 - k_2)^2 + i\delta = 0 \tag{4.39}$$

$$\longrightarrow k_{2,0}^{\pm} = p_0 - k_{1,0} \pm \left(|\vec{k}_1 + \vec{k}_2 - \vec{p}| - \frac{i\delta}{2|\vec{k}_1 + \vec{k}_2 - \vec{p}|} \right).$$

We can then evaluate the $dk_{2,0}$ integral by using the residue theorem, averaging over the closing in the two hemispheres of the complex plane, as we did in the one-loop case. The integral then becomes

$$I_{bub}(k_1) = \frac{1}{2} \sum_{i=1}^{2} \sum_{r=\{+,\}} I_{bub}^{i,r}(k_1). \tag{4.40}$$

We can explicitly compute the residue of the cut at the pole $k_{2,0} = |\vec{k}_2| - i\delta/2|\vec{k}_2|$. The residue formula yields a factor of $1/2|\vec{k}_2|$, while the remaining propagator evaluates to

$$
\begin{aligned}
(p - k_1 - k_2)^2 + i\delta &= \left(p_0 - k_{1,0} - |\vec{k}_2| + \frac{i\delta}{2|\vec{k}_2|} \right)^2 \\
&\quad - |\vec{p} - \vec{k}_1 - \vec{k}_2|^2 + i\delta \\
&= (p_0 - k_{1,0} - |\vec{k}_2|)^2 - |\vec{p} - \vec{k}_1 - \vec{k}_2|^2 \\
&\quad + i\delta + \frac{p_0 - k_{1,0} - |\vec{k}_2|}{|\vec{k}_2|} i\delta \\
&= (p_0 - k_{1,0} - |\vec{k}_2|)^2 - |\vec{p} - \vec{k}_1 - \vec{k}_2|^2 \\
&\quad + \frac{p_0 - k_{1,0}}{|\vec{k}_2|} i\delta
\end{aligned}
\tag{4.41}
$$

thus, the corresponding contribution to the sum in Eq.(4.40) is given by

$$
I_{bub}^{1,+} = -i \int \frac{d^{D-1}k_2}{(2\pi)^{D-1}2|\vec{k}_2|} \times
$$
$$
\frac{1}{(p_0 - k_{1,0} - |\vec{k}_2|)^2 - |\vec{p} - \vec{k}_1 - \vec{k}_2|^2 + \frac{p_0-k_{1,0}}{|\vec{k}_2|}i\delta}
\tag{4.42}
$$

with the remaining contributions being computed in similar fashion. In the next step, we would like to apply the residue theorem in the complex $k_{1,0}$ plane. However, the resulting integrals have a more complicated structure, due to the prefactor in front of the $i\delta$ in Eq.(4.42). In a regular Feynman integral, the propagators have the usual Feynman prescription to separate the position of the poles in a symmetric fashion between both hemispheres of the complex plane. In this case, the position of the poles of the dual propagator in the $k_{1,0}$ plane depends on the sign of $(p_0 - k_{1,0})$. Keeping track of these signs represents the main difficulty in writing down a general LTD formula beyond one-loop and is the reason behind the mismatch found in Fig. 4.1: a naive application of the residue theorem is insensitive to the constraints which relate the different loop momenta, which cannot be ignored if one is to obtain a correct LTD representation of an arbitrary loop integral.

We would like to find a LTD formula for integrals of arbitrary loop order which preserves the structure of the residues found in the one-loop case; that is, that the singularity structure of the cut propagators is defined directly by the Feynman propagators before the introduction of any dual prescription. In order to do this, we will first introduce some general notation to refer more easily to each of the different properties of the integrals that are important to the derivation, as well as a proper definition of a multidimensional residue.

Consider a graph $\Gamma \in U_{L,n}$. Let $E_\Gamma = \{e_1, e_2, ..., e_N\}$ denote the set of internal edges of Γ. We can obtain a cut graph $\Gamma_{cut} \in U_{0,n+2L}$ by cutting open

L internal edges, for example, $\{e_{\sigma_1}, ..., e_{\sigma_L}\}$. We denote by $\sigma = \{\sigma_1, ..., \sigma_L\}$ the set of indices of the cut edges.

We let

$$p_1, p_2, ..., p_n$$

be the external momenta of the graph Γ, while

$$k_1, k_2, ..., k_N$$

denote in the momenta of the internal edges. Notice that there is no single way to define the integrand associated to the graph Γ, since we have the freedom to pick L out of the N momenta in $k_1, ..., k_N$ as the independent loop momenta that we integrate against, while the remaining $(N - L)$ internal momenta become linear combinations of the independent loop momenta and the external momenta. Thus, we will assume that the first L momenta $k_1, k_2, ..., k_L$ form a basis of independent loop momenta. For each internal edge, we define the inverse propagator

$$D_j = k_j^2 - m_j^2 + i\delta, \ e_j \in E_\Gamma \tag{4.43}$$

where, as in the one-loop case, we assume $D_i \neq D_j$ for $i \neq j$ without loss of generality, since the case where two propagators are equal to each other amounts to considering an integral with fewer propagators, where one of the propagators is raised to a higher power.

We let $f(k)$ denote any function which depends on the D-dimensional momentum $k = (E, \vec{k})$. We also use the notation $f(E, \vec{k})$ when we want to emphasize the dependence of f on its energy component. We denote by

$$\int \frac{d^{D-1}k}{(2\pi)^{D-1}2\sqrt{\vec{k}^2 + m^2}} f(\pm\sqrt{\vec{k}^2 + m^2}, \vec{k}) \tag{4.44}$$

the integral of the function f over the forward (+) and backward (-) on-shell hyperboloid $k^2 = m^2$. Such integrals would be obtained by computing residues of loop integrals where the real part of the pole is positive or negative, respectively. Anticipating the appearance of an average over the two possible contour closings associated to the poles of a single propagator, we introduce the shorthand notation

$$dk^{cut} = \frac{d^{D-1}k}{(2\pi)^{D-1}2\sqrt{\vec{k}^2 + m^2}} \tag{4.45}$$

for the integration measure of the cut integrals, and

$$\int_\pm dk^{cut} f(k) = \int dk^{cut} \sum_{\lambda=\{\pm\}} f(\lambda\sqrt{\vec{k}^2 + m^2}, \vec{k}) \tag{4.46}$$

for the sum of the integrals over both hyperboloids. Our object of interest is the general loop integral

$$I_L = \int \left(\prod_{i=1}^{L} \frac{d^D k_i}{(2\pi)^D} \right) \frac{P_\Gamma}{\prod_{e_j \in E_\Gamma} D_j^{\nu_j}} \tag{4.47}$$

where P_Γ is a polynomial in the independent loop momenta $k_1, ..., k_L$ and the external momenta $p_1, ..., p_n$. We further demand that P_Γ be such that all energy integrations over half-circles at infinity vanishes. This conditions is always satisfied, for example, in the case of scalar integrals where $P_\Gamma = 1$. Now, we proceed to separate the energy integrations and write

$$I_L = \int \left(\prod_{i=1}^{L} \frac{d^{D-1} k_i}{(2\pi)^{D-1}} \right) \frac{1}{(2\pi)^L} \int \frac{P_\Gamma}{\prod_{e_j \in E_\Gamma} D_j^{\nu_j}} dE_1 \wedge dE_2 \wedge ... \wedge dE_L \tag{4.48}$$

where we have interpreted the integrand over the energy components as an L-form. We want to perform the L energy integrations using the residue theorem. The first issue we must address is how to properly define the residue of a function of multiple complex variables.

To begin, let σ denote some indices defining a spanning tree, and choose the independent loop momenta to be the momenta flowing through the lines indexed by σ. Furthermore, let

$$E_\sigma^{(\alpha)} = (E_{\sigma_1}^{(\alpha)}, \ldots, E_{\sigma_L}^{(\alpha)}) \tag{4.49}$$

be a solution to the set of equations

$$D_{\sigma_1} = \cdots = D_{\sigma_L} = 0 \tag{4.50}$$

where $\alpha = \pm 1$ denotes the sign of the real part of each solution. Since there are two solutions to each of the equations $D_{\sigma_i} = 0$ for a given propagator, we can see that there will be a total of 2^L solutions E_σ^α, which can in general be written as

$$\left(\pm \sqrt{|\vec{k}_{\sigma_1}|^2 + m_{\sigma_1}^2 - i\delta}, \cdots \pm \sqrt{|\vec{k}_{\sigma_L}|^2 + m_{\sigma_L}^2 - i\delta} \right) \tag{4.51}$$

Now, we consider the L-fold residues of the differential form

$$\frac{P_\Gamma}{\prod_{e_j \in E_\Gamma} D_j^{\nu_j}} dE_1 \wedge dE_2 \wedge ... \wedge dE_L := f \, dE_1 \wedge dE_2 \wedge \cdots \wedge dE_L \tag{4.52}$$

where we have introduced a short-hand notation for the integrand of Eq.(4.47). These residues are calculated around the poles defined by the equations in Eq.(4.50). We can define the local residue [90] at $E_\sigma^{(\alpha)}$ as the contour integral

$$res(f, E_\sigma^{(\alpha)}) = \frac{1}{(2\pi)^L} \oint_{\gamma_\epsilon} f \, dE_1 \wedge dE_2 \wedge \cdots \wedge dE_L \tag{4.53}$$

where the integration region in $\mathbb{C}^L$

$$\gamma_\epsilon = \{(E_1, \ldots, E_L) \in \mathbb{C}^L \mid |D_{\sigma_i}| = \epsilon \, \forall i \in (1, \ldots, L)\} \tag{4.54}$$

encircles the point $E_\sigma^{(\alpha)}$ with orientation

$$d \arg D_{\sigma_1} \wedge d \arg D_{\sigma_2} \wedge \cdots \wedge d \arg D_{\sigma_L} \geq 0. \tag{4.55}$$

Each local residue around $E_\sigma^{(\alpha)}$ corresponds to the contribution to the integral obtained from a single cut of L internal propagators. From their definition, these residues can be calculated as a simple generalization of the residue theorem in one complex variable, which we will perform shortly. However, we will first show that the value of the L-fold residue of f is not given by the sum of the residues, but rather by a sum weighted by combinatorial factors. The result to prove is that

$$\frac{1}{(2\pi)^L} \int f \, dE_1 \wedge dE_2 \wedge \cdots \wedge dE_L$$
$$= (-i)^L \sum_{\sigma \in \mathcal{C}_\Gamma} \sum_{\alpha} S_{\sigma\alpha}(-1)^{n_\sigma^{(\alpha)}} res(f, E_\sigma^{(\alpha)}) \tag{4.56}$$

where, as in the previous chapter, $\mathcal{C}_\Gamma$ is the set of all possible indices of cut edges, and n_σ^α denotes the number of entries with negative real part in $E_\sigma^{(\alpha)}$. The following derivation follows the lines of [1].

As a first step, let us pick a set of L integration variables indexed by an element $\tilde{\sigma} \in \mathcal{C}_\Gamma$ and let us assume that the integration is performed in an iterative fashion. Let $\tilde{\pi} \in S_L$ denote the order in which the integrations are performed; that is, we integrate first over $k_{\tilde{\sigma}_{\pi_1}}$ all the way up to $k_{\tilde{\sigma}_{\pi_L}}$. We remind ourselves that in the intermediate steps after the first m integrations, the position of the poles in the remaining integration variables will depend on the values of the Euclidean components of $(k_{\tilde{\sigma}_{\pi_1}}, \ldots, k_{\tilde{\sigma}_{\pi_m}})$.

Let $\tilde{k} = (\tilde{k}_1, \ldots, \tilde{k}_L) = (k_{\tilde{\sigma}_{\pi_1}}, \ldots, k_{\tilde{\sigma}_{\pi_L}})$ denote the ordered set of integration momenta and $\tilde{\alpha} = (\gamma_1, \ldots, \gamma_L)$ denote the ordered set of winding numbers. Each $\alpha_i = \pm 1$, and its value denotes whether the integration contour in the variable $\tilde{k}_i$ is closed above (+1) or below (-1) in the complex plane.

Furthermore, let us specify by $\sigma \in \mathcal{C}_L$ a particular cut of the graph Γ associated to the Feynman integral we are calculating. This cut can be taken by cutting L lines one after the other, and in analogy to the integration process, we denote by $\pi \in S_L$ the order in which the edges e_{σ_i} are cut, such that the first cut edge is $e_{\sigma_{\pi_1}}$ and the last is $e_{\sigma_{pi_L}}$. Also, we let $\alpha = (\lambda_1, \ldots, \lambda_L)$ denote

the signs of the real part of the cut under consideration, meaning that $\lambda_i = 1$ is related to a cut whose residue has a positive energy with respect to the orientation of the cut edge $e_{\sigma_{\pi_i}}$.

Now, let the momenta of the cut edges be specified by the ordered set $\hat{k} = (\hat{k}_1, \ldots, \hat{k}_L) = (k_{\sigma_{\pi_1}}, \ldots, k_{\sigma_{\pi_L}})$. Recall that we would like to choose the pick the independent loop momenta, which will be our integrations variables, to match with the momenta of the cut edges. Noticing that either $\tilde{k}$ or $\hat{k}$ can be chosen as bases of independent loop momenta, we can relate them as

$$\hat{k}_i = \sum_{j=1}^{L} \Sigma_{ij} \tilde{k}_j + q_i \tag{4.57}$$

where q_i is a linear combination of external momenta and Σ_{ij} is an $L \times L$ matrix whose entries are all in the set $\{-1, 0, 1\}$. Before we proceed, let us consider the familiar example of the sunrise integral to see how to construct Σ_{ij}.

The momenta of the three propagators of the sunrise integral are related through momentum conservation at either of the vertices as

$$k_1 + k_2 + k_3 = p \tag{4.58}$$

Consider the $(1, 3)$ cut[3] taken in that order and let us pick the integration variables to be k_1 and k_2, ordered in such a way that we integrate first over k_2 and then over k_1. Thus, our two ordered basis are

$$\tilde{k} = (k_2, k_1) \tag{4.59}$$

for the integration variables and

$$\hat{k} = (k_1, k_3) \tag{4.60}$$

for the momenta of the cut edges. We can rewrite $k_3 = p - k_1 - k_2$, so that

$$\hat{k} = (k_1, -k_1 - k_2 + p). \tag{4.61}$$

Now, in order to identify the elements of the matrix Σ_{ij}, we can set $p = 0$ and look at the coefficients relating the resulting bases $\tilde{k}$ and $\hat{k}$. It is not difficult to see that, treating each of these ordered sets as vectors,

$$\hat{k} = \Sigma \tilde{k} \tag{4.62}$$

with

$$\Sigma = \begin{bmatrix} 0 & 1 \\ -1 & -1 \end{bmatrix} \tag{4.63}$$

It is then straightforward to restore p in the relevant terms. For example,

---

[3]The signs of the energies are not important for this point, so we omit them.

$$\hat{k}_2 = \sum_{j=1}^{2} \Sigma_{2j}\tilde{k}_j + p$$

$$= -k_2 - k_1 + p$$

(4.64)

which, of course, gives the correct result. This process generalizes directly to arbitrary loop order.

Going back to our arbitrary loop integral, we define $\Sigma^{(j)}$ to be the sub-matrix of Σ obtained by deleting rows and columns from $(j+1)$ up to L. Furthermore, in order to perform the integration procedure, we assume that all masses have large imaginary parts which are strongly ordered, meaning that $Im(m_{\sigma_1}) >> Im(m_{\sigma_2}) >> \cdots >> Im(m_{\sigma_L})$. The final result will be independent of this assumption. The point of this assumption is that, during the intermediate integrations, the ordering will allow us to keep track of the location of the poles. After all L integrations have been performed, we can drop the assumption and analytically continue the integrand to any desired kinematic configuration. Given these conditions, we find the intermediate result

$$\frac{1}{(2\pi)^L} \int f \, dE_1 \wedge dE_2 \wedge ... \wedge dE_L$$

$$= \sum_{\sigma \in \mathcal{C}_\Gamma} \sum_{\pi \in S_L} \sum_{\alpha \in \{-1,1\}^L} C_{\sigma\pi\alpha}^{\tilde{\sigma}\tilde{\pi}\tilde{\alpha}} \, res\left(f, E_\sigma^{(\alpha)}\right)$$

(4.65)

where

$$C_{\sigma\pi\alpha}^{\tilde{\sigma}\tilde{\pi}\tilde{\alpha}} = \prod_{i=1}^{L} \Delta^{(i)},$$

(4.66)

with the numbers $\Delta^{(i)}$ defined to be zero if $\det \Sigma^{(i)} = 0$. Otherwise, we let $\Pi^{(i)}$ denote the inverse of $\Sigma^{(i)}$, and set

$$\Delta^{(i)} = \gamma_i \Pi_{ii}^{(i)} \theta \left(\gamma_i Im \left(\sum_{j=1}^{i} \Pi_{ij}^{(i)} \lambda_j m_{\sigma_j} \right) \right)$$

(4.67)

where $\theta(x)$ denotes the Heaviside step function. It is in this definition that the assumption about the strong ordering is important. As before, lets compute a few of these coefficients to understand a bit better the way they work.

Let us consider our previous example, where the Σ matrix is given in Eq.(4.63). From the structure of the coefficients $C_{\sigma\pi\alpha}^{\tilde{\sigma}\tilde{\pi}\tilde{\alpha}}$, it is clear that if a single $\Delta^{(i)}$ vanishes, then the coefficient is zero. In the present case, taking $j = 1$ yields the submatrix

$$\Sigma^{(1)} = 0 \tag{4.68}$$

which, of course, has a vanishing determinant[4]. Therefore, $\Delta^{(1)} = 0$ and the coefficient $C_{\sigma\pi\alpha}^{\breve{\sigma}\breve{\pi}\breve{\alpha}}$ vanishes for the particular choices of $\tilde{k}$ and $\hat{k}$, independent of the values of α and $\tilde{\alpha}$.

Now, let us consider again the $(1,3)$ cut and the integration variables to be k_1 and k_2, but assume instead that the integration is performed first over k_1 and then over k_2. This gives the new ordered basis

$$\tilde{k} = (k_1, k_2) \tag{4.69}$$

for the integration variables, while the basis spanned by the momenta of the cut edges remains $\hat{k} = (k_1, k_3)$. In this case, we find the matrix relating the two bases to be

$$\Sigma = \begin{bmatrix} 1 & 0 \\ -1 & -1 \end{bmatrix} \tag{4.70}$$

Let us further assume that the imaginary part of the masses is ordered according to $Im(m_1) >> Im(m_2) >> Im(m_3)$. Recalling that the permutation σ is related to the cut basis, this means that $m_{\sigma_1} = m_1$ and $m_{\sigma_2} = m_3$ and we have $Im(m_{\sigma_1}) >> Im(m_{\sigma_3})$. Notice that, in order to compute a particular coefficient $C_{\sigma\pi\alpha}^{\breve{\sigma}\breve{\pi}\breve{\alpha}}$, we need to specify the winding numbers and the sign of the energies. Hence, for our example, we will take $\alpha = (1,1)$ and $\tilde{\alpha} = (1,-1)$. We can then see that

$$C_{\sigma\pi\alpha}^{\breve{\sigma}\breve{\pi}\breve{\alpha}} = \Delta^{(1)}\Delta^{(2)} \tag{4.71}$$

where the first coefficient $\Delta^{(1)}$ is computed from the submatrix $\Sigma^{(1)} = 1$; it follows that $\Pi^{(1)} = 1$, and

$$\Delta^{(1)} = \gamma_1 \Pi_{11}^{(1)} \theta \left(\gamma_1 Im \left(\sum_{j=1}^{1} \Pi_{j1}^{(1)} \lambda_j m_{\sigma_j} \right) \right)$$

$$= 1$$

since all of γ_1, $\Pi_{11}^{(1)}$ and λ_1 are equal to one. The matrix $\Sigma^{(2)}$ (and, in general, $\Sigma^{(L)}$) is equal to Σ, since no rows or columns are eliminated. Its determinant is

$$\det \Sigma = -1. \tag{4.72}$$

This matrix is its own inverse, as can be easily checked by matrix multiplication. Then, we can compute

---

[4]We take the value of a scalar as the definition of its determinant

$$\Delta^{(2)} = \gamma_2 \Pi_{22}^{(2)} \theta \left(\gamma_2 Im \left(\Pi_{21}^{(2)} \lambda_1 m_{\sigma_1} + \Pi_{22}^{(2)} \lambda_2 m_{\sigma_2} \right) \right)$$
$$= \theta \left(-Im \left(-m_1 - m_3 \right) \right)$$
$$= 1$$

since both the real and imaginary part of all the masses is taken to be positive. If we had the difference $(m_1 - m_3)$ instead of the sum $-(m_1 + m_3)$ inside the imaginary part, we would have used our assumption on the strong ordering of the masses to determine the sign of the argument of the Heaviside function, which allows us to obtain the value of the coefficient. Putting the two values together, we find that, for our particular choices of the bases, orderings and signs,

$$C_{\sigma \pi \alpha}^{\tilde{\sigma} \tilde{\pi} \tilde{\alpha}} = 1. \tag{4.73}$$

In its actual form, Eq.(4.65) gives a value for the L-fold residue we are looking for. This highlights the fact that the representation of the integrand in terms of cuts is non-unique, since in this form, we are free to choose a set of integration variables, the order in which we take them and the contour closing for each of the energy components.

Following a similar idea to that discussed in the one-loop case, let us consider the calculation of the full L-loop amplitude for some particular scattering process. Via the cutting and sewing procedures, we can relate loop diagrams with fewer external particles to tree diagrams with $2L$ additional external particles, whose momenta is taken to be pair-wise related through a forward limit. If we attempted to construct all the diagrams contributing to the loop amplitude by sewing tree graphs, we would obtain contributions where all possible integration orders and contour closings appear. Therefore, keeping the result of Eq.(4.65) for the integrand will lack the tree-like structure we would like to achieve. With this in mind, we consider instead a weighted average over $\tilde{\sigma}$, $\tilde{\alpha}$ and $\tilde{\pi}$.

In order to perform this average, we need to introduce the concept of a chain graph [24]. The chain graph of an arbitrary graph can be obtained by grouping the internal propagators into chains, which are sets of loop momenta whose elements differ only by a linear combination of external momenta. Then, one picks a representative propagator of each chain, and collapses all the remaining propagators into the representatives. Finally, all external lines are removed. For a given graph $\Gamma \in U_{L,n}$, we let $|\mathcal{C}_{\Gamma^{chain}}|$ denote the number of spanning trees of its corresponding chain graph. For each propagator D_j, we denote by $n^{chain}(j)$ the number of propagators in its chain. Set

$$N^{chain}(\sigma) = \prod_{j=1}^{L} n^{chain}(\sigma_j) \tag{4.74}$$

and then, perform an average where each term is weighted by $1/N^{chain}(\sigma)$. This allows us to obtain

$$
\begin{aligned}
\frac{1}{(2\pi)^L} &\int f\, dE_1 \wedge dE_2 \wedge \ldots \wedge dE_L \\
&= (-i)^L \sum_{\sigma \in \mathcal{C}_\Gamma} \sum_{\alpha} S_{\sigma\alpha} (-1)^{n_\sigma^{(\alpha)}} res\left(f, E_\sigma^{(\alpha)}\right)
\end{aligned}
\tag{4.75}
$$

where the coefficients $S_{\sigma\alpha}$ are given by

$$
S_{\sigma\alpha} = \frac{(-1)^{L+n_\sigma^{(\alpha)}}}{2^L L! |\mathcal{C}_{\Gamma^{chain}}|} \sum_{\pi \in S_L} \sum_{\tilde{\sigma} \in \mathcal{C}_\Gamma} \sum_{\tilde{\pi} \in S_L} \sum_{\tilde{\alpha} \in \{-1,1\}^L} \frac{C_{\sigma\pi\alpha}^{\tilde{\sigma}\tilde{\pi}\tilde{\alpha}}}{N^{chain}(\sigma)}
\tag{4.76}
$$

here, the 2^L comes from the average over $\tilde{\alpha}$ and the $L!$ comes from the average over $\tilde{\pi}$. Le us remark that the values of these coefficients depends only on the structure of the underlying chain graph of the original graph under consideration.

The expression for the coefficients $S_{\sigma\alpha}$ in Eq.(4.76) can be simplified in some cases. At one-loop, we can deduce from our original discussion of LTD that $S_{\sigma\alpha} = 1/2$ for every loop graph. This can be deduced by noticing that, in this case, the sums over π and $\tilde{\pi}$ are trivial, while the only possible chain graph at one-loop is the vacuum bubble.

At two loops, there are only two possible chain graphs: the sunrise without external legs, and the product of two one-loop vacuum bubbles. In the latter case, the graph essentially behaves as the product of two one-loop graphs, and we obtain $S_{\sigma\alpha} = 1/4$. In the former case, if the orientation of the cut lines is chosen to be the same across the cut, then

$$
S_{\sigma\alpha} = \frac{1}{(L+1)} \frac{1}{\binom{L}{n_\sigma^{(\alpha)}}}
\tag{4.77}
$$

which generalizes to L-loop graphs whose underlying chain graph is a vacuum bubble with $(L+1)$ propagators (the so-called banana graphs).

Notice that the formula for the L-fold residue in Eq.(4.75) makes no reference to the structure of the poles, meaning that it is valid for poles of arbitrary order. Let us, then, specialize to the case where every propagator occurs at power one and compute the value of the residue.

As a first ingredient, we need to compute the contribution coming from the residue of the propagator D_{σ_j} at its poles. We write each of the cut propagators as

$$
D_{\sigma_j} = k_{\sigma_j}^2 - m_{\sigma_j}^2 + i\delta
\tag{4.78}
$$

where, according to our previous discussion, we pick the momenta of the cut propagators to be the independent loop momenta. The poles of $1/D_{\sigma_j}$ in the energy component occur at $k_{\sigma_j,0} = \sqrt{|\vec{k}_{\sigma_j}|^2 + m^2_{\sigma_j} - i\delta}$, and we find

$$res\left(\frac{1}{D_{\sigma_j}}, \pm\sqrt{|\vec{k}_{\sigma_j}|^2 + m^2_{\sigma_j} - i\delta}\right) = \pm\frac{1}{2\sqrt{|\vec{k}_{\sigma_j}|^2 + m^2_{\sigma_j}}} \tag{4.79}$$

where we drop the infinitesimal imaginary part $i\delta$ because these factors introduce no additional poles into the integrand. Now, we need to evaluate the uncut propagators at the poles of the cut propagators. In order to do this, notice that the set of indices $\sigma = \{\sigma_1, \ldots, \sigma_L\}$ defines a tree graph, T_{cut}, obtained from the original loop graph Γ by deleting the edges $\{e_{\sigma_1}, \ldots, e_{\sigma_L}\}$. Now, consider the propagator D_j, where the index j is such that $j \notin \sigma$. Thus, cutting this index will produce a two-forest[5] (T_1, T_2). As a convention, we orient the external momenta of T_1 such that all momenta are outgoing. The external edges of T_1 are comprised by e_j, the set of cut edges and possibly a subset of the external edges $\{1, \ldots, n\}$. We let ρ denote the set of indices corresponding to the external edges of T_1 which come from cutting the internal edges of the original graph Γ. For a given element $a \in \rho$, the energy component has an imaginary part which depends on the infinitesimal δ; expanding up to first order, we find that

$$\begin{aligned} k_{\rho_a,0} &= \pm\sqrt{|\vec{k}_{\pi_a}|^2 + m^2_{\pi_a} - i\delta} \\ &= \pm\sqrt{|\vec{k}_{\pi_a}|^2 + m^2_{\pi_a}} \mp \frac{i\delta}{2\sqrt{|\vec{k}_{\pi_a}|^2 + m^2_{\pi_a}}} \\ &\equiv \pm E_{\rho_a} \mp \frac{i\delta}{2E_{\rho_a}} \end{aligned} \tag{4.80}$$

where we have defined the on-shell energy of the line ρ_a as

$$E_{\rho_a} = \sqrt{|\vec{k}_{\pi_a}|^2 + m^2_{\pi_a}}$$

.

This is a straightforward generalization of the behaviour at one-loop. Now, let us evaluate D_j at these values of $k_{\rho_a,0}$:

---

[5] A two-forest is a tree graph whose structure is that of two disjoint trees. In general, one can define an n-forest as a graph with n disjoint trees. This kind of graphs appear in the formulation of the Feynman Tree Theorem [91], which represents the first attempt to evaluate loop integrals in terms of tree-level contributions.

$$D_j = k_{j,0}^2 - |\vec{k}_j|^2 - m_j^2 + i\delta$$

$$= \left(\sum_{a \in \rho} k_{a,0} + \sum_{b \in E_{ext}} k_{b,0}^{ext} \right) - |\vec{k}_j|^2 - m_j^2 + i\delta \qquad (4.81)$$

$$= k_j^2 - m_j^2 + \left(1 + E_j \sum_{a \in \rho} \frac{1}{E_a} \right) i\delta + \mathcal{O}(\delta^2)$$

and we can see that

$$\left(1 + E_j \sum_{a \in \rho} \frac{1}{E_a} \right) = E_j \sum_{a \in \{j\} \cup \rho} \frac{1}{E_a} \equiv \frac{E_j}{E_{||}}. \qquad (4.82)$$

Defining $s_j(\sigma) = \frac{E_j}{E_{||}}$ for every uncut propagator, we obtain the LTD representation for a multi-loop integral with only single poles

$$\int \left(\prod_{j=1}^{L} \frac{d^D k_j}{(2\pi)^L} \right) \frac{P_\Gamma}{\prod_{e_j \in E_\Gamma} (k_j^2 - m_j^2 + i\delta)} \qquad (4.83)$$

$$= (-i)^L \sum_{\sigma \in \mathcal{C}_\Gamma} \int_{\pm} \left(\prod_{j=1}^{L} dk_{\sigma_j}^{cut} \right) S_{\sigma\alpha} \frac{P_\Gamma}{\prod_{j \notin \sigma} (k_j^2 - m_j^2 + i s_j(\sigma)\delta)}$$

where the $\pm$ subscript in the integral sign becomes a short-hand notation for the sum over the energy signs α.

Notice that the $i\delta$ prescription of the dual propagators in the LTD representation, being written explictly in terms of the energies, breaks the Lorentz invariance of the underlying integrand. We can restore this by introducing a reference, light-like vector η with $\eta_0 \geq 0$, and rewrite

$$s_j(\sigma) = \sum_{a \in \{j\} \cup \rho} \frac{\eta \cdot k_j}{\eta \cdot k_a}, \qquad (4.84)$$

so that our derivation corresponds to the choice $\eta = (1, \vec{0})$. Essentially, the reference vector gives the direction of the axis in Minkowski space along which we compute the residues. The structure of the Feynman propagators then allows us to determine that the easiest such choice is to integrate along the energy components.

Let us attempt, once again, to evaluate the one-dimensional two-loop sunrise integral using the new, modified LTD formula with the combinatorial factors $S_{\sigma\alpha}$. In this case, we can use the simplified version of Eq.(4.77). It is easy to see that there are only two possible values these factor can take at two-loops: if $n_\sigma^{(\alpha)} = 0, 2$, then $S_{\sigma\alpha} = 1/3$ and if $n_{\sigma\alpha} = 1$ then $S_{\sigma\alpha} = 1/6$. Thus, all cuts where both energies have the same sign have factor of $1/3$ and

all cuts with mixed energy signs have a factor of $1/6$. The integral is written then in terms of cuts as

$$
\begin{aligned}
I_{sun}^{LTD} = \Bigg(&\frac{1}{3}Cut(1^+,2^+) - \frac{1}{6}Cut(1^+,2^-) - \frac{1}{6}Cut(1^-,2^+) + \frac{1}{3}Cut(1^-,2^-) \\
+ &\frac{1}{3}Cut(1^+,3^+) - \frac{1}{6}Cut(1^+,3^-) - \frac{1}{6}Cut(1^-,3^+) + \frac{1}{3}Cut(1^-,3^-) \\
+ &\frac{1}{3}Cut(2^+,3^+) - \frac{1}{6}Cut(2^+,3^-) - \frac{1}{6}Cut(2^-,3^+) + \frac{1}{3}Cut(2^-,3^-) \Bigg)
\end{aligned}
\tag{4.85}
$$

and, taking $\{i,j,k\}$ to be a permutation of $\{1,2,3\}$, each of these cuts is given by

$$
Cut(i^{\lambda_i}, j^{\lambda_j}) = \frac{\lambda_i \lambda_j}{4m_i m_j} \frac{1}{(\lambda_i m_i + \lambda_j m_j - p)^2 - m_k^2}
\tag{4.86}
$$

in the case of the one-dimensional sunrise and where we again used the notation $\lambda_i = \pm 1$. We can now compare a couple of values of the integrals. A numerical integration of the Feynman parameter integral yields

$$
I_{sun}^{fp}(p = 1, m_1 = 11, m_2 = 13, m_3 = 17, \delta = 0) \approx 2,509745163 \times 10^{-6},
\tag{4.87}
$$

while evaluating the result of the residues, weighted by the appropriate combinatorial factors, results in

$$
I_{sun}^{LTD}(p = 1, m_1 = 11, m_2 = 13, m_3 = 17, \delta = 0) \approx 2,509745157 \times 10^{-6}
\tag{4.88}
$$

which shows that both approaches agree within a high degree of accuracy. We can furthermore compare the behaviour of the integrals as functions of p below the lowest pseudo-threshold, as shown in Figure 4.2. From this graph, it is easy to see that both results agree very precisely. This allows us to verify that the refined approach to the calculation of the residues, beyond one-loop, reproduces the correct results for the Feynman integrals.

4.3   Remarks

Let us give some closing remarks on the multi-loop LTD formula. As we saw in Eq.(4.65), the representation in terms of cuts is not unique. In fact, different ways to perform the multidimensional residue will yield different representations of the cut integrand, which evaluate to the correct integrated result.

One approach, first introduced at one-loop in [88] and subsequently generalized to multi-loop integrals [92, 93] is based on a distributional identity between the Feynman and advanced propagators, namely
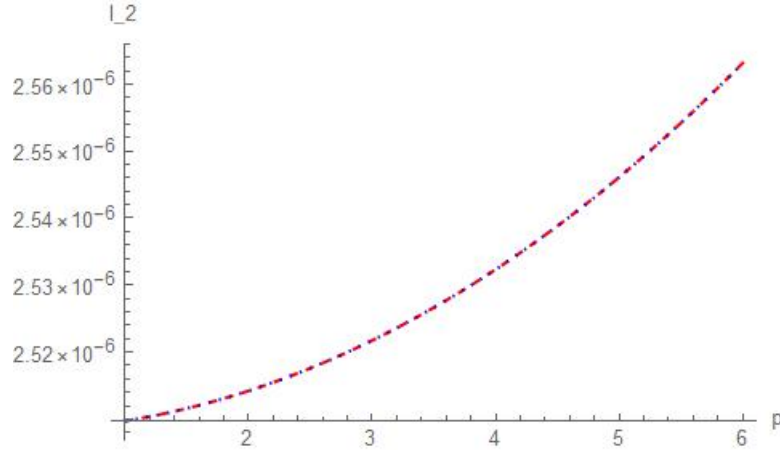
FIGURE 4.2: Plots of the 1D sunrise integral evaluated using the LTD formula of Eq.(4.83) (dotted line) and numerical evaluation of Eq.(4.34)(dashed line) as functions of p for $m_1 = 11, m_2 = 13, m_3 = 17$.

$$\frac{1}{D(k)} = \frac{1}{D_A(k)} + 2\pi i\theta(k_0)\delta(k^2) \tag{4.89}$$

where $D(k) = k^2 - m^2 + i\delta$ and $D_A(k) = k^2 - m^2 - ik_0\delta$ is the inverse advanced propagator. Since the latter has all is residues in the same hemisphere of the complex plane, integrals of products of these advanced propagators can be shown to vanish, thus leading to relations between integrals of Feynman propagators and cut integrals. Applications of this formulation of LTD have been considered in [94–101]. This process, which results analog to computing residues, only takes into account the poles coming from a definite closure of the integration contours. Moreover, the final result depends upon a mixture of Feynman and dual propagators. In contrast, the result obtained by the evaluation of the direct evaluation of the L-fold residue depends exclusively on dual propagators, making the definition of general rules to calculate the integrand simpler to implement. An advantage of the distributional method, however, is that the amounts of terms contributing to the integrand does not grow as rapidly with the number of loops due to the fact that there is no averaging procedure over the possible contour closures. The relation between both formulations has been explored in [102] and further mathematical explorations into the geometrical structure of LTD are pursued in [103, 104].

One final approach is that of [105–108], where the calculation of the residues is performed iteratively as in Eqs.(4.37) and (4.38), with a careful procedure to keep track of the position of the poles at each step of the iteration, while again only considering a single contour closing for each of the loop integrations. This approach results in a formula where the sum is performed over all possible loop momentum bases, in such a way that the complement of each set of propagators defining a basis yields a spanning tree. In this case,

every propagator has a modified prescription for the position of the poles of the uncut propagators, but again no averaging procedure is performed.

In either of these two approaches, the benefits from considering a single contour closing are most evident when computing individual Feynman integrals, since each of these receives a smaller amount of cut contributions. However, when trying to extend this approach to the direct calculation of the loop integrand for a scattering amplitude, the behaviour of the averaged sum of cuts allows to obtain recursion relations, akin to those encountered for tree level amplitudes, which means that one does not have to consider the generation and evaluation of every single Feynman diagram and instead just pick some generic building blocks to build up an amplitude at a fixed loop order with an arbitrary number of external edges. At the time of writing this thesis, no such structure is exhibited in the approaches to LTD where no averaging procedure is performed. The construction of the loop integrand and the recursion relations satisfied by it will be discussed in what follows.

Chapter 5

Integrands of Amplitudes from Loop-Tree Duality

In the previous chapters, we have seen, from different perspectives, how objects with the structure of loops can be related to tree-like objects. On the one hand, we discovered that graphs with internal loops can be cut in several ways to produce tree graphs and how to perform this process backwards by sewing pairs of external edges of tree graphs. We also found that the combinatorial aspects of both kinds of graphs are related to each other by proving that the symmetry factors associated to loop graphs are compensated when cutting the graph open by the different ways to assign markings to the cut lines. In this way, we are able to express a sum of loop graphs weighted with symmetry factors as a sum of tree graphs which can be sewed according to the markings into the original loop graphs.

From the perspective of Feynman integrals, the LTD formula allows to recast the loop integrand as a sum of tree-like quantities with a modified $i\delta$ prescription for the position of the poles in the complex plane. This, in turn, means that the representation of the loop integral in terms of loop Feynman graphs can be decomposed into a sum over tree graphs by suitably modifying the Feynman rules used to translate the graphs into the algebraic expression for the integrand.

Now, we are interested in taking this process one step forward and consider the behaviour of the complete, renormalized L-loop amplitude after applying LTD to each of the its individual contributions. In order to do this, we first do a thorough discussion of the forward limit of tree-like objects. We will introduce a technique that allows the counterterm to be written in a local form, so that they can be put in the same footing as the contributions to the bare amplitude, which allows for the application of the LTD formula to such contributions. Finally, taking advantage of the cancellation of the symmetry factors will allow us to define an integrand for the complete loop amplitude in terms of tree-like objects.

Although it is clear that defining "an" integrand for the loop amplitude is straightforwardly done, for example, by summing up the integrands to each individual Feynman integral contributing to the amplitude, what is not obvious is how to define an integrand with definite factorization properties

or that can be easily computed without first generating all the possible diagrams and extracting their values through the Feynman rules. The construction of integrands for loop amplitudes without explicit reference to the Feynman graphs has been considered in specific field theories and, in some cases, under certain conditions such as the planar limit or specific loop orders [109–122]. In contrast, we will see that the tree-like structure of the integrand defined through the application of LTD allows for its computation using a modified version of the Berends-Giele [123] recursion relations.

5.1   The regularized forward-limit

When we looked at the structure of cut and sewn graphs, we mentioned that tree graphs that can be sewn have the structure of a forward limit, by virtue of the fact that in order to consistently sew two external lines with momenta k and $\bar{k}$, these must satisfy the relation $\bar{k} = -k$. For an arbitrary tree amplitude or tree-like object, the forward limit is in general ill-defined, since some propagators might develop singularities in this limit. In this section, we introduce the regularized forward limit, which gives us a prescription for removing the contributions that become singular in the L-fold forward limit of any tree-like object.

Consider a tree amplitude with $(n + 2L)$ external particles

$$A^{(0)}_{n+2L}(p_1, \ldots, p_n; k_1, \ldots, k_L, \bar{k}_1, \ldots, \bar{k}_L) = \sum_{\Gamma \in U_{n+2L}} f(\Gamma) \tag{5.1}$$

where, for every graph Γ, $f(\Gamma)$ represents the expression obtained for it by application of the Feynman rules of the theory under consideration. We denote the masses of the external particles as

$$p_j^2 = (m_j^{ext})^2, \quad k_j^2 = \bar{k}_j^2 = m_j^2. \tag{5.2}$$

The conditions for a contribution to be singular in the L-fold forward limit

$$\lim_{\bar{k}_1 \to -k_1} \ldots \lim_{\bar{k}_L \to -k_L} A_n \tag{5.3}$$

depend only on the momenta carried by the propagators, meaning that they are independent of the detailed structure of the theory.

There are two different scenarios in which a propagator can become singular in the forward limit. The first one, where the propagator goes on-shell, is divided into two different cases. We can characterize the first of these by choosing a subset of indices $A \in \{1, 2, \ldots, L\}$. Any diagram where a propagator with momenta of the form

$$p_j + \sum_{a \in A} (k_a + \bar{k}_a) \tag{5.4}$$

for some $j \in \{1, ..., n\}$ and mass m_j^{ext} will go on-shell in the forward limit, because the terms in the sum cancel against each other when we take $\bar{k}_a \rightarrow -k_a$. Due to the fact that the momenta of a propagator is determined by the condition that the sum of the momenta entering any given vertex equals the sum of the momenta going out of it, we can see that a combination of the form $(k_a + \bar{k}_a) + p_j$ can only occur if the two lines with momenta k_a and $\bar{k}_a$ are separated by a single propagator. This implies that sewing these two lines yields a self-energy insertion into an external leg.

The second case in which a propagator can go on-shell is when we exchange p_j in Eq.(5.4) for some momenta k_b with $b \notin A$. In this case, the momenta of the singular propagator takes the form

$$k_b + \sum_{a \in A} (k_a + \bar{k}_a) \tag{5.5}$$

and then, if the propagator has mass m_b, it will go on-shell in the forward limit. Again, as in the previous case, the structure of such a propagator implies that any two lines k_a and $\bar{k}_a$ are separated only by a single propagator. In this case, since the line with momenta k_b is to be sewn with the line $\bar{k}_b$, sewing the lines with momenta k_a and $\bar{k}_a$ yields a loop graph with a self-energy insertion into an internal edge.

The second and final scenario where a contribution to the amplitude A_n can develop a singularity in the forward limit is the case where the corresponding diagram has a internal edge with momentum

$$\sum_{a \in A} (k_a + \bar{k}_a), \tag{5.6}$$

which results in a propagator with momentum zero. If the edge associated to this propagator is massless, the diagram will develop a singularity. Given that the only momenta in this propagator has the form of the sum of k_a and $\bar{k}_a$, we can see that sewing the two edges results into a tadpole insertion.

The different types of tree diagrams that develop singularities in the forward limit, after sewing, have the structure of the diagrams that represented problematic contributions to the loop amplitudes. We recognized, in that context, that the contributions coming from tadpoles or self-energy insertions to external legs can be dropped out of the calculation of any on-shell amplitude. In this spirit, let us define the set

$$U_{0,n+2L}^{ns} \tag{5.7}$$

to be the set of all tree graphs where propagators with momenta of the form of Eqs.(5.4), (5.5) and (5.6) are excluded. With this definition in mind, we set

$$\mathcal{R}_f A^{(0)}_{n+2L} = \lim_{\bar{k}_1 \to -k_1} \cdots \lim_{\bar{k}_L \to -k_L} \sum_{\Gamma \in U^{ns}_{0,n+2L}} f(\Gamma) \tag{5.8}$$

to be the regularized *L*-fold forward limit of the tree amplitude.

We can, at this point, define what is meant by a "tree-like object". The map from the Feynman diagrams to the amplitude is given by applying the Feynman rules to each graph Γ that contributes to the amplitude, which we represent by $f(\Gamma)$. The tree-like object associated to this amplitude is obtained by the replacement

$$f(\Gamma) \to S_{\sigma\alpha} f(\Gamma), \tag{5.9}$$

where $S_{\sigma\alpha}$ are the combinatorial factors of Eq.(4.76). This means that a tree-like object is directly related to a (set of) loop graph(s). The properties that characterize the singular behaviour of tree graphs in the forward limit is independent of the appearance of these combinatorial factors. Then, we define the regularized forward limit of a tree-like object in the same way we define it for a tree amplitude.

5.2   Local representation of counterterms and higher-order poles

Notice that, when defining $U^{ns}_{0,n+2L}$, we also exclude diagrams that yield self-energy insertion on internal edges upon sewing. These diagrams, however, can in general contribute to the scattering amplitudes and are characterized by the fact that they contain propagator raised to powers higher than one. From the theory of complex analysis, we know that, in order to compute the residue of a function with higher-order poles, one must compute derivatives of the function. In the case of Feynman integrals, such residues lead to objects that do not possess the structure of trees and, moreover, there is no general, process-independent way to compute them since the derivative will depend on the structure of the numerator of the loop integrand. Therefore, it would be beneficial if we could drop the contributions coming from the residues of diagrams of higher order poles. We now outline a procedure which allows for the construction of local counterterms, therefore solving the issue of putting bare and counterterm graphs at the same footing, which have the additional property of having cuts which cancel the contributions from the bare, higher-order poles. This procedure is showcased at the two-loop order. The ideas of this section follow [87].

We will discuss the technique in the context of ϕ^3 theory. The Lagrangian of this theory can be written as

$$\mathcal{L}_{\phi^3} = \frac{1}{2}\partial_\mu\phi\partial^\mu\phi - \frac{1}{2}m\phi^2 + \frac{\tilde{\lambda}}{3!}\phi^3 + \mathcal{L}_{CT} \tag{5.10}$$
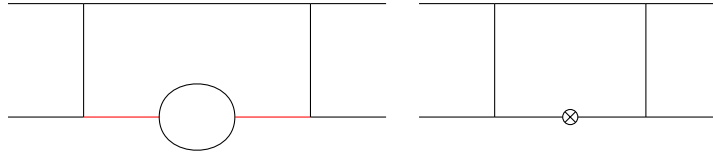
FIGURE 5.1: Two-loop diagram with a self-energy insertion on an internal propagator. The diagram contains a squared propagator, coming from the two red lines. The second diagram is the counterterm that cancels the UV subdivergences that originate from the self-energy insertion.

where we write $\tilde{\lambda} = \mu^\epsilon (4\pi)^\epsilon e^{-\epsilon\gamma} \lambda$ to absorb the usual factors of 4π and Euler's constant γ appearing in dimensional regularization. The counterterm Lagrangian is given by

$$\mathcal{L}_{CT} = -\frac{1}{2} \left(Z_\phi - 1 \right) \phi \partial^2 \phi - \frac{1}{2} \left(Z_\phi Z_m^2 - 1 \right) m^2 \phi^2 + \frac{1}{3!} \left(Z_\phi^{\frac{3}{2}} Z_\lambda - 1 \right) \tilde{\lambda} \phi^3.$$

(5.11)

We are interested in the perturbative expansion of the renormalization constants Z_ϕ and Z_m. These are calculated in detail in Appendix C. We would like to point out that these constants can also be written, up to one-loop order, as

$$Z_m = 1 + \frac{\lambda^2}{16\pi^2} \frac{1}{4m^2} B_0(m^2, m^2, m^2),$$

(5.12)

$$Z_\phi = 1 + \frac{\lambda^2}{16\pi^2} \left(\frac{2-\epsilon}{6m^2} B_0(m^2, m^2, m^2) - \frac{1-\epsilon}{3m^4} A_0(m^2) \right)$$

(5.13)

if one works in the on-shell scheme, in terms of the scalar integrals

$$A_0(m^2) = 16\pi^2 S_\epsilon^{-1} \mu^{2\epsilon} \int \frac{d^D k}{i(2\pi)^D} \frac{1}{k^2 - m^2}$$

(5.14)

and

$$B_0(p^2, m_1^2, m_2^2) = 16\pi^2 S_\epsilon^{-1} \mu^{2\epsilon} \int \frac{d^D k}{i(2\pi)^D} \frac{1}{(k^2 - m_1^2)((k-p)^2 - m_2^2)}.$$

(5.15)

We are interested in the structure of diagrams that contain self-energy insertions on internal edges. An example of such a diagram, with its accompanying counterterm, is shown in Fig. 5.1.

Using the short-hand notation for the propagators

$$D_i = k_i^2 - m_i^2 + i\delta \tag{5.16}$$

we can write the integral expression for the first diagram of Fig. 5.1 as

$$I_2 = \frac{i\lambda^6}{2}\mu^{4\epsilon}S_\epsilon^{-2}\int \frac{d^Dk_1}{(2\pi)^D}\frac{d^Dk_2}{(2\pi)^D}\frac{1}{D_1D_2^2D_3D_4D_5D_6} \tag{5.17}$$

where D_2 denotes the propagator associated to either of the red lines. If we attempted to apply the LTD formula to this diagram, any cut involving either of the red propagators would involve the calculation of the residue when $D_2 = 0$. Since this propagator appears to the power two, we would be forced to compute a derivative if we wanted to find the value of such a residue. This is problematic because the derivative destroys the tree-like structure of the resulting integrand. Moreover, the calculation of the derivative is process-dependant and hence not very well suited for automation. Hence, we will try and see if this contribution can be cancelled against some of the other contributions obtained after cutting.

The second diagram in Fig. 5.1 gives the counterterm contribution that cancels the UV subdivergences of the self-energy insertion in the two-loop bare diagram. Using the Feynman rules for the counterterm Lagrangian, we obtain the value

$$I_2^{CT} = -\frac{\lambda^6}{(4\pi)^2}\mu^{2\epsilon}S_\epsilon^{-1}\int \frac{d^Dk_2}{(2\pi)^D}\frac{Z_\phi^{(1)}k_2^2 - \left(Z_\phi^{(1)} + 2Z_m^{(1)}\right)m^2}{D_2^2D_3D_4D_5}. \tag{5.18}$$

Notice that there is only one integration involved in the definition of the counterterm diagram, while the bare diagram involves two different loop integrations. Therefore, the cancellation of the UV divergences is realized only after all integrations are performed. We would like to find a representation of the counterterm, such that it involves two integrations as well.

Let us introduce the short-hand notation

$$R_2(k_1, k_2) = \frac{1}{2D_1D_2^2D_3D_4D_5D_6} \tag{5.19}$$

for the integrand of the the bare, two-loop diagram. We want to find a representation for the counterterm diagram of the form

$$I_2^{CT} = i\lambda^6\mu^{4\epsilon}S_\epsilon^{-2}\int \frac{d^Dk_1}{(2\pi)^D}\frac{d^Dk_2}{(2\pi)^D}R_2^{CT}(k_1, k_2) \tag{5.20}$$

where $R_2^{CT}(k_1, k_2)$ is a rational function in the energies E_1 and E_2. We would like to impose the following conditions on the counterterm integrand:

1. Integrating over k_1 results in the same expression for the counterterm as in Eq.(5.18).

2. The sum of the bare and counterterm integrands behaves as

$$\lim_{|\vec{k}_1| \to \infty} \left(R_2(k_1, k_2) + R_2^{CT}(k_1, k_2) \right) = \mathcal{O}(|\vec{k}_1|^{-5}) \qquad (5.21)$$

3. Let $p = (E, \vec{p})$ be an arbitrary D-momentum. We can associate to this variable an on-shell momentum via $\tilde{p} = (sgn(E)\sqrt{|\vec{p}|^2 + m^2}, \vec{p})$. With this notation, we also demand that

$$\lim_{k_2^2 \to m^2} \left(R_2(k_1, k_2) + R_2^{CT}(k_1, k_2) \right) = \mathcal{O}\left((E_2 - \tilde{E}_2)^2 \right) \qquad (5.22)$$

that is, the combination of the bare and counterterm integrands vanishes quadratically as k_2 goes on-shell,

4. $R_2^{CT}(k_1, k_2)$ has no poles in E_2.

The first condition is simply the requirement that the candidate integrand R_2^{CT} is consistent with the result for the counterterm obtained from the renormalized Lagrangian. The second requirement implies that the UV divergences associated to the self-energy subgraph are cancelled locally. To understand why, we set $D = 4$. Then, in the limit $|\vec{k}_1| \to \infty$, assuming condition 2 holds,

$$\int d^4k_1 \left(R_2(k_1, k_2) + R_2^{CT}(k_1, k_2) \right) \propto \int d^4k_1 \frac{1}{|\vec{k}_1|^5}$$
$$\propto \int^{\infty} \frac{|\vec{k}_1|^3 dk_1}{|\vec{k}_1|^5} \qquad (5.23)$$
$$= \int^{\infty} \frac{dk_1}{|\vec{k}_1|^2}$$

which means that the sum of the bare and counterterm integrands is regular in the UV region of k_1. Thus, conditions 1 and 2 alone secure that R_2^{CT} would be a proper local counterterm for the bare two-loop diagram. In this regard, we have already managed to solve one of the issues we first mentioned when discussing the structure of counterterms in regards to LTD, which was to put them in the same footing as the bare loop contributions.

The third condition is imposed further to achieve the cancellation of the residue when $D_2 = 0$ of the original loop graph, while the last condition ensures that I_{2L}^{CT} does not receive contributions from cutting both propagators of the self-energy insertion on the loop diagram. It is worth noting that all of these conditions can be imposed only on the structure of the self-energy
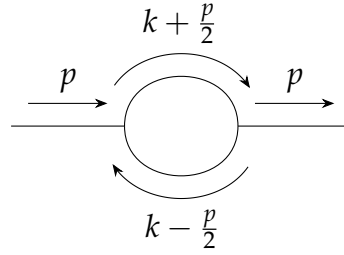
FIGURE 5.2: One-loop self-energy subgraph.

subgraph, and are independent of the remaining parts of the full diagram. Therefore, any diagram with a one-loop self-energy insertion on an internal edge would be constructed in the same fashion, meaning that this procedure is process independent. Given this considerations, it will be sufficient for us to consider the behaviour of the one-loop sub-graph in order to determine the form of R_2^{CT}.

Consider the one-loop self-energy graph, with momenta as in Fig. 5.2. We write the associated integral expression as

$$- i\Sigma_1 = \lambda^2 \mu^{2\epsilon} S_\epsilon^{-1} \int \frac{d^D k}{(2\pi)^D} R_1(k) \tag{5.24}$$

where we define the integrand

$$R_1(k) = \frac{1}{2D_+ D_-} \tag{5.25}$$

in terms of the propagators $D_\pm = \left(k \pm \frac{p}{2}\right)^2 - m^2$. This diagram is accompanied by the counterterm

$$\underline{\quad\quad\otimes\quad\quad} = i \left[(Z_\phi^- 1) p^2 - (Z_\phi Z_m^2 - 1) m^2 \right] \tag{5.26}$$

where, to one-loop order, we only keep the appropriate powers of Z_ϕ and Z_m. If we let $Z_\phi^{(1)}$ and $Z_m^{(1)}$ be the coefficients multiplying $\lambda^2 / 16\pi^2$ in Eqs. (5.13) and (5.12), we can see that the appropriate counterterm at one-loop is given by

$$- i\Sigma_1^{CT} = \frac{i\lambda^2}{16\pi^2} \left[Z_\phi^{(1)} p^2 - (Z_\phi^{(1)} + 2Z_m^{(1)}) m^2 \right]. \tag{5.27}$$

We want to find an integral representation

$$- i\Sigma_1^{CT} = \lambda^2 \mu^{2\epsilon} S_\epsilon^{-1} \int \frac{d^D k}{(2\pi)^D} R_1^{CT}(k) \tag{5.28}$$

satisfying the conditions imposed on the two-loop counterterm, if we identify k with k_1 and p with k_2. We can achieve this by defining

$$\tilde{D}_\pm = \left(k \pm \frac{\tilde{p}}{2} \right)^2 - m^2 \tag{5.29}$$

and expanding the propagators $D_\pm$ around the on-shell kinematics defined by $\tilde{D}_\pm$. To perform this expansion, we first use the identity

$$\frac{1}{(k - q_1)^2 - m_1^2} = \frac{1}{(k - q_2)^2 - m_2^2}$$
$$\times \left[1 - \frac{2(k - q_2) \cdot (q_1 - q_2) - (q_1 - q_2)^2 + m_1^2 - m_2^2}{(k - q_2)^2 - m_2^2} \right]^{-1} \tag{5.30}$$

which is easily shown to hold by simplifying the expression inside the bracket on the right-hand side of the equation. We can use this identity to express the propagators $1/D_\pm$ in terms of $1/\tilde{D}_\pm$, and then expand the bracket in $(p - \tilde{p})$. For example, to expand D_+ in terms of $\tilde{D}_+$, we first notice that $m_1 = m_2 = m$. Then, the last term on the bracket drops out, and

$$\frac{1}{\left(k + \frac{p}{2}\right)^2 - m^2} = \frac{1}{\left(k + \frac{\tilde{p}}{2}\right)^2 - m^2}$$
$$\times \left[1 - \frac{2\left(k + \frac{\tilde{p}}{2}\right) \cdot \left(-\frac{p+\tilde{p}}{2}\right) + \left(-\frac{p}{2} + \frac{\tilde{p}}{2}\right)^2}{\left(k + \frac{\tilde{p}}{2}\right)^2 - m^2} \right]^{-1}$$
$$= \frac{1}{\left(k + \frac{\tilde{p}}{2}\right)^2 - m^2} \tag{5.31}$$
$$\times \left[1 - \frac{4\left(k + \frac{\tilde{p}}{2}\right) \cdot (p - \tilde{p}) + (p - \tilde{p})^2}{4\left(\left(k + \frac{\tilde{p}}{2}\right)^2 - m^2\right)} \right]^{-1}.$$

We can simplify the expression in the numerator inside the bracket, using the fact that $\tilde{p}^2 = m^2$, to obtain

$$4\left(k + \frac{\tilde{p}}{2}\right) \cdot (p - \tilde{p}) + (p - \tilde{p})^2$$
$$= 4k \cdot (p - \tilde{p}) + 2p \cdot \tilde{p} - 2m^2 + p^2 - 2p \cdot \tilde{p} + m^2 \tag{5.32}$$
$$= 4k \cdot (p - \tilde{p}) + p^2 - m^2,$$

and then, using the Taylor expansion

$$(1 + x)^{-1} = 1 - x + \mathcal{O}(x^2) \tag{5.33}$$

we can expand the bracket to first order in $(p - \tilde{p})$ to obtain

$$\frac{1}{D_+} = \frac{1}{\tilde{D}_+} \left[1 - \frac{4k \cdot (p - \tilde{p}) + p^2 - m^2}{4\tilde{D}_+} \right] + \mathcal{O}((p - \tilde{p})^2). \qquad (5.34)$$

An analogous computation yields the expansion of $1/D_-$ around $1/\tilde{D}_-$, and we simply quote the result:

$$\frac{1}{D_-} = \frac{1}{\tilde{D}_-} \left[1 + \frac{4k \cdot (p - \tilde{p}) - p^2 + m^2}{4\tilde{D}_-} \right] + \mathcal{O}((p - \tilde{p})^2). \qquad (5.35)$$

These two results allow us to obtain the expansion of the integrand for the one-loop self-energy around the on-shell kinematics defined by the vector $\tilde{p}$,

$$\begin{aligned}
\frac{1}{2D_+D_-} &\approx \frac{1}{2\tilde{D}_+\tilde{D}_-} \\
&\times \left[1 - \frac{4k \cdot (p - \tilde{p}) + p^2 - m^2}{4\tilde{D}_+} + \frac{4k \cdot (p - \tilde{p}) - p^2 + m^2}{4\tilde{D}_-} \right].
\end{aligned} \qquad (5.36)$$

This expansion fulfills condition 2, since each of the terms in the difference between R_1 and the expansion has three propagators, while having a single power of k in the numerator. Thus, when $k \to \infty$, each of the contributions vanish as $|\vec{k}|^{-5}$ or better. Furthermore, in the limit where p goes on-shell with mass m, the terms linear in $(p^2 - m^2)$ drop out, which means that this difference behaves in the limit as $\mathcal{O}((p^2 - m^2)^2)$. This implies that this term also satisfies condition 3. Furthermore, condition 4 is trivially satisfied since the inverse propagators $\tilde{D}_\pm$ are independent of the energy E associated to p. It only remains to see whether condition 1 is satisfied.

Define E_1^{CT} to be the result of the expansion in Eq.(5.36). We would like to integrate over k and express the result in terms of the counterterm of Eq.(5.27), with $Z_\phi^{(1)}$ and $Z_m^{(1)}$ defined as in Eqs. (5.13) and (5.12). We will need a redefinition of the loop integral $B_0(p^2, m_1^2, m_2^2)$ of Eq.(5.15),

$$B_0(p^2, m_1^2, m_2^2) = 16\pi^2 S_\epsilon^{-1} \mu^{2\epsilon} \int \frac{d^D k}{i(2\pi)^D} \frac{1}{\left((k - \frac{p}{2})^2 - m_1^2 \right)\left((k + \frac{p}{2}))^2 - m_2^2 \right)}, \qquad (5.37)$$

obtained by shifting $k \to k - \frac{p}{2}$. Instead of explicitly evaluating the integrals, we are going to express the integrals resulting from integrating E_1^{CT} over $d^D k$ in terms of $A_0(m^2)$ and $B_0(m^2, m^2, m^2)$. This will require us to perform a tensor reduction [124] in the terms with a non-trivial numerator, as well as the use of integration-by-parts (IBP) relations, which relate integrals with the same number of propagators raised to different powers.

As a first step, let us group the terms of E_1^{CT} in an appropriate fashion, namely

$$
E_1^{CT} = -\frac{1}{2\tilde{D}_+\tilde{D}_-} + \frac{k \cdot (p - \tilde{p})}{2} \left(\frac{1}{\tilde{D}_+^2 \tilde{D}_-} - \frac{1}{\tilde{D}_+\tilde{D}_-^2} \right)
$$
$$
+ \frac{p^2 - m^2}{8} \left(\frac{1}{\tilde{D}_+^2 \tilde{D}_-} + \frac{1}{\tilde{D}_+\tilde{D}_-^2} \right).
\tag{5.38}
$$

We want to integrate E_1^{CT} over k, multiplying by a factor of $\lambda^2 \mu^{2\epsilon} S_\epsilon^{-1}$, express the result in terms of $A_0(m^2)$ and $B_0(m^2, m^2, m^2)$, and then use

$$
Z_m^{(1)} = \frac{1}{4m^2} B_0(m^2, m^2, m^2)
\tag{5.39}
$$

and

$$
Z_\phi^{(1)} = \frac{2 - \epsilon}{6m^2} B_0(m^2, m^2, m^2) - \frac{1 - \epsilon}{3m^4} A_0(m^2)
\tag{5.40}
$$

to write the result in terms of the renormalization constants. In the remainder of this section, we will write $A_0 = A_0(m^2)$ and $B_0 = B_0(m^2, m^2, m^2)$, as well as

$$
\int_k = \mu^{2\epsilon} S_\epsilon^{-1} \int \frac{d^D k}{(2\pi)^D},
\tag{5.41}
$$

in order to shorten the notation. From the definition of the integral B_0 and the fact that $\tilde{p}^2 = m^2$, we can see that

$$
\int_k \frac{1}{\tilde{D}_+\tilde{D}_-} = \frac{i}{16\pi^2} B_0
\tag{5.42}
$$

The two remaining contributions require additional work. We can simplify the calculation by noting that, for any vector q that is independent of k, performing the transformation $k \rightarrow -k$ yields the relation

$$
\int_k \frac{k \cdot q}{\tilde{D}_+^2 \tilde{D}_-} = \int_k \frac{k \cdot q}{\left(\left(k + \frac{\tilde{p}}{2} \right) - m^2 \right)^2 \left(\left(k - \frac{\tilde{p}}{2} \right) - m^2 \right)}
$$
$$
= -\int_k \frac{k \cdot q}{\left(\left(-k + \frac{\tilde{p}}{2} \right) - m^2 \right)^2 \left(\left(-k - \frac{\tilde{p}}{2} \right) - m^2 \right)}
$$
$$
= -\int_k \frac{k \cdot q}{\tilde{D}_+\tilde{D}_-^2}
\tag{5.43}
$$

where we pick a single minus sign due to the power of k in the numerator, while the factor of $(-1)^D$ from the integration measure cancels when we invert the order of the D integrals. By an equivalent argument, we find

$$\int_k \frac{1}{\tilde{D}_+^2 \tilde{D}_-} = \int_k \frac{1}{\tilde{D}_+ \tilde{D}_-^2} \tag{5.44}$$

with which we write

$$\int_k E_1^{CT} = -\frac{1}{2} \int_k \frac{1}{\tilde{D}_+ \tilde{D}_-} + \int_k \frac{k \cdot (p - \tilde{p})}{\tilde{D}_+^2 \tilde{D}_-} + \frac{p^2 - m^2}{4} \int_k \frac{1}{\tilde{D}_+^2 \tilde{D}_-}. \tag{5.45}$$

Given that the first integral is immediate, we only need to perform the other two. The integral with a power of k in the numerator is related to the tensor integral

$$\int_k \frac{k^\mu}{\tilde{D}_+^2 \tilde{D}_-}. \tag{5.46}$$

Notice that, since the only vector left after performing this integral is $\tilde{p}$, the result must be proportional to it. Thus, if we take the ansatz

$$\int_k \frac{k^\mu}{\tilde{D}_+^2 \tilde{D}_-} = a\tilde{p}^\mu \tag{5.47}$$

we find, by contracting each side with $\tilde{p}$ and using the condition $\tilde{p}^2 = m^2$,

$$a = \frac{1}{m^2} \int_k \frac{k \cdot \tilde{p}}{\tilde{D}_+^2 \tilde{D}_-}. \tag{5.48}$$

We can express this integral in terms of integrals with fewer powers of the denominators, using the identity

$$\begin{aligned} 2k \cdot \tilde{p} &= \left(k + \frac{\tilde{p}}{2}\right)^2 - \left(k - \frac{\tilde{p}}{2}\right)^2 \\ &= \tilde{D}_+ - \tilde{D}_- \end{aligned} \tag{5.49}$$

which implies that $k \cdot \tilde{p} = \frac{1}{2}(\tilde{D}_+ - \tilde{D}_-)$, and then

$$\begin{aligned} a &= \frac{1}{2m^2} \int_k \frac{\tilde{D}_+ - \tilde{D}_-}{\tilde{D}_+^2 \tilde{D}_-} \\ &= \frac{1}{2m^2} \int_k \left(\frac{1}{\tilde{D}_+ \tilde{D}_-} - \frac{1}{\tilde{D}_+^2}\right). \end{aligned} \tag{5.50}$$

The first of these two integrals is expressed directly in terms of B_0. The second one, however, has a single propagator squared; we would like to express this integral in terms of A_0 and B_0. In order to do this, we define the family of integrals

$$J(a) = \int_k \frac{1}{(k^2 - m^2)^a} \tag{5.51}$$

which can be seen to be the tadpole integrals discussed previously. We can find relations amongst integrals with different power, by noting that, in D spacetime dimensions,

$$
\begin{aligned}
0 &= \int_k \frac{\partial}{\partial k^\mu} \left(\frac{k^\mu}{(k^2 - m^2)^a} \right) \\
&= DJ(a) - 2a \int_k \frac{k^2}{(k^2 - m^2)^{a+1}} \\
&= DJ(a) - 2a \int_k \frac{k^2 - m^2 + m^2}{(k^2 - m^2)^{a+1}} \\
&= DJ(a) - 2aJ(a) - 2am^2 J(a+1),
\end{aligned}
\tag{5.52}
$$

which is a consequence of the fact that surface terms coming from Feynman integrals vanish. This yields the recurrence relation[1]

$$
J(a+1) = \frac{D - 2a}{2am^2} J(a).
\tag{5.53}
$$

Then, if we notice that

$$
J(1) = \int_k \frac{1}{(k^2 - m^2)} = \frac{i}{16\pi^2} A_0
\tag{5.54}
$$

(shifting $k \to k \pm \frac{\tilde{p}}{2}$ does not change the value of the integral), we find

$$
J(2) = \frac{D - 2}{2m^2} J(1) = \frac{D - 2}{2m^2} \frac{i}{16\pi^2} A_0.
\tag{5.55}
$$

But, from its definition, $J(2)$ is equal to the integral of $1/D_+^2$. Thus, we can finally write, using $D - 2 = 2 - 2\epsilon$,

$$
\begin{aligned}
a &= \frac{1}{2m^2} \left(\frac{i}{16\pi^2} B_0 - \frac{1 - \epsilon}{m^2} \frac{i}{16\pi^2} A_0 \right) \\
&= \frac{i}{32\pi^2 m^2} \left(B_0 - \frac{1 - \epsilon}{m^2} A_0 \right)
\end{aligned}
\tag{5.56}
$$

which gives the final result

$$
\int_k \frac{k \cdot (p - \tilde{p})}{\tilde{D}_+^2 \tilde{D}_-} = \frac{i\tilde{p} \cdot (p - \tilde{p})}{32\pi^2 m^2} \left(B_0 - \frac{1 - \epsilon}{m^2} A_0 \right).
\tag{5.57}
$$

Now, we are left with the last integration, which involves an integrand with three propagators. Let us, then, attempt to derive a set of IBP relations for the family of integrals

$$
I(a_1, a_2) = \int_k \frac{1}{\tilde{D}_+^{a_1} \tilde{D}_-^{a_2}}.
\tag{5.58}
$$

---

[1] This is the simplest example of an IBP relation.

We begin by writing down a formula for the derivatives

$$\frac{\partial}{\partial k^\mu} \tilde{D}_\pm = \frac{\partial}{\partial k^\mu} \left(k \pm \frac{\tilde{p}}{2} \right)^2$$
$$= 2 \left(k_\mu \pm \frac{\tilde{p}_\mu}{2} \right)$$

(5.59)

so that

$$0 = \int_k \frac{\partial}{\partial k^\mu} \left(\frac{k^\mu}{\tilde{D}_+^{a_1} \tilde{D}_-^{a_2}} \right)$$
$$= DI(a_1, a_2) - 2a_1 \int_k \frac{k \cdot \left(k + \frac{\tilde{p}}{2} \right)}{\tilde{D}_+^{a_1+1} \tilde{D}_-^{a_2}} - -2a_2 \int_k \frac{k \cdot \left(k - \frac{\tilde{p}}{2} \right)}{\tilde{D}_+^{a_1} \tilde{D}_-^{a_2+1}}.$$

(5.60)

We proceed to simplify these expressions by rewriting the numerators in terms of the denominators. Using Eq.(5.49), we find

$$k \cdot \left(k + \frac{\tilde{p}}{2} \right) = \frac{3}{4} D_+ + \frac{1}{4} D_- + \frac{3}{4} m^2$$

(5.61)

from which, exchanging $p \to -p$, we obtain

$$k \cdot \left(k - \frac{\tilde{p}}{2} \right) = \frac{1}{4} D_+ + \frac{3}{4} D_- + \frac{3}{4} m^2.$$

(5.62)

This allows us to rewrite

$$0 = DI(a_1, a_2) - \frac{a_1}{2} \left(3I(a_1, a_2) + I(a_1 + 1, a_2 - 1) + 3m^2 I(a_1 + 1, a_2) \right)$$
$$- \frac{a_2}{2} \left(3I(a_1, a_2) + I(a_1 - 1, a_2 + 1) + 3m^2 I(a_1, a_2 + 1) \right)$$
$$= \left(D - \frac{3}{2}(a_1 + a_2) \right) I(a_1, a_2) - \frac{a_1}{2} I(a_1 + 1, a_2 - 1)$$
$$- \frac{a_2}{2} I(a_1 - 1, a_2 + 1) - \frac{3m^2}{2} \left(a_1 I(a_1 + 1, a_2) + a_2 I(a_1, a_2 + 1) \right).$$

(5.63)

We can use these set of identities to find the value of the missing integral, which we can identify with $I(2,1)$. Then, setting $a_1 = a_2 = 1$ and noting that Eq.(5.44) implies that $I(2,1) = I(1,2)$, as well as $I(a,0) = I(0,a)$, we find

$$0 = (D - 3)I(1,1) - I(2,0) - 3m^2 I(2,1)$$

(5.64)

which implies

$$I(2,1) = \int_k \frac{1}{\tilde{D}_+^2 \tilde{D}_-}$$
$$= \frac{i}{48\pi^2 m^2} \left((1-2\epsilon) B_0 - \frac{1-\epsilon}{m^2} A_0 \right). \tag{5.65}$$

Putting everything together, we arrive at the result

$$\lambda^2 \int_k E_1^{CT} = \frac{i\lambda^2}{16\pi^2} \left[-\frac{B_0}{2} + \frac{p \cdot \tilde{p} - m^2}{2m^2} \left(B_0 - \frac{1-\epsilon}{m^2} A_0 \right) \right.$$
$$\left. + \frac{p^2 - m^2}{12m^2} \left((1-2\epsilon) B_0 - \frac{1-\epsilon}{m^2} A_0 \right) \right]. \tag{5.66}$$

We can invert Eqs.(5.39) and (5.40) in order to write the integrals B_0 and A_0 in terms of the renormalization factors as

$$B_0 = 4m^2 Z_m^{(1)}, \tag{5.67}$$

$$A_0 = \frac{2(2-\epsilon)}{1-\epsilon} m^4 Z_m^{(1)} - \frac{3m^4}{1-\epsilon} Z_\phi^{(1)}. \tag{5.68}$$

Substitution of these values in Eq.(5.66) results, after some algebra, in

$$\int_k E_1^{CT} = \frac{i\lambda^2}{16\pi^2} \left[Z_\phi^{(1)} p^2 - (Z_\phi^{(1)} + 2Z_m^{(1)}) m^2 \right.$$
$$\left. + G_1 p^2 + G_2 m^2 + G_3 p \cdot \tilde{p} \right] \tag{5.69}$$

where G_1, G_2 and G_3 are functions linear in $Z_\phi^{(1)}$ and $Z_m^{(1)}$. We can see that the integral of E_1^{CT} does not reproduce the integrated counterterm of Eq. (5.27). This could be anticipated by noting that the prefactor in front of $p \cdot \tilde{p}$ is non-vanishing for generic values of m and there is no such contribution in the integrated counterterm. We must find, then, an additional contribution which still satisfies conditions 2,3 and 4, while ensuring that the additional terms in the integration of E_1^{CT} drop out. With this in mind, the authors of [87] propose

$$R_1^{CT} = -\frac{1}{2\tilde{D}_+ \tilde{D}_-} \left[1 - \frac{4k \cdot (p - \tilde{p}) + p^2 - m^2}{4\tilde{D}_+} + \frac{4k \cdot (p - \tilde{p}) - p^2 + m^2}{4\tilde{D}_-} \right]$$
$$+ \frac{(p - \tilde{p})^2}{8m^2} \left(\frac{2}{\tilde{D}_+ \tilde{D}_-} - \frac{1}{(\tilde{D}_+)^2} - \frac{1}{(\tilde{D}_-)^2} \right). \tag{5.70}$$

Let us denote by M_1^{CT} the correction term in the second line. We can use

the results of Eqs.(5.55) and (5.42) to derive the value of its integral over k, in terms of A_0 and B_0, as

$$
\begin{aligned}
\lambda^2 \int_k M_1^{CT} &= \frac{\lambda^2 (p - \tilde{p})^2}{8m^2} \left(\frac{2i}{16\pi^2} B_0 - \frac{2(1-\epsilon)}{m^2} \frac{i}{16\pi^2} A_0 \right) \\
&= \frac{i\lambda^2}{16\pi^2} \left[\frac{p^2 + m^2}{4m^2} \left(B_0 - \frac{1-\epsilon}{m^2} A_0 \right) \right. \\
&\qquad \left. - \frac{p \cdot \tilde{p}}{2m^2} \left(B_0 - \frac{1-\epsilon}{m^2} A_0 \right) \right] .
\end{aligned}
\tag{5.71}
$$

Comparing with Eq.(5.66), we can see that the terms proportional to $p \cdot \tilde{p}$ are equal and opposite in sign, so they drop out after integration of R_1^{CT}. Adding the remaining contributions, we find

$$
\lambda^2 \int_k R_1^{CT} = \frac{\lambda^2}{16\pi^2} i \left[Z_\phi^{(1)} p^2 - (Z_\phi^{(1)} + 2Z_m^{(1)}) m^2 \right] ,
\tag{5.72}
$$

as required. We can see that the correction M_1^{CT} does not spoil any of the other conditions. Condition 4 is trivial because of the fact that M_1^{CT} depends on p only through the numerator $(p - \tilde{p})^2$. Condition 3 also follows from the polynomial dependence on the numerator. Thus, we must show that condition 2 is also satisfied. We can prove this by noting that

$$
\begin{aligned}
\frac{2}{\tilde{D}_+ \tilde{D}_-} - \frac{1}{(\tilde{D}_+)^2} - \frac{1}{(\tilde{D}_-)^2} &= - \left(\frac{1}{\tilde{D}_+} - \frac{1}{\tilde{D}_-} \right)^2 \\
&= - \left(\frac{\tilde{D}_- - \tilde{D}_+}{\tilde{D}_+ \tilde{D}_-} \right)^2 \\
&= - \frac{(2k \cdot \tilde{p})^2}{\tilde{D}_+^2 \tilde{D}_-^2} \\
&\propto \frac{1}{|\vec{k}|^6}
\end{aligned}
\tag{5.73}
$$

for $|\vec{k}| \to \infty$. Thus, all conditions are satisfied and we have managed to find a local representation for the counterterm. All that is left to show is that the sum of the residues of the counterterm and the bare diagram in the variable k vanish quadratically in the on-shell limit to prove that the contributions coming from cuts of raised propagators vanishes in the sum between bare and counterterm graphs, which is what we need in order to obtain tree-like objects after application of the LTD formula at higher loops.

We will consider the example of one of the poles of the sum $R_1 + R_1^{CT}$ to exhibit the behaviour of the residue in the on-shell limit. The bare integrand R_1, defined by

$$R_1 = \frac{1}{2D_+ D_-} \tag{5.74}$$

with

$$D_\pm = \left(k \pm \frac{p}{2}\right)^2 - m^2 \tag{5.75}$$

has four poles in the variable k_0, the energy component of the loop momentum, that arise when each of the propagators go on-shell. We can find the position of the poles of, say, D_+, by solving

$$D_+ = 0, \quad \rightarrow$$
$$\left(k_0 + \frac{E}{2}\right)^2 = \pm \sqrt{\left|\vec{k} + \frac{\vec{p}}{2}\right|^2 + m^2} \tag{5.76}$$
$$= \pm E_k$$

where we define

$$E_k = \sqrt{\left|\vec{k} + \frac{\vec{p}}{2}\right|^2 + m^2}. \tag{5.77}$$

Let us denote the poles of D_+ by

$$k_0^\pm = -E/2 \pm E_k. \tag{5.78}$$

We compute the residue of R_1 at $k_0 = k_0^+$. As a first step, we factorize

$$D_+ = (k_0 - k_0^+)(k_0 - k_0^-) \tag{5.79}$$

so that, using the standard formula for the residue at a single pole, we find

$$Res\left(\frac{1}{2D_+ D_-}, k_0 = k_0^+\right) = \frac{1}{2} \lim_{k_0 \to k_0^+} \left(\frac{k - k_0^+}{(k_0 - k_0^+)(k_0 - k_0^-)D_-}\right)$$
$$= \frac{1}{2(k_0^+ - k_0^-)} \frac{1}{D_-} \tag{5.80}$$
$$= \frac{1}{2E_k} \frac{1}{D_-}$$

where D_- is understood to be evaluated at $k_0 = k_0^+$. On the other hand, we can see from Eq.(5.70) that R_1^{CT} has double poles in k_0, coming from the squared propagators. For example, the poles of the propagator $\tilde{D}_+$ are located at

$$\tilde{k}_0^\pm = -\frac{\tilde{E}}{2} \pm E_k \tag{5.81}$$

where we used the fact that the spatial components of p and $\tilde{p}$ are equal to each other. Each of the terms in R_1^{CT} has a different pole structure, according to the power of D_+ and D_- that appear in the denominator. Therefore, we compute each residue accordingly. The first contribution is equivalent to the residue of R_1,

$$Res\left(\frac{1}{2\tilde{D}_+\tilde{D}_-}, k_0 = k_0^+\right) = \frac{1}{2E_k}\frac{1}{\tilde{D}_-} \tag{5.82}$$

where, as in the previous calculation, $\tilde{D}_-$ is understood to be evaluated at $k_0 = \tilde{k}_0^+$. To compute the remaining residues, we first note that

$$k \cdot (p - \tilde{p}) = k_0(E - \tilde{E}). \tag{5.83}$$

Hence, writing $\tilde{D}_+ = (k_0 - \tilde{k}_0^+)(k_0 - \tilde{k}_0^-)$, we can compute

$$
\begin{aligned}
Res\left(\frac{k_0(E - \tilde{E})}{2\tilde{D}_+^2\tilde{D}_-}\right) &= \frac{1}{2}\lim_{k_0 \to \tilde{k}_0^+}\frac{d}{dk_0}\left(\frac{k_0(E - \tilde{E})(k_0 - k_0^+)^2}{\tilde{D}_-(k_0 - k_0^-)^2(k_0 - k_0^+)^2}\right) \\
&= \frac{1}{2}\lim_{k_0 \to \tilde{k}_0^+}\frac{d}{dk_0}\left(\frac{k_0(E - \tilde{E})}{\tilde{D}_-(k_0 - k_0^-)^2}\right) \\
&= \frac{E - \tilde{E}}{8\tilde{D}_-E_k^2} - \frac{(E - \tilde{E})(E_k - \tilde{E})\left(E_k - \frac{\tilde{E}}{2}\right)}{2E_k^2\tilde{D}_-^2} \\
&\quad - \frac{(E - \tilde{E})\left(E_k - \frac{\tilde{E}}{2}\right)}{4E_k^3\tilde{D}_-},
\end{aligned}
\tag{5.84}
$$

which illustrates how the computation of derivatives destroys the tree structure of the residues that come from propagators with simple poles. The other residues are calculated in analogous fashion, and we find

$$
\begin{aligned}
Res(R_1^{CT}, k_0 = \tilde{k}_0^+) &= -\frac{1}{4E_k\tilde{D}_-} + \frac{(E - \tilde{E})^2}{8E_k m^2\tilde{D}_-} + \frac{(E - \tilde{E})^2}{32E_k^3 m^2} - \frac{(E - \tilde{E})^2}{32E_k^3\tilde{D}_-} \\
&\quad - \frac{(E_k - \tilde{E})(E - \tilde{E})}{2E_k\tilde{D}_-^2} + \frac{\tilde{E}(E - \tilde{E})^2}{16E_k^2\tilde{D}_-^2}
\end{aligned}
\tag{5.85}
$$

which reproduces the results of [87]. Looking at the result for the residue of R_1^{CT}, we see that most of the contributions already vanish quadratically in the limit where p goes on-shell, because of the explicit factors of $(E - \tilde{E})^2$ in the numerators. When we sum the residues of R_1 and R_1^{CT}, the only term which does not explicitly vanish in this limit is given by

$$\frac{1}{4E_k}\left[\frac{1}{D_-} - \frac{1}{\tilde{D}_-} - \frac{2(E_k - \tilde{E})(E - \tilde{E})}{\tilde{D}_-^2}\right], \tag{5.86}$$

but, recalling that each propagator in this expression is evaluated at k_0^+ and $\tilde{k}_0^+$ for D_- and $\tilde{D}_-$, respectively. This implies that

$$\tilde{D}_- - D_- = (E_k - \tilde{E})^2 - (E_k - E)^2 = (E - \tilde{E})(2E_k - E - \tilde{E}) \qquad (5.87)$$

which in turn means that we can factorize $(E - \tilde{E})$ from the bracket in Eq.(5.86), with the remaining factor given by

$$\frac{2E_k - E - \tilde{E}}{D_- \tilde{D}_-} - \frac{2(E_k - \tilde{E})}{\tilde{D}_-^2}. \qquad (5.88)$$

In the strict on-shell limit, we have $E = \tilde{E}$ and $D_- = \tilde{D}_-$. This implies that the zero-th order term in the Taylor expansion of Eq.(5.88) in $(E - \tilde{E})$ vanishes, meaning that the expansion begins at $\mathcal{O}(E - \tilde{E})$. Taking into account that this expression is multiplied already by an overall factor of $(E - \tilde{E})$, we can see that, in the on-shell limit,

$$\frac{1}{4E_k} \left[\frac{1}{D_-} - \frac{1}{\tilde{D}_-} - \frac{2(E_k - \tilde{E})(E - \tilde{E})}{\tilde{D}_-^2} \right] \sim \mathcal{O}\left((E - \tilde{E})^2 \right). \qquad (5.89)$$

Finally, to obtain the two-loop counterterm R_2^{CT}, simply take the expression for the integrated counterterm in Eq.(5.18) and substitute R_1^{CT}, with p replaced by k_2. This implies that the local structure of the counterterm, even at two-loop order, is completely determined by its one-loop behaviour. This was to be expected due to the fact that the UV divergence of the original bare graph comes from the one-loop self-energy subgraph.

Let us recap what we have achieved: by introducing a local representation for the counterterm that cancel the UV subdivergences of two-loop bare graphs with a self-energy insertion on an internal edge, we have managed not only to put the counterterms in the same footing as the bare contributions (in terms of the number of loop integrations involved in both kind of contributions), but also shown that the residues associated to propagators raised to powers greater than one cancel between the bare and counterterm contributions. Moreover, since such residues are due to one-loop subgraphs, we have been able to construct, in the context of scalar ϕ^3 theory, the appropriate local counterterm that achieves this cancellation in a process-independent fashion. The advantages of this result are twofold.

First, as we have stressed along this section, the appearance of higher-order residues spoils the tree-like structure of the integrand obtained after applying LTD to a given Feynman integral. Realizing the cancellation of such residues after renormalizing the UV divergences allows us to conserve the interpretation of the cut integrand as a tree-like object.

On the other hand, let us comment on the benefits of this result towards the numerical calculation of scattering amplitudes. Within an analytic calculation, higher-order residues can be reduced through IBP relations in the same way we used to show that the proposed local representation integrates to the proper counterterm. Such a procedure, however, is process dependent. This is not well suited for automation, which is a feature one would desire in a numerical calculation. Therefore, being able to extract the a priori process-dependent behaviour and isolate it into a universal building block which depends only on the field theory provides an elegant solution to the problem, paving the way for a suitable automation of the remaining contributions in the calculation.

Local counterterms satisfying the conditions needed to cancel the higher-order residues for QCD are constructed in detail in [87]. One of the consequences of the construction is that a local representation for the fermion propagator counterterm that vanishes quadratically in the on-shell limit is only possible if field and mass renormalization are performed in the on-shell scheme.

Let us close this section by detailing the general structure of the counterterm contributions, which will allow us to apply LTD formula to all terms entering the calculation of an arbitrary L loop scattering amplitude.

In general, a counterterm obtained from the Feynman rules of a given field theory will include fewer than L loop integrations to cancel the UV divergences of its associated bare loop graph. When constructing an integral representation for the counterterm, we introduce an additional number of loop integrations so that both the bare and counterterm contributions are integrated over the same amount of loop momenta. With this in mind, let

$$f^{CT}_{L_{CT}, n_{CT}}(\Gamma) \tag{5.90}$$

for the integrand of a counterterm with L_{CT} additional loop integrations and n_{CT} external legs. For example, the one-loop counterterm R^{CT}_1 of Eq.(5.70) is denoted by $f^{CT}_{1,2}$. As a further assumption, without loss of generality, we take all the external edges n_{CT} to contain momenta only of the remaining loop integrations. Let $i^{CT} \subset \{1, \dots, L\}$ be the set of indices of the loop integrations introduced by the local representation of the counterterm with integrand $f^{CT}_{L_{CT}, n_{CT}}(\Gamma)$, so that $|i_{CT}| = L_{CT}$, and let $(q_1, \dots, q_{n_{CT}})$ be the set of external momenta associated to this counterterm. Then, the integral representation satisfies

1. After integration,

$$\int \left(\prod_{j=1}^{L_{CT}} \frac{d^D k_{i_j}}{(2\pi)^D} \right) f^{CT}_{L_{CT}, n_{CT}}(\Gamma) \tag{5.91}$$

one obtains the analytic representation of the counterterm computed from the Feynman rules,

2. the sum of the bare and counterterm contributions vanishes at least as $\mathcal{O}(|\vec{k}_{i_j}|^{-5})$ when $|\vec{k}_{i_j}| \to \infty$ for each of its associated loop integrations. As in the two-loop case considered earlier, this guarantees that the UV divergences in each loop integration vanish locally between the bare and counterterm contributions,

3. the integral representation has no poles in the energies q_{0i} of the external edges. This ensures that, applying the LTD formula to the integral representation of the counterterm requires exactly L_{CT} cuts,

4. finally, performing the mass and field renormalization in the on-shell scheme, it is possible to construct an integral representation for the propagator counterterms $f_{L_{CT},2}^{CT}$, with external momenta $(q, -q)$, so that the sum of all bare and counterterm two-point integrands contributing to the scattering amplitude vanishes quadratically as q goes on-shell. This condition, as we saw in our two-loop calculation, guarantees that there are no contributions coming from higher-order poles.

These conditions are the generalization of the conditions imposed on R_1^{CT} and R_2^{CT} to arbitrary loop order. We would like to point out that the explicit construction of the counterterms has only been performed up to the two-loop order, which is the main case of interest for practical calculations due to the fact that state of the art algorithms for the automated calculation of loop amplitudes are only available at the one-loop order. However, the one-loop like structure of the integral representation implies that such a construction is always possible at higher-loop orders.

5.3 LTD representation of the integrand for L-loop amplitudes

Having dealt with the problem of higher-order poles and expressing the counterterm contributions as loop integrals with the same amount of integrations as the bare contributions, we have managed to find the last ingredient needed to write down the LTD representation of the loop integrand of the L-loop scattering amplitude with n external particles.

We begin by applying the LTD formula to the integrand $f_{L_{CT},n_{CT}}^{CT}$ of each counterterm diagram that contributes to the L-loop scattering amplitude with n external particles. This results in an integrand over L_{CT}-fold cuts, performed over the spatial components of the L_{CT} loop momenta. Let us denote by

$$V_{L_{CT},n_{CT}}^{CT} \tag{5.92}$$

the result of this cutting procedure. We can regard this result as new vertex of the theory with n_{CT} external edges and L_{CT} pairs of edges $(k_{i_j}, \bar{k}_{i_j})$ which reproduce the integrand $f^{CT}_{L_{CT}, n_{CT}}$ when sewed together. Each of these cuts will have its own combinatorial factor $S_{\sigma\alpha}$, which do not need to be identical of those of its associated bare graph. That this is the case can be seen from the fact that the cuts of bare graphs always involve L cuts, while in general $L_{CT} \leq L$, so that the structure of the cut graph for the counterterm might be different from that of the bare contribution. We identify $V^{CT}_{0, n_{CT}}$, that is, vertices with $L_{CT} = 0$, with the original vertices of the theory.

We can now provide a definition of a tree-amplitude-like object. Recall that in Eq.(5.9) we have defined a tree-like object through the replacement of its usual representation in terms of Feynman graphs by multiplying by the appropriate combinatorial factor. We can generalize this definition, so that the object

$$A^{CT}_{0, n+2(L-L_{CT}), L_{CT}} \tag{5.93}$$

is given by the sum of all tree diagrams with $(n + 2L - 2L_{CT})$ external legs, where the vertices are given by all the possible $V^{CT}_{L_{CT}, n_{CT}}$ and each diagram is weighted by its corresponding combinatorial factor $S_{\sigma\alpha}$. Recalling that an L loop amplitude in an arbitrary field theory is proportional to g^{2L}, where g is the coupling of the theory, we can conclude that the all of the counterterm vertices appearing in $A^{CT}_{0, n+2(L-L_{CT}), L_{CT}}$ are proportional to $g^{2L_{CT}}$. For the bare contributions, we write

$$A_{0, n+2L} = A^{CT}_{0, n+2L, 0} = \sum_{\Gamma \in U_{0, n+2L}} S_{\sigma\alpha} f(\Gamma), \tag{5.94}$$

which is nothing but the tree amplitude with $n + 2L$ external legs where every diagram is weighted by the appropriate combinatorial factor inherited from the cutting procedure. The external momenta of this amplitude are given by

$$\{p_1, ..., p_n; k_1, ..., k_L, \bar{k}_1, ..., \bar{k}_L\}. \tag{5.95}$$

For an arbitrary $L_{CT} \in \{0, 1, ..., L\}$, we define its regularized forward limit

$$\mathcal{R}_f A^{CT}_{0, n+2(L-L_{CT}), L_{CT}} \tag{5.96}$$

in the same fashion as the regularized forward limit of tree amplitudes introduced in Eq.(5.8). Summing the contributions with every possible amount of counterterm insertions, we set

$$\mathcal{B}_{L, n}(p_1, ..., p_n; k_1, ..., k_L, \bar{k}_1, ..., \bar{k}_L) = \sum_{L_{CT}=0}^{L} \mathcal{R}_f A^{CT}_{0, n+2(L-L_{CT}), L_{CT}}, \tag{5.97}$$

which corresponds to the regularized forward limit of a UV-finite sum of weighted tree diagrams. We want to show that the expression in Eq.(5.97) corresponds precisely to the integrand of the L loop amplitude after application of LTD.

As a starting point, we write the L loop amplitude as a sum over Feynman diagrams as

$$A_{L,n}(p_1,...,p_n) = \sum_{\Gamma \in U_{L,n}^S} \frac{(-1)^{n_c(\Gamma)}}{S(\Gamma)} \int \prod_{j=1}^{L} \left(\frac{d^D k_j}{(2\pi)^D} \right) f(\Gamma) \qquad (5.98)$$

where $S(\Gamma)$ is the symmetry factor associated to the graph Γ, as defined in Chapter 3, and $n_c(\Gamma)$ is the number of closed fermion loops of the graph. We can apply LTD individually to each of the graphs, using Eqs.(4.45) and (4.75), to turn each of the loop integrals into a sum of cut integrals

$$A_{L,n}(p_1,...,p_n) = (-i)^L \sum_{\Gamma \in U_{L,n}^S} \frac{(-1)^{n_c(\Gamma)}}{S(\Gamma)} \sum_{\sigma \in C_\Gamma} \int_\pm \prod_{j=1}^{L} dk_{\sigma_j}^{cut} S_{\sigma\alpha} f^{cut}(\Gamma) \quad (5.99)$$

where f^{cut} denotes the loop integrand without the cut propagators and all the remaining propagators are turned into the corresponding dual propagators. For every one of these integrals, it is possible to relabel the loop momenta $(k_{\sigma_1},...,k_{\sigma_L})$ so that the loop momenta becomes $(k_1,...,k_L)$ for all the contributions. For a each set of integrals defined by the same cut, this amounts to performing a linear transformation on the momenta, and there are $L!$ factorial ways to do this, starting from a given basis $(k_{\sigma_1},...,k_{\sigma_L})$ of independent loop momenta. Averaging over all these possibilities, we can exchange the order of the sums and the integration, obtaining

$$A_{L,n}(p_1,...,p_n) = \frac{(-i)^L}{L!} \int_\pm \prod_{j=1}^{L} dk_j^{cut} \sum_{\Gamma \in U_{L,n}^S} \frac{(-1)^{n_c(\Gamma)}}{S(\Gamma)} \sum_{\sigma \in C_\Gamma} \sum_{S_L} S_{\sigma\alpha} f^{cut}(\Gamma)$$

$$\qquad (5.100)$$

where the sum over S_L is the sum over all possible permutations introduced by the averaging procedure. Recall that we introduced the notation

$$\int_\pm dk^{cut} = \int \frac{d^{D-1}k}{(2\pi)^{D-1} 2\sqrt{\vec{k}^2 + m^2}} \sum_{\lambda=\pm} \qquad (5.101)$$

to denote the integration over the spatial components of the loop momenta k, summed over the forward and backwards on-shell hyperboloid. This sum is equivalent to summing over the two possible orientations of the flow of the momentum k. This means that, restoring the sum over the hyperboloids, we can identify that the four remaining sums appearing in Eq. (5.100) make up the set $U_{L,n}^{\otimes L,ns}$, which is the set of non-singular graphs from

the set in Eq.(5.7) where L internal lines have been marked. With this, we can write

$$A_{L,n}(p_1,...,p_n) = \frac{(-i)^L}{L!} \int \prod_{j=1}^{L} dk_j^{cut} \sum_{\Gamma \in U_{L,n}^{\otimes L,ns}} \frac{(-1)^{n_c(\Gamma)}}{S(\Gamma)} f^{cut}(\Gamma) \qquad (5.102)$$

where we have dropped the $\pm$ subscript on the integral since the sum over the hyperboloids has been put together in the sum over the non-singular marked graphs.

Since we are summing over L loop marked graphs, we can use Eq.(3.26) to exchange the summation over marked graphs by a summation over sewed tree graphs. By definition of the loop amplitude, there are no singular contributions coming from self-energy insertions on external legs, nor there are tadpole insertions, if we assume that all fields in the theory have vanishing vacuum expectation values. Moreover, because of the way we constructed the local representation for the counterterms, there are no residues coming from higher-order poles. We can, therefore, recognize the sum over sewed graphs as the regularized forward limit of the sum of weighted tree graphs, which is exactly the definition of $B_{L,n}$. The result of this observation is that

$$A_{L,n}(p_1,...,p_n) = \frac{(-i)^L}{L!} \int \prod_{j=1}^{L} \left(\frac{d^{D-1}k_j}{(2\pi)^{D-1} 2\sqrt{|\vec{k}_j|^2 + m_j^2}} \right) \sum_{L_{CT}=0}^{L} \mathcal{R}_f A_{0,n+2(L-L_{CT}),L_{CT}}^{CT}$$

$$= \frac{(-i)^L}{L!} \int \prod_{j=1}^{L} \left(\frac{d^{D-1}k_j}{(2\pi)^{D-1} 2\sqrt{|\vec{k}_j|^2 + m_j^2}} \right) \mathcal{B}_{L,n}(\{p_i\}, \{k_i, \bar{k}_i\}).$$

$$(5.103)$$

The formula in Eq.(5.103) represents the main result of this thesis, since it provides a definition of the integrand for an arbitrary, renormalized L-loop scattering amplitude which does not depend on the evaluation of individual Feynman diagram as the integral over the spatial components of the loop momenta of the regularized forward limit of a tree-amplitude-like object. An additional caveat of this formula is that, since the momenta of a tree amplitude (and by consequence, the momenta of a tree-amplitude-like object) are completely determined by momentum conservation, this representation of the loop integrand provides a global definition of the loop momenta. As we have already mentioned, the structure of the tree-amplitude-like object not only differs from the tree amplitude by the inclusion of combinatorial factors, but also on the modification of the usual Feynman propagators to dual propagators, whose modified causal prescription is relevant in the remaining integrations to determine in which direction to perform the necessary contour deformation [49, 54, 55, 106, 125] to avoid the non-pinch singularities

of the integrand in a numerical calculation.

We conclude this section by mentioning the remaining generalizations of Eq.(5.103). In theories such as QED or QCD where there are more than one species of particles, we must also perform a sum over all flavours of the $(2L)$ additional particles appearing as external edges of the cut integrand. When cutting lines associated to particles with spin, we perform a sum over both physical and unphysical polarizations, in line with our remarks in Eqs.(3.13) and (3.15) about the cutting of fermion or gauge boson propagators and their numerator structure. Finally, in non-Abelian gauge theories, the bare loop diagrams receive contributions from loops with ghosts and antighosts that cancel the contributions from the longitudinal polarizations of the gauge bosons. In that regard, we must include cut diagrams with external ghosts and antighosts.

Finally, in the context of the SM, it is known that the Higgs field acquires a non-vanishing vacuum expectation value. This means that contributions where a tadpole is inserted into an external line through a Higgs propagator, even though the propagator has momentum zero, the Higgs has a non-vanishing mass, rendering such diagrams finite. In order to accomodate for this new contributions, we would include terms where the internal edges have momenta

$$\sum_a (k_a + \bar{k}_a) \tag{5.104}$$

in the regularized forward limit, whenever the internal edge with this momenta corresponds to a Higgs boson. Since there is no condition on which renormalization scheme to use for the the Higgs sector, we can follow the ideas in **??**, where the renormalization of the Higgs sector is performed under the condition that the vacuum expectation value of the Higgs field matches the physical vacuum expectation value of the interacting theory. This translates to the condition that the tadpole contributions vanish, and therefore, no modification is needed to include the Higgs sector in an application of the LTD formula to a calculation in the SM. If the use of such renormalization scheme is not convenient, one must simply extend the contributions to the regularized forward limit adding the contributions determined by Eq.(5.104).

5.4 Recursion relations for the integrand

In contrast to higher-loop contributions, the structure of tree-level amplitudes is remarkably simple, since these are always rational functions of the external momenta. The singularities of tree amplitudes are also very well understood, given by poles that occur when a propagator goes on-shell. A remarkable property of tree amplitudes is that the residues at the poles exhibit a factorized structure, given by the product of lower point amplitudes.

This factorized structure can be exploited to construct tree amplitudes recursively, and such an approach can be classified broadly into two different kinds.

On one hand, there are the so-called on-shell recursion relations, of which [128, 129], the BCFW recursion relations, is the one most used in the literature. The technique is based on performing a complex deformation of the momenta of a tree amplitude, where some of the momenta are shifted according to $p_i \rightarrow p_i + z q_i$, with z a complex variable, in such a way that the on-shell conditions and conservation of momenta are still satisfied by the shifted momenta. The complexified amplitude then develops poles in z, which can be shown to always be simple and applying the residue theorem to the function $A_n^{(0)}(z)/z$, where $A_n^{(0)}(z)$ denotes the shifted tree amplitude, yields an expansion of the amplitude that takes the schematic form

$$A_n^{(0)} = \sum A_{n_1,R}^{(0)} \frac{1}{P^2} A_{n_2,L}^{(0)} \tag{5.105}$$

with $A_{m,S}^{(0)}$ lower-point amplitudes evaluated at the position of the poles, and P^2 a propagator-like quantity that "connects" the factorized subamplitudes. The seeds for the recursion in this approach are given by the three-point amplitudes of the theory, which are nothing else than the cubic interaction vertices contracted with external wave-functions. In theories of massless particles these three-particle amplitudes vanish unless the momenta is taken to be complex, which is built-in in the formalism via the shifted momenta. Furthermore, a striking property of three-point amplitudes is that their kinematic structure can be completely determined using only the constraints imposed on them by Lorentz symmetry [130]. This means that on-shell recursion relations can be seen to produce tree-level amplitudes without the need to refer to Feynman diagrams, or even Lagrangians. In practice, these kind of relations are very useful in analytic calculations, but not very well suited for numerical computation of amplitudes with arbitrary inputs. The reason for this is that, when the momenta is shifted to obtain the deformed amplitude $A_n^{(0)}(z)$, the position of the physical poles of the original amplitude is also shifted. This means that each of the individual contributions in Eq.(5.105) will contain spurious poles which only cancel once the sum is performed. This results in large cancellations amongst different terms, which reduces the precision of a numerical calculation where the recursion relations are employed. However, when working with specific representations of the kinematic variables [131, 132], the BCFW recursion relations allow to obtain compact closed expressions for tree amplitudes of arbitrary multiplicities, as shown in [133, 134].

The second general approach to the recursive calculation of tree amplitudes are the off-shell recursion relations, first derived in the case of color-ordered gluon amplitudes by Berends and Giele in [123]. In this case, given an arbitrary tree-amplitude, one constructs an object known as an off-shell

current, which corresponds to removing one of the external wave-functions of the amplitude, and contracting it with an additional propagator that corresponds to the same kind of particle whose wave-function was removed. These off-shell currents can be shown to satisfy recursion relations, where the building blocks are given by the vertices, propagators and external wave functions of the theory. Finally, the amplitude is obtained by a contraction with a suitable external wave function. In [135], a comparison is made between the numerical implementation of the different kind of recursion relations, and it is found that off-shell recursion yields the fastest results at high multiplicity. For this reason, given that the ultimate goal of the LTD formalism is to allow for the automated numerical calculation of loop amplitudes, we choose to use off-shell recursion relations for the calculation of the tree-amplitude-like objects. With this in mind, we give a detailed review of the algorithm in the simple case of tree amplitudes in scalar ϕ^3 theory, explaining along the way the necessary modifications to accomodate an arbitrary field theory.

We let

$$\mathcal{J}_{0,j} \tag{5.106}$$

denote an off-shell current, which can be also defined as an object with j external legs with on-shell momenta $(p_1, ..., p_j)$ and an additional external, off-shell leg with momenta p_{j+1}, subject to momentum conservation

$$\sum_{i=1}^{j+1} p_i = 0. \tag{5.107}$$

The first step in the recursion involves setting the values for the $j = 1$ currents. These will be given by

$$\mathcal{J}_{0,1}(p_i) = 1, \qquad i \in \{1, ..., j-1\} \tag{5.108}$$

for the case of ϕ^3 theory, and by the appropriate wave-functions for the case of particles with spin. The one-particle currents serve as the seeds of the recursion.

Higher multiplicity currents are then built by considering the different ways in which to put one-particle currents together. In order to do this, we let γ be a subset of $\{p_1, ..., p_{j-1}\}$[2]. We look for partitions of γ given by subsets $\alpha, \beta \subset \gamma$, that is

$$\alpha \cup \beta = \gamma, \qquad \alpha \cap \beta = \emptyset. \tag{5.109}$$

Furthermore, set $i = |\gamma|$ and $a = |\alpha|$. We define the total momentum of the sets α and β as

---

[2]It suffices to consider only the first $(j-1)$ p_i's due to momentum conservations

$$P_1 = \sum_{p \in \alpha} p, \qquad P_2 = \sum_{p \in \beta} p \tag{5.110}$$

and, finally, we set $P_3 = -P_1 - P_2$. Then, the off-shell currents are constructed recursively according to

$$\mathcal{J}_{0,i}^{amp}(\gamma) = \sum_{\alpha,\beta} V(P_1, P_2, P_3) J_{0,a}(\alpha) J_{0,i-a}(\beta) \tag{5.111}$$

where $V(P_1, P_2, P_3)$ denotes the three-point interaction vertex, and

$$\mathcal{J}_{0,i}(\gamma) = \frac{-i}{D(P_3)} \mathcal{J}_{0,i}^{amp}(\gamma) \tag{5.112}$$

where $D(k) = k^2 - m^2$ are the scalar inverse propagators. In theories with spin, the numerator of $1/D$ is modified to yield the appropriate propagators. In theories with multiple interaction vertices, an additional sum over all the possible types of vertices is introduced and, if there are vertices with valency higher than three, the set γ is partioned into more than two subsets. In particular, for four-point vertices such as the four gluon vertex of QCD, one must construct threefold partitions.

Finally, the amplitude is obtained as

$$A_n^{(0)}(p_1, ..., p_n) = \mathcal{J}_{0,1}(p_n) \mathcal{J}_{0,n-1}^{amp}(p_1, ..., p_{n-1}) \tag{5.113}$$

where the contraction with $\mathcal{J}_{0,1}(p_n)$ is only relevant for theories with spin. We can put this algorithm to test with a simple calculation by computing the 4-point scalar amplitude. Working from the bottom up, we want to obtain

$$A_4^{(0)}(p_1, ..., p_4) = \mathcal{J}_{0,3}^{amp}(p_1, p_2, p_3) \tag{5.114}$$

From the definition of Eq.(5.111), we need to set $\gamma = \{p_1, p_2, p_3\}$, which implies $i = |\gamma| = 3$. There are three possible partitions of this set into two disjoint sets, namely

$$\begin{aligned} \alpha_1 &= \{p_1, p_2\}, & \beta_1 &= \{p_3\} \\ \alpha_2 &= \{p_1, p_3\}, & \beta_2 &= \{p_2\} \\ \alpha_3 &= \{p_2, p_3\}, & \beta_3 &= \{p_1\}. \end{aligned} \tag{5.115}$$

Since the only vertex in ϕ^3 theory is given by the coupling $V(q_1, q_2, q_3) = -i\lambda$ for any set of momenta $\{q_1, q_2, q_3\}$, we can write

$$\mathcal{J}_{0,3}(\gamma) = -i\lambda \sum_{\alpha,\beta} \mathcal{J}_{0,a}(\alpha) \mathcal{J}_{0,3-a}(\beta). \tag{5.116}$$

Now, we can see that in every possible partition, we have $a = 2$, which implies that all the currents $\mathcal{J}_{0,3-a}(\beta) = \mathcal{J}_{0,1}(p_i) = 1$. This means that the off-shell current simplifies to

$$\mathcal{J}_{0,3}(\gamma) = -i\lambda \sum_{\alpha} \mathcal{J}_{0,2}(\alpha). \tag{5.117}$$

We only need to compute the currents $\mathcal{J}_{0,2}$. We first notice that, since all of the sets α have only two momenta, the only possible partition is given by splitting the set into two sets with a single momenta each. Thus, if the momenta in the set α are (k_1, k_2), then we have $P_3 = -k_1 - k_2$, and

$$\mathcal{J}_{0,2}(\alpha) = \frac{-i}{(k_1 + k_2)^2 - m^2} \mathcal{J}_{0,2}^{amp}(\alpha). \tag{5.118}$$

Finally, since the partitions of the two-particle sets are given by single element sets, we can see that the recursion terminates, since all the $\mathcal{J}_{0,a}$ and $\mathcal{J}_{0,i-a}$ entering the definition of $\mathcal{J}_{0,2}^{amp}$ are the one-point currents, which for scalar are simply defined to be 1. Thus, the two-point amputated current is simply given by the vertex $-i\lambda$, and we find

$$
\begin{aligned}
\mathcal{J}_{0,3}^{amp}(\gamma) &= -i\lambda \left(\mathcal{J}_{0,2}(\alpha_1) + \mathcal{J}_{0,2}(\alpha_2) + \mathcal{J}_{0,2}(\alpha_3) \right) \\
&= i\lambda \left(\frac{i\mathcal{J}_{0,2}^{amp}(\alpha_1)}{D(p_1 + p_2)} + \frac{i\mathcal{J}_{0,2}^{amp}(\alpha_2)}{D(p_2 + p_3)} + \frac{i\mathcal{J}_{0,2}^{amp}(\alpha_3)}{D(p_1 + p_3)} \right) \\
&= i\lambda^2 \left(\frac{1}{D(p_1 + p_2)} + \frac{1}{D(p_2 + p_3)} + \frac{1}{D(p_1 + p_3)} \right)
\end{aligned}
\tag{5.119}
$$

which coincides with the four-point amplitude as computed from the Feynman rules. With this off-shell current, moreover, one could construct the five scalar amplitude in a more efficient fashion than by generating the complete set of Feynman diagrams contributing to the amplitude.

Now, we can address the issue of modifying the recursive algorithm in order to calculate the tree-amplitude-like object $\mathcal{B}_{l,n}$ introduced in Eq. (5.97).

The first modification we have to perform is the inclusion of the combinatorial factors $S_{\sigma\alpha}$ appearing in Eq.(4.76). We will show that, up to three-loop order, it is possible to dress the vertices and propagators that make up the recursion relations in order to reproduce the appropriate combinatorial factors.

To begin, we recall that the combinatorial factors depend only on the structure of the underlying chain graph Γ_{chain} of a given graph Γ. We specify a cut through the set of permutations

$$(\sigma_1^{\alpha_1}, \ldots, \sigma_L^{\alpha_L}). \tag{5.120}$$

A general property of the combinatorial factors is that they are invariant if we change the energy signs $\alpha_j \to -\alpha_j$ for all of the cut lines. Thus, it is
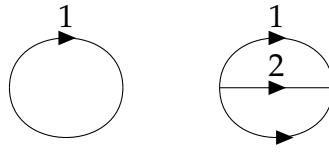
FIGURE 5.3: Chain graphs up to two-loops.

sufficient to consider only a limited amount of cases to derive the remaining factors.

At one-loop order, the only possible chain graph is the vacuum bubble, and as we argued previously, all the one loop combinatorial factors are given by $S_{\sigma\alpha} = 1/2$. Thus, we introduce the vertex rule

$$\text{(diagram)} = \frac{1}{2}, \tag{5.121}$$

where the blobs indicate the parts of the diagram where the cut lines k_1^+ and $\overline{k}_1^-$ attach to. Similarly, at two-loop order, the only possible chain graphs are given by a product of two one-loop vacuum bubbles, and by the sunrise graph with no external legs. The first occurs for graphs whose integral expression factorizes into the product of two independent one-loop integrals. These chain graphs are shown in Fig. 5.3.

At the two-loop level, we can use Eq. (4.77) to find that the only possible combinatorial factors at this order are given by $1/3$ when the sign of the energies of both cut lines is equal and by $1/6$ when the sign of the energies are different from each other. With this in mind, we introduce the vertex factors

$$\text{(diagram)} = \frac{1}{\sqrt{3}}, \qquad \text{(diagram)} = \frac{1}{\sqrt{6}}. \tag{5.122}$$

The reason for the square roots is easy to explain: each of these vertices is accompanied by a second vertex, where k_i for $i = 1, 2$ is exchanged with $\overline{k}_i$. These second vertices will have then the same factor, so that when building up the complete tree diagram associated to the cut, we recover the correct
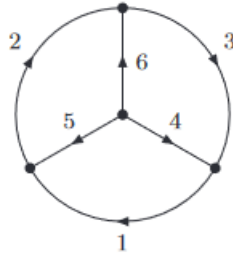
FIGURE 5.4: Irreducible three-loop chain graph. Figure taken
from [2].

combinatorial factors.

Finally, the three-loop case requires to be more careful. The basic chain graph at three loops is shown in Fig. 5.4. The combinatorial factors associated to this graph need only be computed once, and any three-loop graph whose chain graph has this structure will inherit those values. Using Eq.(4.76), we find

Three-loop chain:

Cut	$(1^+, 2^+, 3^+)$	$(1^+, 2^+, 3^-)$
$S_{\sigma\alpha}$	$\frac{3}{64}$	$\frac{29}{192}$
Cut	$(1^+, 2^-, 3^+)$	$(1^+, 2^-, 3^-)$
$S_{\sigma\alpha}$	$\frac{29}{192}$	$\frac{29}{192}$
Cut	$(1^+, 2^+, 4^+)$	$(1^+, 2^+, 4^-)$
$S_{\sigma\alpha}$	$\frac{5}{96}$	$\frac{19}{192}$
Cut	$(1^+, 2^-, 4^+)$	$(1^+, 2^-, 4^-)$
$S_{\sigma\alpha}$	$\frac{19}{192}$	$\frac{1}{4}$

(5.123)

In addition to the six-propagator three-loop graph in Fig. (5.4), there are two additional two chain-graphs that can be seen as subtopologies of this graph, obtained by pinching one or two pairs of vertices together. These are shown in Fig. 5.5).

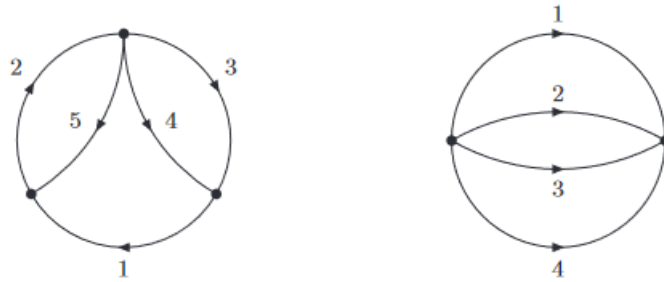The combinatorial factors for these graphs are given by

FIGURE 5.5: Non-factorizable suptopologies of the irreducible three-loop chain graph. Figure taken from [2].
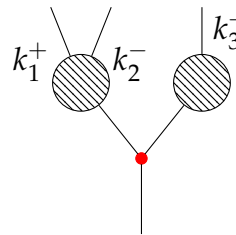
5-propagator chain:

Cut	$(3^+,4^+,5^+)$	$(3^+,4^+,5^-)$
$S_{\sigma\alpha}$	$\frac{1}{4}$	$\frac{11}{96}$
Cut	$(3^+,4^-,5^+)$	$(3^+,4^-,5^-)$
$S_{\sigma\alpha}$	$\frac{13}{192}$	$\frac{13}{192}$
Cut	$(1^+,3^+,5^+)$	$(1^+,3^+,5^-)$
$S_{\sigma\alpha}$	$\frac{1}{8}$	$\frac{11}{192}$
Cut	$(1^+,3^-,5^+)$	$(1^+,3^-,5^-)$
$S_{\sigma\alpha}$	$\frac{37}{192}$	$\frac{1}{8}$

(5.124)

for the graph on the left of Fig. 5.5, and
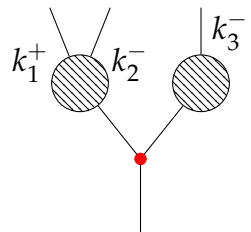
4-propagator chain:

Cut	$(1^+,2^+,3^+)$	$(1^+,2^+,3^-)$
$S_{\sigma\alpha}$	$\frac{1}{4}$	$\frac{1}{12}$
Cut	$(1^+,2^-,3^+)$	$(1^+,2^-,3^-)$
$S_{\sigma\alpha}$	$\frac{1}{12}$	$\frac{1}{4}$

(5.125)

for the remaining chain graph. These last coefficients, due to the "banana-like" structure of the four-propagator chain graph, can be computed using the simplified formula of Eq. (4.77). These combinatorial factors can be distributed among vertices of cut graphs according to
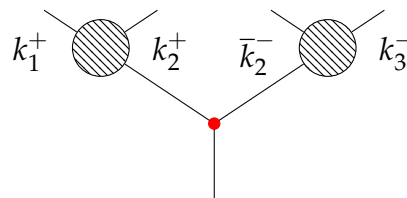

$$= \frac{1}{2}\sqrt{3},$$

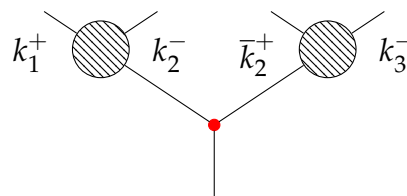(5.126)

$$\text{(diagram)} = \frac{1}{4}\sqrt{5},$$
(5.127)

$$\text{(diagram)} = \frac{19}{80}\sqrt{10},$$
(5.128)

$$\text{(diagram)} = \frac{29}{64}\sqrt{6},$$
(5.129)

and

$$\text{(diagram)} = \frac{9}{32}\sqrt{6}.$$
(5.130)

Using these vertex factors, it is possible to reproduce the combinatorial factors of any graph whose underlying chain graph is given by any of the graphs in Fig. 5.4 or 5.5. However, at three-loop order, one encounters an additional vacuum graph which is not a chain graph. This is shown in Fig. 5.6. Its underlying chain graph is given by the five-propagator graph of Fig. 5.5. However, the vertex rules introduced so far are not sufficient to reproduce the correct combinatorial factors for the cuts of the ladder graph. These cuts can be classified according to two different sets, and each of those will require the introduction of an additional factor to dress the internal propagators of the cut graphs associated with the lines with a shared momenta.

The first class of cut can be represented by cutting the lines $(3, 4, 5)$. In this case, the lines $(1, 6)$, which share the same momenta, are uncut. Then, we pick either one of lines 1 or 6, but not both, an attach factors
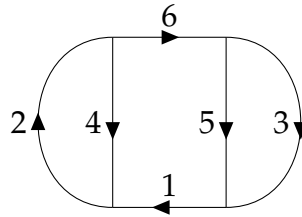
FIGURE 5.6: Three-loop vacuum graph with six propagators. The lines labelled by 1 and 6 carry the same momenta, which implies that this is not a chain graph.
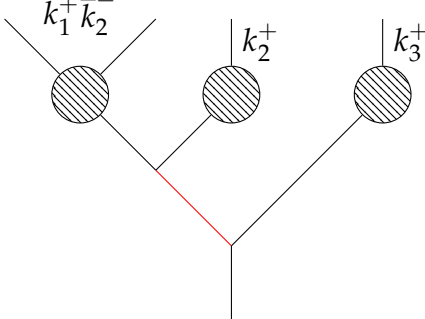

$$= 1, \tag{5.131}$$

$$= \frac{220}{361}, \tag{5.132}$$

$$= \frac{13}{10}, \tag{5.133}$$
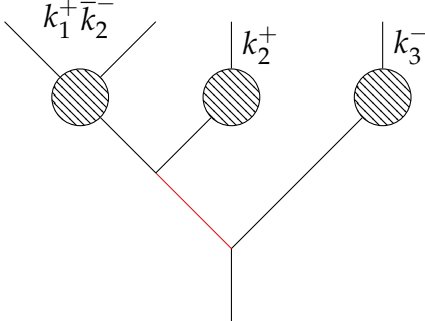
and
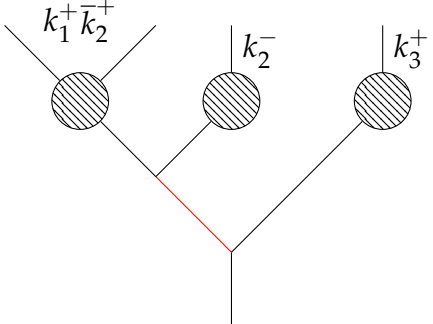

$$= \frac{13}{10}. \tag{5.134}$$

to one of the chosen propagators. The other type of cut can be character-ized by either the sets $(1, 3, 5)$ or $(3, 5, 6)$. Without loss of generality, we work with a cut of the type $(1, 3, 5)$. In this case, the propagator 6 is left uncut, and we attach to it the factors
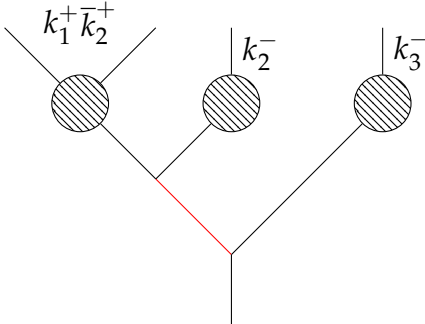
$$\text{(diagram)} = \frac{24}{19}, \tag{5.135}$$

$$\text{(diagram)} = \frac{11}{10}, \tag{5.136}$$

$$\text{(diagram)} = \frac{370}{361}, \tag{5.137}$$

and, finally

$$\text{(diagram)} = \frac{24}{19}. \tag{5.138}$$

Dressing the cut graphs with these vertex and propagator factors allows to reproduce the combinatorial factors associated to the cut graphs, eliminat-ing the need to use Eq. (4.76). Although we have limited ourselves to doing

this construction up to three-loop order, it is in principle possible to perform this same analysis for four and higher order loop graphs. The main complication in these scenarios is the appearance of more chain and non-chain vacuum graphs, which imply the need to introduce a bigger amount of vertex and propagator factors.

The remaining two modifications we need to make to the recursion relations in order to succesfully apply them to compute $\mathcal{B}_{L,n}$ are to include all possible counterterm vertices, as defined in Eq. (5.92), and to define the recursion relations to exclude contributions which would lead to singular propagators.

The quantities entering the recursion relations are off-shell currents

$$\mathcal{J}_{L_{CT},j}(q_1,...,q_j) \tag{5.139}$$

with j external on-shell edges and that contain counterterm vertices of order $g^{2L_{CT}}$. The momenta of these edges is chosen to be a subset of

$$\{p_1,\ldots,p_n;k_1,\ldots,k_L;\bar{k}_1,\ldots,\bar{k}_L\}, \tag{5.140}$$

where the dependence of $\mathcal{J}_{L_{CT},j}$ on the momenta of the cut lines is pairwise, i.e. it always depends on pairs $(k_a,\bar{k}_a)$, of which there are exactly L_{CT}. The combinatorial factors will be distributed among the vertices and propagators appearing in the recursion. Attaching the vertex factors is straightforward, since the structure of each vertex is independent on where the off-shell current attaches to. However, one can only identify if a propagator needs the insertion of a particular combinatorial factor after the off-shell currents are contracted into another vertex. We solve this issue by treating currents which might result in non-trivial combinatorial factors as currents of different flavour and group the off-shell currents according to which have the same propagator factor. These are later combined after being attached into a new vertex. The recursive algorithm in this case, detailed for ϕ^3 theory, starts by setting

$$\begin{aligned}
\mathcal{J}_{0,1}(q_i) &= 1, \quad i \in \{1,...,j-1\} \\
\mathcal{J}_{k,1}(q_i) &= 0, \quad k \geq 1,
\end{aligned} \tag{5.141}$$

meaning that there are no one-particle currents with counterterms. In other words, we only need the external states of the theory to initialize the recursion. Then, as before, we pick a subset γ of the momenta $\{p_1,\ldots,p_{j-1}\}$ and partition it into subsets α and β satisfying

$$\alpha \cup \beta = \gamma, \quad \alpha \cap \beta = \varnothing. \tag{5.142}$$

Then, with $i = |\gamma|$ and $a = |\alpha|$ being the amount of elements in each set, and the total momenta

$$Q_1 = \sum_{q \in \alpha} q, \quad Q_2 = \sum_{q \in \beta} q, \quad Q_3 = -Q_1 - Q_2, \tag{5.143}$$

we define the off-shell currents recursively through

$$\mathcal{J}^{amp}_{L_{CT},i,f}(\gamma) = \sum_{L_1+L_2+L_3=L_{CT}} \sum_{\alpha,\beta}{}' \sum_{f1,f2} C_V V^{CT}_{L_3,3}(Q_1,Q_2,Q_3) \\ \times C_\alpha \mathcal{J}_{L_1,a,f_1}(\alpha) C_\beta \mathcal{J}_{L_2,i-a,f_2}(\beta), \tag{5.144}$$

where the primed sum is over all subsets of γ forming a partition and such that only contributions with the same combinatorial factor for the propagator are selected. The possible combinatorial factors for the propagators are indexed by f, and we sum over all such possibilites for the lower-order currents. Furthermore, the vertices $V^{CT}_{L_3,3}$ denote the possible tri-valent vertices of order L_{CT}, and C_V denotes the combinatorial factor associated to this vertex. Finally, C_α and C_β denote the propagator combinatorial factors for the sub-currents $\mathcal{J}_{L_1,a,f_1}(\alpha)$ and $\mathcal{J}_{L_2,i-a,f_2}(\beta)$, respectively.

At this stage, we veto the singular kinematic configurations. If the momentum Q_3 is of the form of Eqs. (5.4), (5.5) or (5.6), we set

$$\mathcal{J}_{L_{CT},i,f}(\gamma) = 0, \tag{5.145}$$

otherwise,

$$\mathcal{J}_{L_{CT},i,f}(\gamma) = \frac{-i}{D(Q_3)} \mathcal{J}^{amp}_{L_{CT},i,f}(\gamma) \\ + \sum_{L_1+L_2=L_{CT}} \left(\frac{-i}{D(Q_3)}\right)^2 V^{CT}_{L_2,2}(Q_3,-Q_3) \mathcal{J}^{amp}_{L_1,i,f}(\gamma) \tag{5.146}$$

where $V^{CT}_{L_2,2}$ denote propagator counterterm vertices. Since there are no further counterterms in ϕ^3 besides the vertex and propagator counterterms, we have exhausted all possibilites. In theories with with additional vertices, both bare and coming from counterterms, the extension of these formulation is equivalent to the extension of the recursion relations for tree amplitudes from scalar theories to any other field theory. From this currents, then, one obtains

$$\mathcal{R}_f A^{CT}_{0,n+2(L-L_{CT}),L_{CT}}(p1,\ldots,p_n;k_{\alpha_1},\ldots,k_{\alpha_{L-L_{CT}}},\bar{k}_{\alpha_1},\ldots,\bar{k}_{\alpha_{L-L_{CT}}}) = \\ \mathcal{J}^{amp}_{L_{CT},n-1+2(L-L_{CT})}(p1,\ldots,p_n;k_{\alpha_1},\ldots,k_{\alpha_{L-L_{CT}}},\bar{k}_{\alpha_1},\ldots,\bar{k}_{\alpha_{L-L_{CT}}}) \tag{5.147}$$

from which all regularized forward limits can be computed, and then their sum yields $\mathcal{B}_{L,n}$.

Chapter 6

Summary and outlook

In this thesis, we have explored techniques for the calculation of scattering amplitudes and cross-sections in various quantum field theories, with an aim to develop a formulation that allows the efficient and automated computation of two-loop amplitudes and beyond.

To reach this goal, we introduced in Chapter 2 the fundamental principles of QFT and their application to the calculation of amplitudes and cross-sections. We started by looking at the Lagrangian formulation of gauge theories, and found the relation between amplitudes, defined as transition amplitudes of asymptotic in and out states, and cross-sections, which provide the main kind of observables measured at collider experiments. It was then shown that, within the framework of perturbation theory, scattering amplitudes can be computed as a series in the couplings of the field theory where each of the coefficients to be determined can be organized in the language of Feynman diagrams. There, we argued that beyond the leading order contributions, these diagrams translate into integrals of rational functions over some set of unconstrained momenta. We then saw that these integrals develop multiple singularities associated to different energy regimes and discussed the various technicalities needed in order to remove these divergences.

The first step in this direction was the need for regularization, which allows to parametrize the divergences of a given integral. Amongst the many possible regularization schemes, the one we chose to use along our work was dimensional regularization. The singularities associated to the high-energy modes (UV) were shown to cancel with the introduction of counterterms, which can be computed after the theory has been renormalized. Such a process was performed at the Lagrangian level, showing that defining field theories in terms of physical parameters allows a separation of the degrees of freedom in such a way that the divergences of the theory are absorbed into unobservable quantities. We discussed the different kinds of renormalization schemes, which are conditions imposed on the observables of the theory defined at some energy scale so that the divergences can be cancelled successfully. These cancellations occur at the level of the scattering amplitudes.

Singularities associated to low-energy modes (IR), however, were shown

to persist after renormalization. These singularities cancel between the virtual corrections, coming from higher-loop diagrams, and real or radiative corrections, which come from diagrams with additional external particles[1]. We then argued that in gauge theories, both Abelian and non-Abelian the KLN theorem guarantees the cancellation of IR divergences among these contributions. Finally, in order to illustrate this principle, we performed a one-loop calculation in QED to show how the cancellation of IR divergences manifests itself in the calculation of the real and virtual corrections to the cross-section. There, we saw that these cancellations occur only after all integrations have been performed, since the different type of corrections live in spaces of different dimensions and their integrations measures are different to one another. Although the result itself is consistent, the fact that one must perform the calculation of each contribution separately and keep track of the regulator in each one of them is not very well suited for the use in numerical calculations, since the treatment of every contributions highly depends on the process under consideration.

Chapter 3 is devoted to graph-theoretical study of the relation between loop and tree graphs. We first work out which kind of diagrams contribute the the scattering amplitude at a given perturbative order, reaching the conclusion that only connected graphs are to be considered in the calculation of amplitudes. Moreover, we saw that there are special types of graphs, namely those which contain insertions of tadpoles or self-energies on external edges, which give rise to singular contributions. In the case of tadpoles, it was argued that, given that the vacuum expectation values of the fields in the theory vanish, one can always ignore such contributions. On the other hand, we introduced the LSZ formula and argued that using the formula to calculate a scattering amplitude by computing the simple poles of off-shell correlation functions imply that diagrams with self-energy insertions on external edges, which produced higher-order poles in the correlation functions, do not contribute to the amplitude themselves but rather provide the basis for the calculation of the wave-function renormalization constants, which are then seen to associate the bare and renormalized amplitudes to one another.

Having discussed which kind of diagrams contribute to scattering amplitudes, we proceed to do a brief classification of diagrams with n external edges and L internal loops, with our without counterterm insertions. From this basic definitions, we look at ways to relate loop graphs and tree graphs, finding that these can be relate through the operations of cutting and sewing, which are inverse to each other. The essential idea is then that, given a loop graph, one can cut open one of its internal edges within a loop to reduce the loop order by one and increase the number of external edges by two. Picking exactly L internal edges of a L graph and cutting them open then yields

---

[1]This does not mean that there are no radiative corrections that include loops. For example, the IR divergences associated to the two-loop corrections to some process are cancelled against one-loop corrections with one additional external particle, as well as tree contributions with two extra external particles.

a connected tree graph with $2L$ additional external edges. We also saw that the loop graph can be recovered after cutting by identifying pairs of external edges and putting them together. We then took a detour from our graphic theoretic discussion by looking at the necessary conditions that must be imposed on the algebraic quantities associated to Feynman graphs in order for the cutting and sewing operations to make sense beyond being purely pictorial relations, emphasizing the way in which cutting behaves in theories with spin. Finally, we discussed the role of symmetry factors of loop graphs and how these factors cancel when cutting exactly L internal edges. We were able to prove that these symmetry factors cancel against the overcounting of equivalent tree graphs obtained by different cuts. This result is summarized in the equation

$$\sum_{\Gamma \in U_{L,n}^{\otimes L}} \frac{1}{S(\pi_f(\Gamma))} F(\pi_f(\Gamma)) = \sum_{\Gamma \in U_{0,n+2L}^{L-Sew}} F(B(\Gamma)), \tag{6.1}$$

where the sets summed over represent, on the loop side, the set of all L loop graphs were a marking is introduced to each of its internal edges and, on the tree side, the set of all graphs which give, by sewing exactly $2L$ legs, the L loop graph on the left-hand side of the equations. We wrote this relation such that it was valid for the linear combination of any operator acting on the graphs, implying that this equation holds for the sum of Feynman diagrams that contribute to a scattering amplitude at any loop order.

Chapter 4 takes the graph-theoretical discussion of Chapter 3 and translates it into the context of Feynman integrals. This is done through the derivation of the LTD formula, both at one- and multi-loop level, which constitute the first principal result of this thesis. As a first step, we provide the derivation of the LTD formula at one-loop for integrals where all the propagators occur at the power one. It is shown that the pole structure of the propagators allows for the application of the residue theorem to perform the integration over the energy component of the loop momenta. The resulting integrand is then argued to have the structure of a tree diagram, and we see that this tree diagram can be interpreted as a cut diagram, tying up with our previous discussion of the graph-theoretical relation between loop and tree graphs. It is also seen that the modification induced by the residue computation is to change the causal prescription for the poles of the propagators, introducing a dependence on the momenta of the external particles. We discuss the fact that one might average over all possible contour closings and argue why this is benefitial in order to obtain a tree-like structure for the integrand of the complete scattering amplitude after applying LTD to each of its individual contributions. Before deriving the LTD formula at multi-loop order, we perform a simple calculation to show the consistency of the LTD formula at one-loop by calculating a three-point scalar one-loop integral through the explicit evaluation of the cut integrals resulting from the application of the theorem.

In order to perform the derivation of the multi-loop LTD formula, a discussion of the differences between the one-loop and higher-loop cases is done by considering the behaviour of the two-loop two point function, given in terms of the so-called sunrise integral. We see that a naive application of the residue theorem in which we assume that the residues in the energies of the two loop momenta can be computed independently by finding the position of the poles through the original Feynman propagators leads to inconsistent results. A more careful approach is then taken, by first computing the residue in a single energy variable and looking at the dependence of the result on the second, unintegrated energy component. This leads to the discovery that the causal prescription of the poles is modified by an amount dependent on the momenta of the cut propagators. This dependence reveal the inconsistency of treating the residues separately, and we proceed to show that a representation in terms of cuts for multi-loop integrals, where the structure of the poles is determined completely by the original Feynman propagators, can be obtained at the cost of introducing a set of combinatorial factors, which in a sense account for the way in which a given pole "distributes itself" among the different possible contours as a function of the momenta of the remaining loop momenta. These combinatorial factors are rational numbers and are shown to depend only on the structure of the underlying chain graph of the loop graph under consideration. The resulting expression for the integral over the energy components of the integrand f at L-loops is then

$$
\frac{1}{(2\pi)^L} \int f \, dE_1 \wedge dE_2 \wedge \ldots \wedge dE_L
$$
$$
= (-i)^L \sum_{\sigma \in \mathcal{C}_\Gamma} \sum_\alpha S_{\sigma\alpha} (-1)^{n_\sigma^{(\alpha)}} res\left(f, E_\sigma^{(\alpha)}\right) \tag{6.2}
$$

with the coefficients $S_{\sigma\alpha}$ given by

$$
S_{\sigma\alpha} = \frac{(-1)^{L+n_\sigma^{(\alpha)}}}{2^L L! |\mathcal{C}_{\Gamma^{chain}}|} \sum_{\tilde{\pi} \in S_L} \sum_{\tilde{\sigma} \in \mathcal{C}_\Gamma} \sum_{\tilde{\pi} \in S_L} \sum_{\tilde{\alpha} \in \{-1,1\}^L} \frac{C_{\sigma\pi\alpha}^{\tilde{\sigma}\tilde{\pi}\tilde{\alpha}}}{N^{chain}(\sigma)}, \tag{6.3}
$$

where the possibility of propagators raised to powers higher than one is considered by leaving the expression for the residue of f at each of its poles without evaluation. Specializing the result to single poles results in an integrand where every contribution has the structure of a tree graph, and the modified causal prescription for the propagators of the dual integrand is derived. Finally, to further probe the consistency of our formula, we show a numerical comparison of the sunrise integral calculated using the corrected LTD formula and a direct Monte-Carlo evaluation, finding excellent agreement between the two results.

The second main result of this thesis is derived in Chapter 5. By taking into account the loop graphs which do not contribute to the scattering amplitude, we define the regularized forward limit of tree amplitude with $n + 2L$

external edges. This object is shown to be the kinematic limit of a set of non-singular tree graphs, and the criteria to choose which diagrams to omit according to the momenta flowing through their propagators is constructed. Afterwards, we provide a first definition of a "tree-like object" as a quantity constructed from the standard Feynman graph expansion of a tree amplitude or correlation function, where each graph is weighted by a combinatorial factor inherited from some loop graph which, after cutting, yields the tree graph under consideration.

We then perform a thorough treatment of counterterms, stemming from the need to express them in a local representation which allows for the application of the LTD formula to all contributions to the scattering amplitude. We show that it is possible to find local representation for the counterterms that make them match the loop order of the bare contributions, while cancelling the UV singularities at the level of the integrand. Moreover, the local representation can also be constructed to cancel the contributions coming from residues of higher-order poles, such as those of diagrams with self-energy insertions on an internal edge. This is a result of utmost importance, since higher-order poles require the calculation of derivatives, which presents a roadblock in the attempt to automate the calculation of amplitudes through the use of the LTD formalism since not only the tree structure of the integrands is lost, but also non-trivial numerators of the loop integrand, which naturally appear in theories with spin, make the calculation of such residues a process-dependent operation. Therefore, since the counterterms have a universal structure that depends only on the loop order and the field theory under consideration, one can preserve both the tree structure and the process-independence of the LTD formula by suitably constructing the counterterms. The explicit construction of such counterterms if performed in ϕ^3 theory up to two-loop order, and we mention how the analogous result for QCD amplitudes implies that the only consistent renormalization scheme in which these cancellations can be realized at a local level for fermion self-energies is the on-shell scheme. Finally, we introduce a general notation for the integral representation of an arbitrary counterterm, paving the way for the application of the LTD formula to the counterterm contributions.

The LTD formula is then applied to the sum of graphs that yield the L loop amplitude in an arbitrary field theory. All of the previous results are put together at this moment, showing that after application of the LTD formula to each individual graph, it is possible to use the formula relating the sum of loop graphs weighted by symmetry factors to sewn tree graphs to express the integrand as a sum of regularized forward limits of tree-like objects with counterterm insertions going from 0 to L. This result is contained in the equation

$$A_{L,n}(p_1,...,p_n) = \frac{(-i)^L}{L!} \int \prod_{j=1}^{L} \left(\frac{d^{D-1}k_j}{(2\pi)^{D-1}2\sqrt{|\vec{k}_j|^2 + m_j^2}} \right) \mathcal{B}_{L,n}(\{p_i\}, \{k_i, \bar{k}_i\})$$

(6.4)

where

$$\mathcal{B}_{L,n}(p_1,...,p_n; k_1,...,k_L, \bar{k}_1,...,\bar{k}_L) = \sum_{L_{CT}=0}^{L} \mathcal{R}_f A_{0,n+2(L-L_{CT}),L_{CT}}^{CT},$$

(6.5)

is the UV-regularized tree-amplitude like object, constructed from regularized forward limits of tree graphs with all possible orders of counterterm insertions. This formula suggests that the structure of loop corrections, and thus of all the calculable observables in a given QFT, is completely determined by the tree structure of the theory. This is an observation also implied by other modern approaches to the calculation of scattering amplitudes [110, 112, 136–139]. For our applications, the implications of this are two-fold.

On one hand, having a representation of the loop corrections given in terms of phase-space-like integrals suggests that there is a way to put the virtual and real corrections together at an integrand level such that the IR divergences become integrable. Finding a representation of cross-sections satisfying this property would provide a mayor breakthrough in the field of higher-order calculations, since the implementation of an automated Monte Carlo computation of the cross-sections would be much easier to perform if one is working with single, convergent integrands, instead of the sum of divergent integrands which have to be rendered finite separately. This kind of calculation, where the IR divergences are cancelled separately in the virtual and real contributions, is one of the many techniques used nowadays for the calculation of cross-sections [140–144], and such cancellation is achieved by the introduction of additional IR counterterms[2] that can be integrated over a single-particle phase-space by the definition of mappings which allow the phase-space measure to factorize appropriately.

On the other hand, the fact that the loop integrand possesses a tree-like structure allows the construction of recursion relations to calculate the integrand without referring to individual Feynman diagrams. The construction of off-shell recursion relations is reviewed in the familiar context of tree amplitudes, followed by a discussion of the necessary modification that have to be implemented to adjust the algorithm for the calculation of the loop integrand $\mathcal{B}_{L,n}$. We first see how it is possible to distribute the combinatorial factors obtained from cutting the loop graphs into vertices and propagators

---

[2] These are not derived from the systematic renormalization of the Lagrangian and should not be confused with the UV counterterms.

of the resulting cut graphs. Afterwards, including all possible counterterm vertices and vetoing the singular configurations yields the modified recursion relations for the calculation of the loop integrand.

It is important to emphasize that, although our work provides a big step towards the application of LTD to numerical computations, there are still some hurdles to overcome. First, in order to numerically evaluate the virtual contributions, it is not sufficient to achieve the cancellation of the IR divergences with the real contributions in order to obtain purely integrable singularities. One needs, for some of the singularities, an algorithm of contour deformation to avoid some of the poles of the unphysical poles of the integrand. Moreover, realizing the local cancellation of IR divergences is by itself a very difficult task. In alternate approaches to LTD, such cancellations have been shown to occur in simple one-loop processes [108]. However, a framework in which this cancellations occur at two or higher loop levels is not currently known. From a technical point of view, one of the main difficulties in achieving these cancellations lies in the fact that the phase-space integrations of the real and virtual corrections include delta functions with support on different sets of momenta satisfying by themselves momentum conservation. Therefore, it is only possible to obtain maps from one into the other in kinematicly degenerate regions of phase-space, close to where the IR divergences occur. Although there are known solutions to both problems in the standard treatment of the calculations, the adaptation of these techniques to the LTD approach represents an open problem which, in the author's opinion, would pave the way for an efficient automation of the calculation of two-loop cross-sections.

Appendix A

Feynman Rules for Select Quantum Field Theories

In this appendix, we list the Feynman rules for ϕ^3 theory and QED. The ϕ^3 theory Lagrangian of Eq.(2.1) can be written, after renormalization, as

$$\mathcal{L}_{\phi^3} = \frac{1}{2}\partial_\mu\phi\partial^\mu\phi - \frac{1}{2}m^2\phi^2 + \frac{\tilde{\lambda}}{3!}\phi^3 + \mathcal{L}_{CT} \tag{A.1}$$

where we write $\tilde{\lambda} = \mu^\epsilon(4\pi)^{-\frac{\epsilon}{2}}e^{\frac{\epsilon\gamma}{2}}\lambda$ to absorb the usual factors of $\log(4\pi)$ and Euler's constant γ appearing in dimensional regularization. The counterterm Lagrangian is given by

$$\mathcal{L}_{CT} = -\frac{1}{2}\left(Z_\phi - 1\right)\phi\partial^2\phi - \frac{1}{2}\left(Z_\phi Z_m^2 - 1\right)m^2\phi^2 + \frac{1}{3!}\left(Z_\phi^{\frac{3}{2}}Z_\lambda - 1\right)\tilde{\lambda}\phi^3 \tag{A.2}$$

where the renormalization constants Z_a for $a = \phi, m, \lambda$ have an expansion in the coupling λ

$$Z_a = 1 + \sum_{n=1}^{\infty} Z_a^{(n)}\left(\frac{\lambda^2}{(4\pi)^2}\right)^n. \tag{A.3}$$

From the first line, we read off the Feynman rule for the propagator and the interaction vertex,

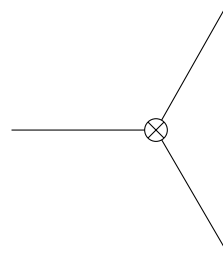$$\underline{} = \frac{i}{p^2 - m^2 + i\delta} \tag{A.4}$$

$$= i\tilde{\lambda} \tag{A.5}$$

In addition, there are two further vertices coming from the counterterm Lagrangian,

$$\underline{}\otimes\underline{} = i\left[(Z_\phi - 1)p^2 - (Z_\phi Z_m^2 - 1)m^2\right] \tag{A.6}$$

for the propagator counterterm, and

$$= i(Z_\phi^{\frac{3}{2}} Z_\lambda - 1)\tilde{\lambda} \qquad (A.7)$$
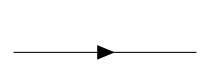
for the vertex counterterm.

For QED, we quote the Lagrangian from Eq.(2.47)

$$\mathcal{L}_{EM} = -\frac{1}{4} F_{\mu\nu} F^{\mu\nu} + \overline{\Psi}(i\slashed{\partial} - m)\Psi - e\overline{\Psi}\gamma_\mu A^\mu \Psi + \mathcal{L}_{CT} \qquad (A.8)$$
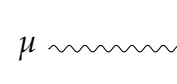
and the counterterm Lagrangian from Eq.(2.48)

$$\mathcal{L}_{CT} = -\frac{1}{4} \delta_3 F_{\mu\nu} F^{\mu\nu} + \overline{\Psi}(i\delta_2 \slashed{\partial} - \delta_m)\Psi - e\delta_1 \overline{\Psi}\gamma_\mu A^\mu \Psi \qquad (A.9)$$

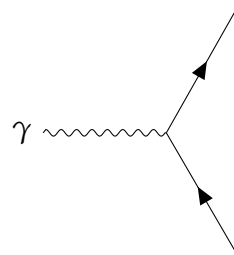Again, we use the first line of the Lagrangian to obtain the propagators

$$\longrightarrow \qquad = \frac{i(\slashed{p} + m)}{p^2 - m^2 + i\delta} \qquad (A.10)$$
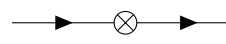
for the fermions,

$$\mu \;\sim\!\sim\!\sim\!\sim\; \mu \quad = \frac{-i g_{\mu\nu}}{p^2 + i\delta} \qquad (A.11)$$

for the photons, and finally

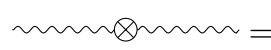$$= -ie\gamma^\mu \qquad (A.12)$$

for the interaction vertex. Similarly, the counterterm Lagrangian gives three additional vertices: one for each propagator
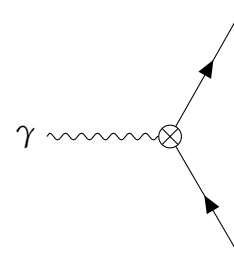
$$\longrightarrow\!\otimes\!\longrightarrow \qquad = -i(\slashed{p}\delta_2 - \delta_m) \qquad (A.13)$$

for the fermion,

$$\sim\!\sim\!\otimes\!\sim\!\sim \qquad = -i(g^{\mu\nu} p^2 - p^\mu p^\nu)\delta_3 \qquad (A.14)$$

in the case of the photon, and

$$\gamma \sim\!\!\sim\!\!\sim\!\!\otimes \qquad = -ie\gamma^{\mu}\delta_1 \qquad\qquad\qquad \text{(A.15)}$$

for the vertex counterterm.

Appendix B

Trace calculation for the process $\gamma^* \rightarrow e^+ e^- \gamma$

In this appendix, we perform the detailed calculation of the traces that appear after expanding the argument of Eq.(2.93). We would like to point out that the computation of traces of an arbitrary number of Gamma matrices can be performed with single lines of code using the Mathematica packages Form [145] or FeynCalc [146–148]. However, because of the relative simplicity of these traces, we show the detailed calculation.

The four traces to be computed are given by

$$
\begin{aligned}
T_1 &= Tr\left(\slashed{p}_1(2p_1^\alpha \gamma^\mu + \gamma^\alpha \slashed{k} \gamma^\mu)\slashed{p}_2(2p_{1\alpha}\gamma_\mu + \gamma_\mu \slashed{k} \gamma_\alpha)\right), \\
T_2 &= Tr\left(\slashed{p}_1(2p_1^\alpha \gamma^\mu + \gamma^\alpha \slashed{k} \gamma^\mu)\slashed{p}_2(2p_{2\alpha}\gamma_\mu + \gamma_\alpha \slashed{k} \gamma_\mu)\right), \\
T_3 &= Tr\left(\slashed{p}_1(2p_2^\alpha \gamma^\mu + \gamma^\mu \slashed{k} \gamma^\alpha)\slashed{p}_2(2p_{1\alpha}\gamma_\mu + \gamma_\mu \slashed{k} \gamma_\alpha)\right), \\
T_4 &= Tr\left(\slashed{p}_1(2p_2^\alpha \gamma^\mu + \gamma^\mu \slashed{k} \gamma^\alpha)\slashed{p}_2(2p_{2\alpha}\gamma_\mu + \gamma_\alpha \slashed{k} \gamma_\mu)\right).
\end{aligned}
\tag{B.1}
$$

First, we notice that T_4 can be obtained from T_1 by the replacement $p_2 \rightarrow p_1$ and the cyclic properties of the trace. Furthermore, reversing the order of the Gamma matrices and relabelling the dummy Lorentz indices shows that $T_2 = T_3$. Thus, we only need to compute T_1 and T_2.

A straightforward, if lengthy calculation reveals

$$
\begin{aligned}
T_1 &= Tr\left(\slashed{p}_1(2p_1^\alpha \gamma^\mu + \gamma^\alpha \slashed{k} \gamma^\mu)\slashed{p}_2(2p_{1\alpha}\gamma_\mu + \gamma_\mu \slashed{k} \gamma_\alpha)\right) \\
&= Tr\left((2p_1^\alpha \slashed{p}_1 \gamma^\mu + \slashed{p}_1 \gamma^\alpha \slashed{k} \gamma^\mu)(2p_{1\alpha}\slashed{p}_2\gamma_\mu + \slashed{p}_2 \gamma_\mu \slashed{k} \gamma_\alpha)\right) \\
&= Tr\left(2p_1^\alpha \slashed{p}_1 \gamma^\mu \slashed{p}_2 \gamma_\mu \slashed{k} \gamma_\alpha + \slashed{p}_1 \gamma^\alpha \slashed{k} \gamma^\mu \slashed{p}_2 \gamma_\mu \slashed{k} \gamma_\alpha\right) \\
&= Tr\left(\gamma_\alpha \slashed{p}_1 \gamma^\alpha \slashed{k} \gamma^\mu \slashed{p}_2 \gamma_\mu \slashed{k}\right) \\
&= 4(1-\epsilon)^2 Tr\left(\slashed{p}_1 \slashed{k} \slashed{p}_2 \slashed{k}\right) \\
&= 16(1-\epsilon)^2 \left((p_1 \cdot k)(p_2 \cdot k) - k^2(p_1 \cdot p_2) + (p_1 \cdot k)(p_2 \cdot k)\right) \\
&= 32(1-\epsilon)^2(p_1 \cdot k)(p_2 \cdot k).
\end{aligned}
\tag{B.2}
$$

To get to the third line, we used $p_1^2 = 0$ and the cyclic property of the trace to obtain $\slashed{p}_1 \slashed{p}_1 = p_1^2 = 0$, which cancels two of the contributions. To get the

fourth line, we again use the cyclicity of the trace to obtain the product $\not{p}_1 \not{p}_1$, leaving only a single trace to be calculated. To perform the contraction of the Lorentz indices, we use the identity

$$\gamma^\alpha \gamma^\nu \gamma_\alpha = -(D-2)\gamma^\nu = -2(1-\epsilon)\gamma^\nu, \tag{B.3}$$

allowing us to obtain the fifth line. Finally, we use the trace identity

$$Tr(\gamma^{\mu_1}\gamma^{\mu_2}\gamma^{\mu_3}\gamma^{\mu_4}) = 4(g^{\mu_1\mu_2}g^{\mu_3\mu_4} - g^{\mu_1\mu_3}g^{\mu_2\mu_4} + g^{\mu_1\mu_4}g^{\mu_2\mu_3}) \tag{B.4}$$

and $k^2 = 0$ to obtain the desired result. We can see that the value of the trace is invariant under the exchange of p_1 and p_2, which implies that, also,

$$T_4 = 32(1-\epsilon)^2(p_1 \cdot k)(p_2 \cdot k). \tag{B.5}$$

The remaining trace is given by

$$\begin{aligned}
T_2 &= Tr\left(\not{p}_1(2p_1^\alpha\gamma^\mu + \gamma^\alpha\not{k}\gamma^\mu)\not{p}_2(2p_{2\alpha}\gamma_\mu + \gamma_\alpha\not{k}\gamma_\mu)\right) \\
&= Tr\left((2p_1^\alpha\not{p}_1\gamma^\mu + \not{p}_1\gamma^\alpha\not{k}\gamma^\mu)(2p_{2\alpha}\not{p}_2\gamma_\mu + \not{p}_2\gamma_\alpha\not{k}\gamma_\mu)\right) \\
&= Tr\left(4p_1 \cdot p_2\not{p}_1\gamma^\mu\not{p}_2\gamma_\mu + 2p_1^\alpha\not{p}_1\gamma^\mu\not{p}_2\gamma_\alpha\not{k}\gamma_\mu \right. \\
&\quad \left. +2p_{2\alpha}\not{p}_1\gamma^\alpha\not{k}\gamma^\mu\not{p}_2\gamma_\mu + \not{p}_1\gamma^\alpha\not{k}\gamma^\mu\not{p}_2\gamma_\alpha\not{k}\gamma_\mu\right) \\
&= -8(1-\epsilon)p_1 \cdot p_2 Tr(\not{p}_1\not{p}_2) - 4(1-\epsilon)Tr(\not{p}_1\not{p}_2\not{p}_1\not{k}) \\
&\quad - 4(1-\epsilon)Tr(\not{p}_1\not{p}_2\not{k}\not{p}_2) + Tr(\not{p}_1(-2\not{p}_2\gamma^\mu\not{k} + 2\epsilon\not{k}\gamma^\mu\not{p}_2)\not{k}\gamma^\mu) \\
&= -32(1-\epsilon)(p_1 \cdot p_2)^2 - 8(1-\epsilon)p_1 \cdot p_2 Tr(\not{p}_1\not{k}) \\
&\quad - 8(1-\epsilon)p_1 \cdot p_2 Tr(\not{p}_2\not{k}) + 2\epsilon Tr(\not{p}_1\not{k}\gamma^\mu\not{p}_2\not{k}\gamma_\mu) \\
&= -32(1-\epsilon)(p_1 \cdot p_2)(p_1 \cdot p_2 + p_1 \cdot k + p_2 \cdot k) \\
&\quad + 2\epsilon Tr(\not{p}_1\not{k}(4p_2 \cdot k - 2\epsilon\not{p}_2\not{k})) \\
&= -32(1-\epsilon)(p_1 \cdot p_2)(p_1 \cdot p_2 + p_1 \cdot k + p_2 \cdot k) \\
&\quad + 32\epsilon(1-\epsilon)(p_1 \cdot k)(p_2 \cdot k)
\end{aligned} \tag{B.6}$$

where, apart from the contraction identity we used in the previous computation, we also used the identities

$$\gamma^\alpha\gamma^{\mu_1}\gamma^{\mu_2}\gamma_\alpha = 4g^{\mu_1\mu_2} - 2\epsilon\gamma^{\mu_1}\gamma^{\mu_2} \tag{B.7}$$

and

$$Tr(\gamma^{\mu_1}\gamma^{\mu_2}) = 4g^{\mu_1\mu_2}. \tag{B.8}$$

Appendix C

Computation of the Wave-Function Renormalization

In this Appendix, we compute the wave-function renormalization constants at one-loop order for fermions in QED and scalars in a theory with a cubic interaction.

In order to compute the renormalization factor Z_2 for the fermion wave-function at the one-loop order, we begin by calculating the self-energy contribution

$$-i\Sigma_2(\not{p}) = \underset{}{}$$

$$= -e^2 \int \frac{d^D k}{(2\pi)^D} \frac{(D-2)(\not{k} - \not{p}) + Dm}{(k^2 - m_\gamma^2)((k-p)^2 - m^2)}$$

where we have written the integral in dimensional regularization. Also, to regulate the possible IR divergences coming from the photon propagator, we include an small mass m_γ, which should cancel in the computation of any physical observable. Introducing Feynman parameters, we turn the product of the two propagators into

$$\frac{1}{(k^2 - m_\gamma^2)((k-p)^2 - m^2)} = \int_0^1 dx \frac{1}{[(k-(1-x)p)^2 - \Delta(x)]^2} \qquad \text{(C.1)}$$

where we define

$$\Delta(x) = (1-x)(m^2 - xp^2) + xm_\gamma^2. \qquad \text{(C.2)}$$

We can perform the shift $k \to k + xp$ and introduce the renormalization scale μ to obtain

$$-i\Sigma_2(\not{p}) = -e^2 \mu^{2\epsilon} \int_0^1 dx \int \frac{d^D k}{(2\pi)^D} \frac{(D-2)(\not{k} - x\not{p}) + Dm}{(k^2 - \Delta(x))^2} \qquad \text{(C.3)}$$

Now, since the denominator is an even function in k, the term with $\not{k}$ in the numerator vanishes. The resulting momentum integral is then the tadpole integral of Eq.(2.28) in the special case $b = 2$, with a "squared mass" $\Delta(x)$. Then, using the general result of Eq.(2.35), with $D = 4 - 2\epsilon$, we arrive at the intermediate result

$$-i\Sigma_2(\not{p}) = \frac{ie^2\mu^{2\epsilon}}{8\pi^2}\frac{\Gamma(\epsilon)}{(4\pi)^{-\epsilon}}\int_0^1 dx\,[(1-\epsilon)x\not{p} - (2-\epsilon)m]\,(\Delta(x))^{-\epsilon} \quad \text{(C.4)}$$

At the same order in the electric charge, the counterterm Lagrangian gives a contribution to the two-point function, given by

$$-i\Sigma_2^{CT}(\not{p}) = \underline{\quad\otimes\quad} = i(\not{p}\delta_2 - \delta_m). \quad \text{(C.5)}$$

Thus, the second renormalization condition, $\left.\frac{d\Sigma}{d\not{p}}\right|_{\not{p}=m} = 0$, results directly in an expression for the counterterm δ_2 in the on-shell scheme

$$
\begin{aligned}
\delta_2 &= \left.\frac{d\Sigma_2}{d\not{p}}\right|_{\not{p}=m} \\
&= -\frac{e^2\mu^{2\epsilon}}{8\pi^2}\Gamma(\epsilon)\int_0^1 \frac{dx}{[(1-x)^2m^2 + xm_\gamma^2]^\epsilon} \\
&\quad \times \left[(1-\epsilon)x - \epsilon\frac{2x(1-x)m^2}{(1-x)^2m^2 + xm_\gamma^2}(x - 2 + \epsilon(1-x))\right]
\end{aligned}
\quad \text{(C.6)}
$$

which agrees with the result of [20]. Notice that all the UV divergences of δ_2 are contained in the first term in the brackets, since the appearance of ϵ in the numerator of the second term cancels the pole from the Gamma function.

Now, we will compute the factor Z_ϕ for ϕ^3 theory, using the Lagrangian and Feynman rules of Appendix A. At one-loop, there are two corrections to the Fermion propagator, denoted by $M^{(1)}(p^2)$, which we write as

$$M^{(1)}(p^2) = \underbrace{\overset{\overset{k}{\frown}}{\underset{p\quad\quad\quad p}{}}}_{M^{(1)}_{bare}(p^2)} + \underbrace{\underline{\quad\otimes\quad}}_{M^{(1)}_{CT}(p^2)}. \quad \text{(C.7)}$$

The value of the second contribution is given by the Feynman rule for the counterterm. Thus, we only need to compute the bare contribution, which is given by the integral

$$M^{(1)}_{bare}(p^2) = \frac{\tilde{\lambda}^2}{2}\int\frac{d^Dk}{(2\pi)^D}\frac{1}{(k^2 - m^2 + i\delta)((k-p)^2 - m^2 + i\delta)} \quad \text{(C.8)}$$

where the factor of 2 in the denominator is the symmetry factor associated to the bubble diagram. As in the case of QED, we introduce Feynman parameters. In this case, both propagators have mass m, and we find

$$
\frac{1}{(k^2 - m^2 + i\delta)((k-p)^2 - m^2 + i\delta)}
= \int_0^1 dx \frac{1}{[(k-xp)^2 - m^2 + x(1-x)p^2]^2}
\tag{C.9}
$$

thus, shifting $k \to k + xp$ in the loop integration and using again the tadpole integral of Eq.(2.28), we find, setting $D = 4 - 2\epsilon$ as in all our previous calculations,

$$
\begin{aligned}
M^{(1)}_{bare}(p^2) &= \frac{i\tilde{\lambda}^2}{2(4\pi)^{\frac{D}{2}}} \Gamma\left(2 - \frac{D}{2}\right) \int_0^1 dx \left(m^2 - x(1-x)p^2\right)^{-2+\frac{D}{2}} \\
&= \frac{i\mu^{2\epsilon}(4\pi)^{-\epsilon}e^{\epsilon\gamma}\lambda^2}{2(4\pi)^{2-\epsilon}} \Gamma(\epsilon) \int_0^1 dx (m^2 - x(1-x)p^2)^{-\epsilon} \\
&= \frac{i\lambda^2}{32\pi^2} \left(\frac{m^2}{\mu^2}\right)^{-\epsilon} e^{\epsilon\gamma}\Gamma(\epsilon) \int_0^1 dx \left(1 - x(1-x)\frac{p^2}{m^2}\right)^{-\epsilon}.
\end{aligned}
\tag{C.10}
$$

Putting this contribution together with the counterterm, the one-loop correction to the propagator is given by

$$
\begin{aligned}
M^{(1)}(p^2) &= \frac{i\lambda^2}{32\pi^2} \left(\frac{m^2}{\mu^2}\right)^{-\epsilon} e^{\epsilon\gamma}\Gamma(\epsilon) \int_0^1 dx \left(1 - x(1-x)\frac{p^2}{m^2}\right)^{-\epsilon} \\
&\quad + i\left((Z_\phi - 1)p^2 - (Z_\phi Z_m^2 - 1)m^2\right)
\end{aligned}
\tag{C.11}
$$

Similar to the case of QED, we impose the renormalization conditions

$$
\begin{aligned}
M(p^2 = m^2) &= 0 \\
\left.\frac{dM}{dp^2}\right|_{p^2=m^2} &= 0
\end{aligned}
\tag{C.12}
$$

We can directly obtain Z_ϕ from the second condition, since the counterterm contribution is linear in p^2 at one-loop order. We find

$$
\begin{aligned}
Z_\phi - 1 &= -\frac{\lambda^2}{32\pi^2} \left(\frac{m^2}{\mu^2}\right)^{-\epsilon} e^{\epsilon\gamma}\Gamma(\epsilon) \int_0^1 dx \frac{\partial}{\partial p^2} \left(1 - x(1-x)\frac{p^2}{m^2}\right)^{-\epsilon}\Bigg|_{p^2=m^2} \\
&= -\frac{\lambda^2}{32\pi^2 m^2} \left(\frac{m^2}{\mu^2}\right)^{-\epsilon} e^{\epsilon\gamma}\epsilon\Gamma(\epsilon) \int_0^1 dx \left(1 - x(1-x)\right)^{-\epsilon-1} x(1-x).
\end{aligned}
\tag{C.13}
$$

At this point, we can see that the appearance of ϵ in the numerator of this expression, which we find after computing the derivative, will cancel the pole of the Gamma function. Since all remaining terms are finite when $\epsilon \to 0$, we can simply take $\epsilon = 0$, giving us the final result

$$Z_\phi = 1 - \frac{\lambda^2}{32\pi^2 m^2} \int_0^1 dx \frac{x(1-x)}{1 - x(1-x)}. \tag{C.14}$$

Since the remaining integral is just a number, this result shows that, at one-loop order, the renormalization constant Z_ϕ in ϕ^3 theory is independent of the regulator.

Bibliography

[1] R. Runkel, Z. Szőr, J. P. Vesga and S. Weinzierl, "Causality and loop-tree duality at higher loops," Phys. Rev. Lett. **122** (2019) no.11, 111603 [erratum: Phys. Rev. Lett. **123** (2019) no.5, 059902] doi:10.1103/PhysRevLett.122.111603 [arXiv:1902.02135 [hep-ph]].

[2] R. Runkel, Z. Szőr, J. P. Vesga and S. Weinzierl, "Integrands of loop amplitudes within loop-tree duality," Phys. Rev. D **101** (2020) no.11, 116014 doi:10.1103/PhysRevD.101.116014 [arXiv:1906.02218 [hep-ph]].

[3] R. Runkel, Z. Szőr, J. P. Vesga and S. Weinzierl, "A new formulation of the loop-tree duality at higher loops," doi:10.22323/1.375.0073 [arXiv:1911.09610 [hep-ph]].

[4] B. P. Abbott *et al.* [LIGO Scientific and Virgo], "GW170814: A Three-Detector Observation of Gravitational Waves from a Binary Black Hole Coalescence," Phys. Rev. Lett. **119** (2017) no.14, 141101 doi:10.1103/PhysRevLett.119.141101 [arXiv:1709.09660 [gr-qc]].

[5] J. de Blas, R. Franceschini, F. Riva, P. Roloff, U. Schnoor, M. Spannowsky, J. D. Wells, A. Wulzer, J. Zupan and S. Alipour-Fard, *et al.* doi:10.23731/CYRM-2018-003 [arXiv:1812.02093 [hep-ph]].

[6] CLICdp, CLIC collaboration, The Compact Linear Collider (CLIC) - 2018 Summary Report, 2018.

[7] FCC collaboration, Future Circular Collider: Vol. 1 Physics opportunities, 2018.

[8] FCC collaboration, Future Circular Collider: Vol. 2 The Lepton Collider (FCC-ee), 2018.

[9] FCC collaboration, Future Circular Collider: Vol. 3 The Hadron Collider (FCC-hh), 2018.

[10] FCC collaboration, Future Circular Collider: Vol. 4 The High-Energy LHC (HE-LHC), 2018.

[11] P. Bambade, T. Barklow, T. Behnke, M. Berggren, J. Brau, P. Burrows, D. Denisov, A. Faus-Golfe, B. Foster and K. Fujii, *et al.* "The International Linear Collider: A Global Project," [arXiv:1903.01629 [hep-ex]].

[12] CEPC-SPPC Study Group collaboration, CEPC-SPPC Preliminary Conceptual Design Report. 1. Physics and Detector, 2015.

[13] CEPC-SPPC Study Group collaboration, CEPC-SPPC Preliminary Conceptual Design Report. 2. Accelerator, 2015.

[14] J. Alwall, R. Frederix, S. Frixione, V. Hirschi, F. Maltoni, O. Mattelaer, H. S. Shao, T. Stelzer, P. Torrielli and M. Zaro, "The automated computation of tree-level and next-to-leading order differential cross sections, and their matching to parton shower simulations," JHEP **07** (2014), 079 doi:10.1007/JHEP07(2014)079 [arXiv:1405.0301 [hep-ph]].

[15] J. M. Campbell, R. K. Ellis and C. Williams, "Vector boson pair production at the LHC," JHEP **07** (2011), 018 doi:10.1007/JHEP07(2011)018 [arXiv:1105.0020 [hep-ph]].

[16] C. F. Berger, Z. Bern, L. J. Dixon, F. Febres Cordero, D. Forde, H. Ita, D. A. Kosower and D. Maitre, "An Automated Implementation of On-Shell Methods for One-Loop Amplitudes," Phys. Rev. D **78** (2008), 036003 doi:10.1103/PhysRevD.78.036003 [arXiv:0803.4180 [hep-ph]].

[17] Z. Bern, L. J. Dixon, F. Febres Cordero, S. Höche, H. Ita, D. A. Kosower, D. Maître and K. J. Ozeren, "The BlackHat Library for One-Loop Amplitudes," J. Phys. Conf. Ser. **523** (2014), 012051 doi:10.1088/1742-6596/523/1/012051 [arXiv:1310.2808 [hep-ph]].

[18] D. J. Gross and F. Wilczek, "Ultraviolet Behavior of Non-abelian Gauge Theories," Phys. Rev. Lett. **30** (1973), 1343-1346 doi:10.1103/PhysRevLett.30.1343

[19] H. D. Politzer, "Reliable Perturbative Results for Strong Interactions?," Phys. Rev. Lett. **30** (1973), 1346-1349 doi:10.1103/PhysRevLett.30.1346

[20] M. E. Peskin and D. V. Schroeder, "An Introduction to quantum field theory," ISBN:9780201503975

[21] M. D. Schwartz, "Quantum Field Theory and the Standard Model," ISBN:9781107034730

[22] S. Weinberg, "Photons and Gravitons in *S*-Matrix Theory: Derivation of Charge Conservation and Equality of Gravitational and Inertial Mass," Phys. Rev. **135** (1964), B1049-B1056 doi:10.1103/PhysRev.135.B1049

[23] S. Weinberg, "Infrared photons and gravitons," Phys. Rev. **140** (1965), B516-B524 doi:10.1103/PhysRev.140.B516

[24] T. Kinoshita, "Mass singularities of Feynman amplitudes," J. Math. Phys. **3** (1962), 650-677 doi:10.1063/1.1724268

[25] T. D. Lee and M. Nauenberg, 'Degenerate Systems and Mass Singularities," Phys. Rev. **133** (1964), B1549-B1562 doi:10.1103/PhysRev.133.B1549

[26] A. V. Kotikov, "Differential equations method: New technique for massive Feynman diagrams calculation," Phys. Lett. B **254** (1991), 158-164 doi:10.1016/0370-2693(91)90413-K

[27] A. V. Kotikov, "Differential equation method: The Calculation of N point Feynman diagrams," Phys. Lett. B **267** (1991), 123-127 [erratum: Phys. Lett. B **295** (1992), 409-409] doi:10.1016/0370-2693(91)90536-Y

[28] Z. Bern, L. J. Dixon and D. A. Kosower, "Dimensionally regulated pentagon integrals," Nucl. Phys. B **412** (1994), 751-816 doi:10.1016/0550-3213(94)90398-0 [arXiv:hep-ph/9306240 [hep-ph]].

[29] T. Gehrmann and E. Remiddi, "Differential equations for two loop four point functions," Nucl. Phys. B **580** (2000), 485-518 doi:10.1016/S0550-3213(00)00223-6 [arXiv:hep-ph/9912329 [hep-ph]].

[30] S. Müller-Stach, S. Weinzierl and R. Zayadeh, "Picard-Fuchs equations for Feynman integrals," Commun. Math. Phys. **326** (2014), 237-249 doi:10.1007/s00220-013-1838-3 [arXiv:1212.4389 [hep-ph]].

[31] L. Adams, E. Chaubey and S. Weinzierl, "Simplifying Differential Equations for Multiscale Feynman Integrals beyond Multiple Polylogarithms," Phys. Rev. Lett. **118** (2017) no.14, 141602 doi:10.1103/PhysRevLett.118.141602 [arXiv:1702.04279 [hep-ph]].

[32] J. M. Henn, "Multiloop integrals in dimensional regularization made simple," Phys. Rev. Lett. **110** (2013), 251601 doi:10.1103/PhysRevLett.110.251601 [arXiv:1304.1806 [hep-th]].

[33] A. B. Goncharov, "Multiple polylogarithms, cyclotomy and modular complexes," Math. Res. Lett. **5** (1998), 497-516 doi:10.4310/MRL.1998.v5.n4.a7 [arXiv:1105.2076 [math.AG]].

[34] E. Remiddi and J. A. M. Vermaseren, "Harmonic polylogarithms," Int. J. Mod. Phys. A **15** (2000), 725-754

doi:10.1142/S0217751X00000367 [arXiv:hep-ph/9905237 [hep-ph]].

[35] S. Weinzierl, "Feynman integrals and multiple polylogarithms," IRMA Lect. Math. Theor. Phys. **15** (2009), 247-270 doi:10.4171/073-1/8 [arXiv:0705.0900 [hep-ph]].

[36] J. M. Henn and V. A. Smirnov, "Analytic results for two-loop master integrals for Bhabha scattering I," JHEP **11** (2013), 041 doi:10.1007/JHEP11(2013)041 [arXiv:1307.4083 [hep-th]].

[37] T. Gehrmann, A. von Manteuffel, L. Tancredi and E. Weihs, "The two-loop master integrals for $q\bar{q} \to VV$," JHEP **06** (2014), 032 doi:10.1007/JHEP06(2014)032 [arXiv:1404.4853 [hep-ph]].

[38] L. Adams, C. Bogner and S. Weinzierl, "The two-loop sunrise graph in two space-time dimensions with arbitrary masses in terms of elliptic dilogarithms," J. Math. Phys. **55** (2014) no.10, 102301 doi:10.1063/1.4896563 [arXiv:1405.5640 [hep-ph]].

[39] L. Adams, C. Bogner and S. Weinzierl, "The two-loop sunrise integral around four space-time dimensions and generalisations of the Clausen and Glaisher functions towards the elliptic case," J. Math. Phys. **56** (2015) no.7, 072303 doi:10.1063/1.4926985 [arXiv:1504.03255 [hep-ph]].

[40] L. Adams, C. Bogner, A. Schweitzer and S. Weinzierl, "The kite integral to all orders in terms of elliptic polylogarithms," J. Math. Phys. **57** (2016) no.12, 122302 doi:10.1063/1.4969060 [arXiv:1607.01571 [hep-ph]].

[41] L. Adams and S. Weinzierl, "The ε-form of the differential equations for Feynman integrals in the elliptic case," Phys. Lett. B **781** (2018), 270-278 doi:10.1016/j.physletb.2018.04.002 [arXiv:1802.05020 [hep-ph]].

[42] S. Catani and M. H. Seymour, "A General algorithm for calculating jet cross-sections in NLO QCD," Nucl. Phys. B **485** (1997), 291-419 [erratum: Nucl. Phys. B **510** (1998), 503-504] doi:10.1016/S0550-3213(96)00589-5 [arXiv:hep-ph/9605323 [hep-ph]].

[43] L. Phaf and S. Weinzierl, "Dipole formalism with heavy fermions," JHEP **04** (2001), 006 doi:10.1088/1126-6708/2001/04/006 [arXiv:hep-ph/0102207 [hep-ph]].

[44] S. Catani, S. Dittmaier, M. H. Seymour and Z. Trocsanyi, "The Dipole formalism for next-to-leading order QCD calculations with massive partons," Nucl. Phys. B **627** (2002), 189-265 doi:10.1016/S0550-3213(02)00098-6 [arXiv:hep-ph/0201036 [hep-ph]].

[45] M. Assadsolimani, S. Becker and S. Weinzierl, "A Simple formula for the infrared singular part of the integrand of one-loop QCD amplitudes," Phys. Rev. D **81** (2010), 094002 doi:10.1103/PhysRevD.81.094002 [arXiv:0912.1680 [hep-ph]].

[46] D. E. Soper, "QCD calculations by numerical integration," Phys. Rev. Lett. **81** (1998), 2638-2641 doi:10.1103/PhysRevLett.81.2638 [arXiv:hep-ph/9804454 [hep-ph]].

[47] D. E. Soper, "Techniques for QCD calculations by numerical integration," Phys. Rev. D **62** (2000), 014009 doi:10.1103/PhysRevD.62.014009 [arXiv:hep-ph/9910292 [hep-ph]].

[48] Z. Nagy and D. E. Soper, "General subtraction method for numerical calculation of one loop QCD matrix elements," JHEP **09** (2003), 055 doi:10.1088/1126-6708/2003/09/055 [arXiv:hep-ph/0308127 [hep-ph]].

[49] W. Gong, Z. Nagy and D. E. Soper, "Direct numerical integration of one-loop Feynman diagrams for N-photon amplitudes," Phys. Rev. D **79** (2009), 033005 doi:10.1103/PhysRevD.79.033005 [arXiv:0812.3686 [hep-ph]].

[50] M. Assadsolimani, S. Becker, C. Reuschle and S. Weinzierl, "Infrared singularities in one-loop amplitudes," Nucl. Phys. B Proc. Suppl. **205-206** (2010), 224-229 doi:10.1016/j.nuclphysbps.2010.08.047 [arXiv:1006.4609 [hep-ph]].

[51] S. Becker, C. Reuschle and S. Weinzierl, "Numerical NLO QCD calculations," JHEP **12** (2010), 013 doi:10.1007/JHEP12(2010)013 [arXiv:1010.4187 [hep-ph]].

[52] S. Becker, D. Goetz, C. Reuschle, C. Schwan and S. Weinzierl, "NLO results for five, six and seven jets in electron-positron annihilation," Phys. Rev. Lett. **108** (2012), 032005 doi:10.1103/PhysRevLett.108.032005 [arXiv:1111.1733 [hep-ph]].

[53] S. Becker, C. Reuschle and S. Weinzierl, "Efficiency Improvements for the Numerical Computation of NLO Corrections," JHEP **07** (2012), 090 doi:10.1007/JHEP07(2012)090 [arXiv:1205.2096 [hep-ph]].

[54] S. Becker and S. Weinzierl, "Direct contour deformation with arbitrary masses in the loop," Phys. Rev. D **86** (2012), 074009 doi:10.1103/PhysRevD.86.074009 [arXiv:1208.4088 [hep-ph]].

[55] S. Becker and S. Weinzierl, "Direct numerical integration for multi-loop integrals," Eur. Phys. J. C **73** (2013) no.2, 2321 doi:10.1140/epjc/s10052-013-2321-1 [arXiv:1211.0509 [hep-ph]].

[56] D. Götz, C. Reuschle, C. Schwan and S. Weinzierl, "NLO corrections to Z production in association with several jets," PoS **LL2014** (2014), 009 doi:10.22323/1.211.0009 [arXiv:1407.0203 [hep-ph]].

[57] S. Seth and S. Weinzierl, "Numerical integration of subtraction terms," Phys. Rev. D **93** (2016) no.11, 114031 doi:10.1103/PhysRevD.93.114031 [arXiv:1605.06646 [hep-ph]].

[58] C. Anastasiou and G. Sterman, "Removing infrared divergences from two-loop integrals," JHEP **07** (2019), 056 doi:10.1007/JHEP07(2019)056 [arXiv:1812.03753 [hep-ph]].

[59] J. Gluza, K. Kajda and D. A. Kosower, "Towards a Basis for Planar Two-Loop Integrals," Phys. Rev. D **83** (2011), 045012 doi:10.1103/PhysRevD.83.045012 [arXiv:1009.0472 [hep-th]].

[60] D. A. Kosower and K. J. Larsen, "Maximal Unitarity at Two Loops," Phys. Rev. D **85** (2012), 045017 doi:10.1103/PhysRevD.85.045017 [arXiv:1108.1180 [hep-th]].

[61] S. Caron-Huot and K. J. Larsen, "Uniqueness of two-loop master contours," JHEP **10** (2012), 026 doi:10.1007/JHEP10(2012)026 [arXiv:1205.0801 [hep-ph]].

[62] Y. Zhang, "Integrand-Level Reduction of Loop Amplitudes by Computational Algebraic Geometry Methods," JHEP **09** (2012), 042 doi:10.1007/JHEP09(2012)042 [arXiv:1205.5707 [hep-ph]].

[63] M. Sogaard and Y. Zhang, "Unitarity Cuts of Integrals with Doubled Propagators," JHEP **07** (2014), 112 doi:10.1007/JHEP07(2014)112 [arXiv:1403.2463 [hep-th]].

[64] K. J. Larsen and Y. Zhang, "Integration-by-parts reductions from unitarity cuts and algebraic geometry," Phys. Rev. D **93** (2016) no.4, 041701 doi:10.1103/PhysRevD.93.041701 [arXiv:1511.01071 [hep-th]].

[65] H. Ita, "Two-loop Integrand Decomposition into Master Integrals and Surface Terms," Phys. Rev. D **94** (2016) no.11, 116015 doi:10.1103/PhysRevD.94.116015 [arXiv:1510.05626 [hep-th]].

[66] A. von Manteuffel and R. M. Schabinger, "A novel approach to integration by parts reduction," Phys. Lett. B **744** (2015), 101-104 doi:10.1016/j.physletb.2015.03.029 [arXiv:1406.4513 [hep-ph]].

[67] T. Peraro, "Scattering amplitudes over finite fields and multivariate functional reconstruction," JHEP **12** (2016), 030 doi:10.1007/JHEP12(2016)030 [arXiv:1608.01902 [hep-ph]].

[68] T. Peraro, "FiniteFlow: multivariate functional reconstruction using finite fields and dataflow graphs," JHEP **07** (2019), 031 doi:10.1007/JHEP07(2019)031 [arXiv:1905.08019 [hep-ph]].

[69] S. Badger, C. Brønnum-Hansen, H. B. Hartanto and T. Peraro, "First look at two-loop five-gluon scattering in QCD," Phys. Rev. Lett. **120** (2018) no.9, 092001 doi:10.1103/PhysRevLett.120.092001 [arXiv:1712.02229 [hep-ph]].

[70] S. Badger, C. Brønnum-Hansen, T. Gehrmann, H. B. Hartanto, J. Henn, N. A. Lo Presti and T. Peraro, "Applications of integrand reduction to two-loop five-point scattering amplitudes in QCD," PoS **LL2018** (2018), 006 doi:10.22323/1.303.0006 [arXiv:1807.09709 [hep-ph]].

[71] S. Badger, C. Brønnum-Hansen, H. B. Hartanto and T. Peraro, "Analytic helicity amplitudes for two-loop five-gluon scattering: the single-minus case," JHEP **01** (2019), 186 doi:10.1007/JHEP01(2019)186 [arXiv:1811.11699 [hep-ph]].

[72] S. Abreu, F. Febres Cordero, H. Ita, M. Jaquier and B. Page, "Subleading Poles in the Numerical Unitarity Method at Two Loops," Phys. Rev. D **95** (2017) no.9, 096011 doi:10.1103/PhysRevD.95.096011 [arXiv:1703.05255 [hep-ph]].

[73] S. Abreu, F. Febres Cordero, H. Ita, M. Jaquier, B. Page and M. Zeng, "Two-Loop Four-Gluon Amplitudes from Numerical Unitarity," Phys. Rev. Lett. **119** (2017) no.14, 142001 doi:10.1103/PhysRevLett.119.142001 [arXiv:1703.05273 [hep-ph]].

[74] S. Abreu, F. Febres Cordero, H. Ita, B. Page and M. Zeng, "Planar Two-Loop Five-Gluon Amplitudes from Numerical Unitarity," Phys. Rev. D **97** (2018) no.11, 116014 doi:10.1103/PhysRevD.97.116014 [arXiv:1712.03946 [hep-ph]].

[75] S. Abreu, J. Dormans, F. Febres Cordero, H. Ita and B. Page, "Analytic Form of Planar Two-Loop Five-Gluon Scattering Amplitudes in QCD," Phys. Rev. Lett. **122** (2019) no.8, 082002 doi:10.1103/PhysRevLett.122.082002 [arXiv:1812.04586 [hep-ph]].

[76] S. Abreu, J. Dormans, F. Febres Cordero, H. Ita, B. Page and V. Sotnikov, "Analytic Form of the Planar Two-Loop Five-Parton Scattering Amplitudes in QCD," JHEP **05** (2019), 084 doi:10.1007/JHEP05(2019)084 [arXiv:1904.00945 [hep-ph]].

[77] W. Pauli and F. Villars, "On the Invariant regularization in relativistic quantum theory," Rev. Mod. Phys. **21** (1949), 434-444 doi:10.1103/RevModPhys.21.434

[78] K. G. Wilson, "Confinement of Quarks," Phys. Rev. D **10** (1974), 2445-2459 doi:10.1103/PhysRevD.10.2445

[79] C. G. Bollini and J. J. Giambiagi, "Dimensional Renormalization: The Number of Dimensions as a Regularizing Parameter," Nuovo Cim. B **12** (1972), 20-26 doi:10.1007/BF02895558

[80] G. 't Hooft and M. J. G. Veltman, "Regularization and Renormalization of Gauge Fields," Nucl. Phys. B **44** (1972), 189-213 doi:10.1016/0550-3213(72)90279-9

[81] S. Weinberg, "New approach to the renormalization group," Phys. Rev. D **8** (1973), 3497-3509 doi:10.1103/PhysRevD.8.3497

[82] S. Weinzierl, "The infrared structure of $e^+e^- \rightarrow$ 3 jets at NNLO reloaded," JHEP **07** (2009), 009 doi:10.1088/1126-6708/2009/07/009 [arXiv:0904.1145 [hep-ph]].

[83] C. Bogner and S. Weinzierl, "Feynman graph polynomials," Int. J. Mod. Phys. A **25** (2010), 2585-2618 doi:10.1142/S0217751X10049438 [arXiv:1002.3458 [hep-ph]].

[84] Bondy, J. A., Murty, U. S. R. "Graph Theory with Applications." MacMillan, London, 1976.

[85] J. C. Collins, "Renormalization: An Introduction to Renormalization, The Renormalization Group, and the Operator Product Expansion," doi:10.1017/CBO9780511622656

[86] H. Lehmann, K. Symanzik and W. Zimmermann, "On the formulation of quantized field theories," Nuovo Cim. **1** (1955), 205-225 doi:10.1007/BF02731765

[87] R. Baumeister, D. Mediger, J. Pečovnik and S. Weinzierl, "Vanishing of certain cuts or residues of loop integrals with higher powers of the propagators," Phys. Rev. D **99** (2019) no.9, 096023 doi:10.1103/PhysRevD.99.096023 [arXiv:1903.02286 [hep-ph]].

[88] S. Catani, T. Gleisberg, F. Krauss, G. Rodrigo and J. C. Winter, "From loops to trees by-passing Feynman's theorem," JHEP **09** (2008), 065 doi:10.1088/1126-6708/2008/09/065 [arXiv:0804.3170 [hep-ph]].

[89] R. K. Ellis and G. Zanderighi, "Scalar one-loop integrals for QCD," JHEP **02** (2008), 002 doi:10.1088/1126-6708/2008/02/002 [arXiv:0712.1851 [hep-ph]].

[90] P. Griffiths, J. Harris, "Principles of Algebraic Geometry," DOI:10.1002/9781118032527

[91] R. P. Feynman, "Quantum theory of gravitation," Acta Phys. Polon. **24** (1963), 697-722

[92] I. Bierenbaum, S. Catani, P. Draggiotis and G. Rodrigo, "A Tree-Loop Duality Relation at Two Loops and Beyond," JHEP **10** (2010), 073 doi:10.1007/JHEP10(2010)073 [arXiv:1007.0194 [hep-ph]].

[93] I. Bierenbaum, S. Buchta, P. Draggiotis, I. Malamos and G. Rodrigo, "Tree-Loop Duality Relation beyond simple poles," JHEP **03** (2013), 025 doi:10.1007/JHEP03(2013)025 [arXiv:1211.5048 [hep-ph]].

[94] G. F. R. Sborlini, F. Driencourt-Mangin, R. Hernandez-Pinto and G. Rodrigo, "Four-dimensional regularization of higher-order computations: FDU approach," PoS **EPS-HEP2017** (2017), 547 doi:10.22323/1.314.0547 [arXiv:1710.04516 [hep-ph]].

[95] F. Driencourt-Mangin, G. Rodrigo, G. F. R. Sborlini and W. J. Torres Bobadilla, "Universal four-dimensional representation of $H \to \gamma\gamma$ at two loops through the Loop-Tree Duality," JHEP **02** (2019), 143 doi:10.1007/JHEP02(2019)143 [arXiv:1901.09853 [hep-ph]].

[96] J. J. Aguilera-Verdugo, F. Driencourt-Mangin, J. Plenter, S. Ramírez-Uribe, G. Rodrigo, G. F. R. Sborlini, W. J. Torres Bobadilla and S. Tracz, "Causality, unitarity thresholds, anomalous thresholds and infrared singularities from the loop-tree duality at higher orders," JHEP **12** (2019), 163 doi:10.1007/JHEP12(2019)163 [arXiv:1904.08389 [hep-ph]].

[97] J. J. Aguilera-Verdugo, F. Driencourt-Mangin, R. J. Hernández-Pinto, J. Plenter, S. Ramirez-Uribe, A. E. Renteria Olivo, G. Rodrigo, G. F. R. Sborlini, W. J. Torres Bobadilla and S. Tracz, "Open Loop Amplitudes and Causality to All Orders and Powers from the Loop-Tree Duality," Phys. Rev. Lett. **124** (2020) no.21, 211602 doi:10.1103/PhysRevLett.124.211602 [arXiv:2001.03564 [hep-ph]].

[98] J. Plenter and G. Rodrigo, "Asymptotic expansions through the loop-tree duality," Eur. Phys. J. C **81** (2021) no.4, 320 doi:10.1140/epjc/s10052-021-09094-9 [arXiv:2005.02119 [hep-ph]].

[99] J. J. Aguilera-Verdugo, R. J. Hernandez-Pinto, G. Rodrigo, G. F. R. Sborlini and W. J. Torres Bobadilla, "Causal representation of multi-loop Feynman integrands within the loop-tree duality," JHEP **01** (2021), 069 doi:10.1007/JHEP01(2021)069 [arXiv:2006.11217 [hep-ph]].

[100] S. Ramírez-Uribe, R. J. Hernández-Pinto, G. Rodrigo, G. F. R. Sborlini and W. J. Torres Bobadilla, "Universal opening of four-loop scattering amplitudes to trees," JHEP

04 (2021), 129 doi:10.1007/JHEP04(2021)129 [arXiv:2006.13818 [hep-ph]].

[101] S. Ramírez-Uribe, A. E. Rentería-Olivo, G. Rodrigo, G. F. R. Sborlini and L. Vale Silva, [arXiv:2105.08703 [hep-ph]].

[102] J. Jesús Aguilera-Verdugo, R. J. Hernández-Pinto, G. Rodrigo, G. F. R. Sborlini and W. J. Torres Bobadilla, "Mathematical properties of nested residues and their application to multi-loop scattering amplitudes," JHEP **02** (2021), 112 doi:10.1007/JHEP02(2021)112 [arXiv:2010.12971 [hep-ph]].

[103] W. J. Torres Bobadilla, "Loop-tree duality from vertices and edges," JHEP **04** (2021), 183 doi:10.1007/JHEP04(2021)183 [arXiv:2102.05048 [hep-ph]].

[104] G. F. R. Sborlini, "Geometrical approach to causality in multiloop amplitudes," Phys. Rev. D **104** (2021) no.3, 036014 doi:10.1103/PhysRevD.104.036014 [arXiv:2102.05062 [hep-ph]].

[105] Z. Capatti, V. Hirschi, D. Kermanschah and B. Ruijl, "Loop-Tree Duality for Multiloop Numerical Integration," Phys. Rev. Lett. **123** (2019) no.15, 151602 doi:10.1103/PhysRevLett.123.151602 [arXiv:1906.06138 [hep-ph]].

[106] Z. Capatti, V. Hirschi, D. Kermanschah, A. Pelloni and B. Ruijl, "Numerical Loop-Tree Duality: contour deformation and subtraction," JHEP **04** (2020), 096 doi:10.1007/JHEP04(2020)096 [arXiv:1912.09291 [hep-ph]].

[107] Z. Capatti, V. Hirschi, D. Kermanschah, A. Pelloni and B. Ruijl, "Manifestly Causal Loop-Tree Duality," [arXiv:2009.05509 [hep-ph]].

[108] Z. Capatti, V. Hirschi, A. Pelloni and B. Ruijl, "Local Unitarity: a representation of differential cross-sections that is locally free of infrared singularities at any order," JHEP **04** (2021), 104 doi:10.1007/JHEP04(2021)104 [arXiv:2010.01068 [hep-ph]].

[109] N. Arkani-Hamed, J. L. Bourjaily, F. Cachazo, S. Caron-Huot and J. Trnka, "The All-Loop Integrand For Scattering Amplitudes in Planar N=4 SYM," JHEP **01** (2011), 041 doi:10.1007/JHEP01(2011)041 [arXiv:1008.2958 [hep-th]].

[110] N. Arkani-Hamed and J. Trnka, "The Amplituhedron," JHEP **10** (2014), 030 doi:10.1007/JHEP10(2014)030 [arXiv:1312.2007 [hep-th]].

[111] N. Arkani-Hamed and J. Trnka, "Into the Amplituhedron," JHEP **12** (2014), 182 doi:10.1007/JHEP12(2014)182 [arXiv:1312.7878 [hep-th]].

[112] Y. Geyer, L. Mason, R. Monteiro and P. Tourkine, "Loop Integrands for Scattering Amplitudes from the Riemann Sphere," Phys. Rev. Lett. **115** (2015) no.12, 121603 doi:10.1103/PhysRevLett.115.121603 [arXiv:1507.00321 [hep-th]].

[113] Y. Geyer, L. Mason, R. Monteiro and P. Tourkine, "One-loop amplitudes on the Riemann sphere," JHEP **03** (2016), 114 doi:10.1007/JHEP03(2016)114 [arXiv:1511.06315 [hep-th]].

[114] Y. Geyer, L. Mason, R. Monteiro and P. Tourkine, "Two-Loop Scattering Amplitudes from the Riemann Sphere," Phys. Rev. D **94** (2016) no.12, 125029 doi:10.1103/PhysRevD.94.125029 [arXiv:1607.08887 [hep-th]].

[115] Y. Geyer and R. Monteiro, "Gluons and gravitons at one loop from ambitwistor strings," JHEP **03** (2018), 068 doi:10.1007/JHEP03(2018)068 [arXiv:1711.09923 [hep-th]].

[116] Y. Geyer and R. Monteiro, "Two-Loop Scattering Amplitudes from Ambitwistor Strings: from Genus Two to the Nodal Riemann Sphere," JHEP **11** (2018), 008 doi:10.1007/JHEP11(2018)008 [arXiv:1805.05344 [hep-th]].

[117] F. Cachazo, S. He and E. Y. Yuan, "One-Loop Corrections from Higher Dimensional Tree Amplitudes," JHEP **08** (2016), 008 doi:10.1007/JHEP08(2016)008 [arXiv:1512.05001 [hep-th]].

[118] B. Feng, "CHY-construction of Planar Loop Integrands of Cubic Scalar Theory," JHEP **05** (2016), 061 doi:10.1007/JHEP05(2016)061 [arXiv:1601.05864 [hep-th]].

[119] S. He and O. Schlotterer, "New Relations for Gauge-Theory and Gravity Amplitudes at Loop Level," Phys. Rev. Lett. **118** (2017) no.16, 161601 doi:10.1103/PhysRevLett.118.161601 [arXiv:1612.00417 [hep-th]].

[120] S. He, O. Schlotterer and Y. Zhang, "New BCJ representations for one-loop amplitudes in gauge theories and gravity," Nucl. Phys. B **930** (2018), 328-383 doi:10.1016/j.nuclphysb.2018.03.003 [arXiv:1706.00640 [hep-th]].

[121] G. Salvatori and S. L. Cacciatori, "Hyperbolic Geometry and Amplituhedra in 1+2 dimensions," JHEP **08** (2018), 167 doi:10.1007/JHEP08(2018)167 [arXiv:1803.05809 [hep-th]].

[122] G. Salvatori, "1-loop Amplitudes from the Halohedron," JHEP **12** (2019), 074 doi:10.1007/JHEP12(2019)074 [arXiv:1806.01842 [hep-th]].

[123] F. A. Berends and W. T. Giele, "Recursive Calculations for Processes with n Gluons," Nucl. Phys. B **306** (1988), 759-808 doi:10.1016/0550-3213(88)90442-7

[124] G. Passarino and M. J. G. Veltman, "One Loop Corrections for e+ e- Annihilation Into mu+ mu- in the Weinberg Model," Nucl. Phys. B **160** (1979), 151-207 doi:10.1016/0550-3213(79)90234-7

[125] S. Buchta, G. Chachamis, P. Draggiotis and G. Rodrigo, "Numerical implementation of the loop–tree duality method," Eur. Phys. J. C **77** (2017) no.5, 274 doi:10.1140/epjc/s10052-017-4833-6 [arXiv:1510.00187 [hep-ph]].

[126] D. A. Ross and J. C. Taylor, "Renormalization of a unified theory of weak and electromagnetic interactions," Nucl. Phys. B **51** (1973), 125-144 [erratum: Nucl. Phys. B **58** (1973), 643-643] doi:10.1016/0550-3213(73)90505-1

[127] M. Bohm, H. Spiesberger and W. Hollik, "On the One Loop Renormalization of the Electroweak Standard Model and Its Application to Leptonic Processes," Fortsch. Phys. **34** (1986), 687-751 doi:10.1002/prop.19860341102

[128] R. Britto, F. Cachazo and B. Feng, "New recursion relations for tree amplitudes of gluons," Nucl. Phys. B **715** (2005), 499-522 doi:10.1016/j.nuclphysb.2005.02.030 [arXiv:hep-th/0412308 [hep-th]].

[129] R. Britto, F. Cachazo, B. Feng and E. Witten, "Direct proof of tree-level recursion relation in Yang-Mills theory," Phys. Rev. Lett. **94** (2005), 181602 doi:10.1103/PhysRevLett.94.181602 [arXiv:hep-th/0501052 [hep-th]].

[130] P. Benincasa and F. Cachazo, "Consistency Conditions on the S-Matrix of Massless Particles," [arXiv:0705.4305 [hep-th]].

[131] F. A. Berends, R. Kleiss, P. De Causmaecker, R. Gastmans and T. T. Wu, "Single Bremsstrahlung Processes in Gauge Theories," Phys. Lett. B **103** (1981), 124-128 doi:10.1016/0370-2693(81)90685-7

[132] F. A. Berends, R. Kleiss, P. De Causmaecker, R. Gastmans, W. Troost and T. T. Wu, "Multiple Bremsstrahlung in Gauge Theories at High-Energies. 2. Single Bremsstrahlung," Nucl. Phys. B **206** (1982), 61-89 doi:10.1016/0550-3213(82)90489-8

[133] J. M. Drummond and J. M. Henn, "All tree-level amplitudes in N=4 SYM," JHEP **04** (2009), 018 doi:10.1088/1126-6708/2009/04/018 [arXiv:0808.2475 [hep-th]].

[134] L. J. Dixon, J. M. Henn, J. Plefka and T. Schuster, "All tree-level amplitudes in massless QCD," JHEP **01** (2011), 035 doi:10.1007/JHEP01(2011)035 [arXiv:1010.3991 [hep-ph]].

[135] M. Dinsdale, M. Ternick and S. Weinzierl, "A Comparison of efficient methods for the computation of Born gluon amplitudes," JHEP **03** (2006), 056 doi:10.1088/1126-6708/2006/03/056 [arXiv:hep-ph/0602204 [hep-ph]].

[136] F. Cachazo, S. He and E. Y. Yuan, "Scattering in Three Dimensions from Rational Maps," JHEP **10** (2013), 141 doi:10.1007/JHEP10(2013)141 [arXiv:1306.2962 [hep-th]].

[137] F. Cachazo, S. He and E. Y. Yuan, "Scattering equations and Kawai-Lewellen-Tye orthogonality," Phys. Rev. D **90** (2014) no.6, 065001 doi:10.1103/PhysRevD.90.065001 [arXiv:1306.6575 [hep-th]].

[138] F. Cachazo, S. He and E. Y. Yuan, "Scattering of Massless Particles in Arbitrary Dimensions," Phys. Rev. Lett. **113** (2014) no.17, 171601 doi:10.1103/PhysRevLett.113.171601 [arXiv:1307.2199 [hep-th]].

[139] F. Cachazo, S. He and E. Y. Yuan, "Scattering of Massless Particles: Scalars, Gluons and Gravitons," JHEP **07** (2014), 033 doi:10.1007/JHEP07(2014)033 [arXiv:1309.0885 [hep-th]].

[140] L. Magnea, E. Maina, P. Torrielli and S. Uccirati, "Towards analytic local sector subtraction at NNLO," PoS **RADCOR2017** (2018), 035 doi:10.22323/1.290.0035 [arXiv:1801.06458 [hep-ph]].

[141] L. Magnea, E. Maina, P. Torrielli and S. Uccirati, "Factorization and subtraction," PoS **RADCOR2017** (2018), 043 doi:10.22323/1.290.0043 [arXiv:1801.06462 [hep-ph]].

[142] L. Magnea, E. Maina, G. Pelliccioli, C. Signorile-Signorile, P. Torrielli and S. Uccirati, "Local analytic sector subtraction at NNLO," JHEP **12** (2018), 107 [erratum: JHEP **06** (2019), 013] doi:10.1007/JHEP12(2018)107 [arXiv:1806.09570 [hep-ph]].

[143] L. Magnea, E. Maina, G. Pelliccioli, C. Signorile-Signorile, P. Torrielli and S. Uccirati, "Factorisation and Subtraction beyond NLO," JHEP **12** (2018), 062 doi:10.1007/JHEP12(2018)062 [arXiv:1809.05444 [hep-ph]].

[144] L. Magnea, G. Pelliccioli, C. Signorile-Signorile, P. Torrielli and S. Uccirati, "Analytic integration of soft and collinear radiation in factorised QCD cross sections at NNLO," JHEP **02** (2021), 037 doi:10.1007/JHEP02(2021)037 [arXiv:2010.14493 [hep-ph]].

[145] J. Vermaseren, "The use of computer algebra in QCD," Lect. Notes Phys. **479** (1997), 255-298 doi:10.1007/BFb0104292

[146] R. Mertig, M. Bohm and A. Denner, "FEYN CALC: Computer algebraic calculation of Feynman amplitudes," Comput. Phys. Commun. **64** (1991), 345-359 doi:10.1016/0010-4655(91)90130-D

[147] V. Shtabovenko, R. Mertig and F. Orellana, "New Developments in FeynCalc 9.0," Comput. Phys. Commun. **207** (2016), 432-444 doi:10.1016/j.cpc.2016.06.008 [arXiv:1601.01167 [hep-ph]].

[148] V. Shtabovenko, R. Mertig and F. Orellana, "FeynCalc 9.3: New features and improvements," Comput. Phys. Commun. **256** (2020), 107478 doi:10.1016/j.cpc.2020.107478 [arXiv:2001.04407 [hep-ph]].